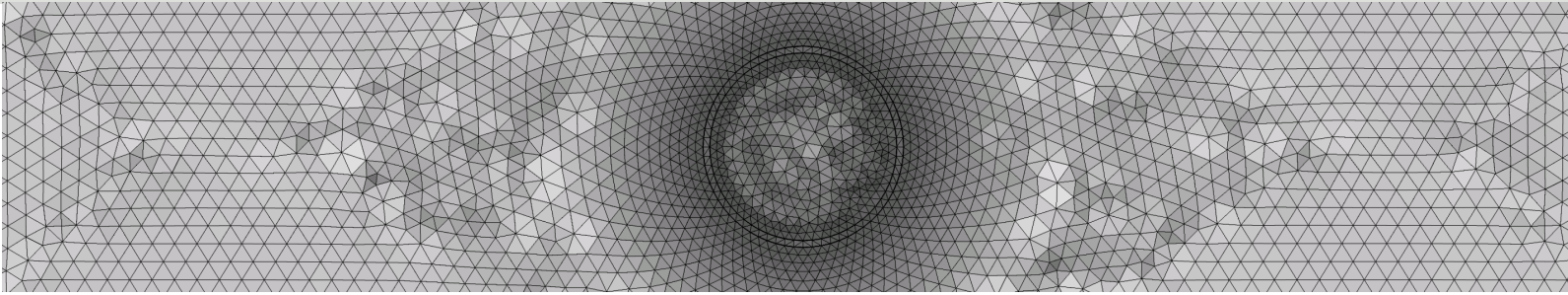




Schweizerische Eidgenossenschaft
Confédération suisse
Confederazione Svizzera
Confederaziun svizra

Eidgenössisches Nuklearsicherheitsinspektorat ENSI
Inspection fédérale de la sécurité nucléaire IFSN
Ispettorato federale della sicurezza nucleare IFSN
Swiss Federal Nuclear Safety Inspectorate ENSI



Assessment of Geomechanical Properties, Maximum Depth below Ground Surface and EDZ Impact on Long Term Safety

Expertenbericht

im Rahmen der Beurteilung des Vorschlags von mindestens zwei geologischen Standortgebieten pro Lagertyp, Etappe 2, Sachplan geologische Tiefenlager

**F. Amann, S. Löw, M. Perras
ETH Zürich Ingenieurgeologie**

November 2015

Sachplan Geologische Tiefenlager, Etappe 2

**Assessment of Geomechanical Properties, Maximum
Depth below Ground Surface and EDZ Impact on
Long Term Safety**

Florian Amann, Simon Löw, Matthew Perras

ETH Zürich, Chair of Engineering Geology

October 29, 2015

ENSI Report No. 33/460

Zusammenfassung

Die maximale Tiefe der HAA- und SMA-Lager aus bautechnischer und sicherheitstechnischer Sicht stellt ein wichtiges Kriterium für die Optimierung der Lagerperimeter und die Auswahl der Standortgebiete in SGT Etappe 2 dar. Bei der bautechnischen Machbarkeit geologischer Tiefenlager ist die minimale Schädigung der geologischen Barriere zu berücksichtigen. Dafür spielen die felsmechanischen Grundlagen v. a. des Opalinustons eine wichtige Rolle. Die Professur für Ingenieurgeologie der ETH wurde vom ENSI beauftragt, die Grundlagen, die Beurteilungen und die Bewertungen der Nagra betreffend der Indikatoren Nr. 1 (Tiefenlage im Hinblick auf bautechnische Machbarkeit) und Nr. 29 (Auflockerungszone im Nahbereich der Untertagebauten) zu prüfen. Folgende Leitfragen waren von der ETH zu beantworten:

- 1) Sind die von der Nagra dokumentierten felsmechanischen Grundlagen und orientierenden felsmechanischen Berechnungen für den Opalinuston nachvollziehbar, vollständig und korrekt?
- 2) Sind die Berechnungen und Hinweise auf die maximale Tiefenlage im NAB 14-81 aus Sicht des felsmechanischen Gebirgsverhalten nachvollziehbar?
- 3) Ist der Schritt der optimierten Abgrenzung der Lagerperimeter im NTB 14-01 bezüglich maximaler Tiefenlage und deren Bewertung nachvollziehbar?
- 4) Werden von der Nagra mögliche Einflüsse der EDZ auf die Langzeitsicherheit nach Verschluss des Lagers aufgezeigt und bewertet? Sind diese nachvollziehbar und plausibel?

Stoffansatz, Gesteins- und Gebirgskennwerte

Der Stoffansatz und die Gesteinskennwerte des Opalinustons werden in einem separaten Bericht der Prüfexperten (Amann und Vogelhuber 2015) bewertet. Dieser Bericht zeigt, dass der von der NAGRA beschriebene Stoffansatz im Einklang mit vielen anderen Studien an Tonsteinen (z.B. Aristorenas 1992) ist. Der Stoffansatz ist übersichtlich beschrieben und sowohl mit Literatur als auch Laborergebnissen dokumentiert. Um den Einschränkungen der numerischen Methoden, die für die Machbarkeitsstudie verwendet werden, gerecht zu werden, hat die NAGRA Vereinfachungen des Stoffansatzes eingeführt. Eine starke Vereinfachung ist dabei das Weglassen der Roscoe Fliessgrenze und damit das Einführen eines linear-elastischen Stoffverhaltens bevor im effektiven Spannungsraum die Hvorslev Bruchgrenze oder die Zugspannungsbegrenzung erreicht wird. Die Vereinfachungen der NAGRA werden für Machbarkeitsbetrachtungen nur dann als zulässig erachtet, wenn die Konsequenzen des Weglassens der Roscoe Fliessgrenze durch eine geeignete Wahl der elastischen Eigenschaften berücksichtigt werden. Zudem berücksichtigen die Stoffmodelle der analytischen und numerischen Methoden der NAGRA die Abhängigkeit der Festigkeit und Steifigkeit mit zunehmender effektiver Spannung / Tiefe nicht. Demzufolge definiert die NAGRA effektive Scherfestigkeiten und Steifigkeiten für eine Tiefenlage bis 400 m und zwischen 400 – 900 m. Im relevanten Tiefenbereich zwischen 400 bis 900 m bleibt der Effekt der zunehmenden Tiefe auf die Festigkeit und Steifigkeit unberücksichtigt, was relevante Folgen für Festlegung der maximalen Tiefenlage nach sich ziehen kann.

Gemäss Amann und Vogelhuber (2015) ist die Datenbasis an belastbaren Versuchen sehr klein, überschätzen die von der NAGRA abgeleiteten effektiven Gesteins-Festigkeiten und die undrainierten Scherfestigkeiten die tatsächlichen Festigkeiten (u.a. aufgrund von Laborversuchen an teilgesättigten Proben), und ist das Ausmass der Überschätzung nicht quantifizierbar. Die von der Nagra vorgeschlagenen undrainierten Festigkeiten beruhen auf einem Datensatz welcher die Anforderung zur Bestimmung der undrainierten Scherfestigkeit zum grossen Teil nicht erfüllt. Die von der NAGRA vorgeschlagenen Werte sind zudem nicht konsistent mit den vorgeschlagenen effektiven Festigkeiten und überschätzen die tatsächlichen undrainierten Festigkeiten deutlich.

Die Kennwerte des tektonisch geschwächten Gebirges werden konzeptuell in verschiedene Gebirgsklassen (oder nach NAGRA „Gebirgsmodelle“) eingeteilt und den tektonisch unterschiedlich stark überprägten Standortgebieten und Arealen zugeteilt. Die von der NAGRA abgeleiteten Gebirgsfestigkeiten überschätzen die tatsächliche Festigkeit, insbesondere im Fall der undrainierten Gebirgsscherfestigkeit. Die Gebirgssteifigkeit bleibt gemäss NAGRA trotz zunehmender Schwächung des Gebirges konstant, was aus Sicht der Experten nicht zulässig ist.

Spannungsbedingungen

Die regionale Verteilung der Spannungsorientierungen in der Nordschweiz wurde systematisch aufgrund von Bohrlochrandausbrüchen und Hydrofrac-Versuchen kompiliert und mit Paläospannungs-Analysen und Modellrechnungen verglichen. Die regionalen Analysen der Spannungsmagnituden wurden sorgfältig dokumentiert. Die lokalen Spannungsverhältnisse in den Standortgebieten und kleinräumige Spannungsheterogenitäten werden nicht systematisch beschrieben. Dafür decken die verwendeten Spannungs-Szenarien die zu erwartenden Bandbreiten konservativ ab.

Entwurfsindikatoren

Die Anforderungen an die maximale Tiefenlage des Tiefenlagers für hochaktive Abfälle (HAA) werden von der NAGRA systematisch, basierend auf übergeordneten sicherheits- und bautechnischen Zielsetzungen abgeleitet und mittels 5 Entwurfsindikatoren (EI) in einer Serie von Detailstudien untersucht, wobei sich 3 auf die Langzeitsicherheit (EI-1 bis EI3) und 2 (EI4, EI5) auf die bautechnische Machbarkeit beziehen. Diese Entwurfsindikatoren umfassen: die gemittelte Ausdehnung der Auflockerungszone oder „plastifizierte Zone“ (EI-1), die über den Ausbruchsquerschnitt gemittelte Tunnelkonvergenz (EI-2, EI-3, EI-4), und die Beurteilung der Tragfähigkeit des Ausbaus (EI-5). Die Bewertung dieser Entwurfsindikatoren basiert dabei auf einer Serie unterschiedlicher empirischer, analytischer und numerischer Verfahren, auf felsmechanischen Eigenschaften des Opalinustons, welche aus Laborversuchen abgeleitet wurden, und den in-situ Spannungsverhältnissen an den zur Diskussion stehenden Standortgebieten für SMA- und HAA-Tiefenlager.

Sicherheitstechnische Beurteilung der maximalen Tiefenlage

Die Wahl und die Bewertungsskala des ersten Entwurfsindikators zur maximalen Tiefenlage aus Sicht der Langzeitsicherheit (Ausdehnung der plastifizierte Zone) sind für die Prüfexperten nachvollziehbar. Aufgrund grosser Sicherheitsreserven (d.h. genügend vertikaler Mächtigkeit des ungestörten Opalinustons zwischen AUZ und der Formationsgrenze) ergeben sich bei Anwendung dieses Entwurfsindikators im betrachteten Tiefenbereich bis 900 m keine zusätzlichen Einschränkungen. Aus Sicht der Prüfexperten führt die grundsätzliche Beziehung, dass sich die Auflockerungszone und die Verformungen mit zunehmender Tiefe vergrössern (unter der Voraussetzung eines gleich bleibenden Ausbauwiderstandes und gleich bleibender Gebirgsfestigkeit), zu einer schlechteren relativen Bewertung tieferliegender Standortareale. In Anbetracht des Stoffansatzes der NAGRA, der von den Experten als zutreffend erachtet wird, ist aber mit einer zunehmenden Festigkeit und Steifigkeit mit zunehmender Tiefe zu rechnen. Im relevanten Tiefenbereich zwischen 400 und 900m wird dieser Effekt von der NAGRA nicht berücksichtigt und kann anhand der vorliegenden Laborversuche nur für die Steifigkeit aber nicht für die Festigkeit quantifiziert werden kann. Demzufolge verbleiben grosse Unsicherheiten bei der vergleichenden Bewertung der AUZ Tiefe bei stark unterschiedlichen Tiefenlagen.

Die transportwirksamen Eigenschaften der Auflockerungszone (EI-2) und die Qualität der Einbaubedingungen der technischen Barriere (EI-3) werden durch die NAGRA mit jeweils einem Konvergenzkriterium beurteilt. Die Wahl dieser beiden Kriterien ist für die Prüfexperten nicht nachvollziehbar, da die berechneten Tunnelkonvergenzen auch substantiell von den elastischen Gebirgseigenschaften abhängen, welche keine Auswirkung auf die bruchhaften Verformungen in der Auflockerungszone und damit die hydraulische Durchlässigkeit und Leitfähigkeit haben, sich jedoch

deutlich auf die totalen Tunnelverformungen und somit die Bewertung auswirken. Letzteres steht insbesondere im Zusammenhang mit der Wahl der elastischen Eigenschaften der NAGRA (undrainierter statt drainierter E-Modul für effektive Spannungsberechnungen; nicht Berücksichtigung der Konsequenzen der Vereinfachungen des Stoffmodells auf die Wahl des E-Moduls; nicht Berücksichtigung der experimentell belegten, deutlichen Zunahme des drainierten E-Modul im relevanten Tiefenbereich zwischen 400 und 900 m). Zudem sind die Erschwernisse beim Einbau der technischen Barrieren vor allem auch von lokalen Niederbrüchen und Ausbrüchen (Überprofilen) abhängig und nicht von einer gemittelten Konvergenz. In Bezug auf EI-3 wurden von der NAGRA zudem typische, im Labor ermittelte axiale Stauchungen beim Erreichen der Restfestigkeit mit der tangentialen Stauchung und damit der diametralen Tunnelverzerrung gleich gesetzt, um Grenzwerte festzulegen. Dieses Vorgehen ist grundsätzlich ungeeignet und die Herleitung der Grenzwerte zudem nicht korrekt.

Die Bewertung der quantitativen Zusammenhänge zwischen gemittelten Konvergenzen und der hydraulischen Leitfähigkeit der Auflockerungszone kann im Rahmen der vorliegenden Arbeitsberichte nicht nachvollzogen werden. So fehlt insbesondere eine nachvollziehbare Herleitung der Beziehung zwischen dem geforderten hydraulischen Leitvermögen von $1E-7 \text{ m}^3/\text{s}$ und der entsprechenden maximal zulässigen Tunnelkonvergenz von 4%.

Bautechnische Beurteilung der maximalen Tiefenlage

Während die bautechnische Machbarkeit eines Tunnels in tonreichen Gesteinen wie dem Opalinuston selbst bei stark druckhaften Verhältnissen in tektonisch gestörten Zonen bis in grosse Tiefenlagen (> 1000 m unter OKT) gegeben ist, unterliegt die Bewertung der bautechnischen Machbarkeit eines HAA-Tiefenlagers Einschränkungen der zur Verfügung stehenden Stützmittel. Im Fall der HAA-Lagerstollen bestehen aus Sicht der Langzeitsicherheit (z.B. Gasbildung, Lösungshohlräume, geochemische Alterationen von Bentonit und Wirtgestein) starke Einschränkungen in der Wahl der Sicherungsmittel. Diese umfassen nach NAGRA eine Begrenzung der Spritzbetonstärke auf 30 cm, sowie eine nicht quantifizierte Beschränkung der Menge an Stahl und Organika (wie zum Beispiel GFK-Anker). Zudem wirken sich unerwünschte Ereignisse wie Niederbrüche oder eine weit ausgedehnte Auflockerungszone, die im klassischen Tunnelbau beherrscht werden oder von geringer Relevanz sind, auf die Langzeitsicherheit negativ aus.

Bautechnisch kritisch für die HAA-Lagerstollen und ihre maximale Tiefenlage sind vor allem die Versiegelungsstrecken, bei welchen aus sicherheitstechnischen Überlegungen gefordert wird, dass der Bentonit optimal (d.h. ohne grössere Ausbrüche) eingebracht und verdichtet werden kann und über grosse Flächen im direkten Kontakt zum Wirtgestein steht. In diesen Versiegelungsstrecken kommen nach NAGRA alle 0.7 m TH25-Stahlbögen mit Gleitschlössern und Bewehrungsnetze als Steinschlagschutz zur Anwendung. Basierend auf den bisherigen Erfahrungen scheinen Bewehrungsnetze insbesondere in grossen Tiefen keine genügenden Stützmittel zwischen den Stahlbögen zu sein. Vermutlich sind andere temporäre Sicherungskonzepte wie zum Beispiel Verzugsbleche zwischen den Bögen für die Längsstabilität der Stahlbögen und als Sicherung gegen Niederbrüche notwendig.

Das erste bautechnische Entwurfskriterium (EI-4) erachten die Prüfexperten als nicht zweckmässig, da sich 1) die kritischen Gefährdungsbilder (lokale Aus- und Niederbrüche, spannungs- oder strukturkontrolliert) nicht mit einer gemittelten Konvergenz bewerten lassen und 2) die totalen Tunnelkonvergenzen, wie bereits oben erwähnt, auch von der Wahl der elastischen Eigenschaften abhängen. Zudem wurde der Entwurfsindikator EI-4 aus Empfehlungen in der Literatur abgeleitet, welche die diametrale Tunnelverzerrung mit bautechnischen Schwierigkeiten gleich setzten. Diese Empfehlungen erlauben aus mehreren Gründen keine quantitativen Beurteilungen und geben nur einen generellen Hinweis darauf, dass mit zunehmender Tiefenlage die bautechnischen Schwierigkeiten zunehmen könnten.

Die Beurteilung der Gebirgstragfähigkeit und des Tragwiderstandes des Ausbaus erfolgt mit dem Entwurfsindikator EI-5 (zweites bautechnisches Entwurfskriterium). Zwei Ausbauprinzipien werden von der NAGRA betrachtet: das Widerstandsprinzip, bei dem der Tunnelausbau im Abstand von einem Tunneldurchmesser (ca. 3 m) hinter der Ortsbrust erfolgt und das Ausweichprinzip, bei dem der Tunnelausbau bzw. das Erreichen des vollen Ausbauwiderstandes im Abstand von drei Tunneldurchmesser (ca. 9 m) hinter der Ortsbrust erfolgt. Im ersteren Fall zeigen die Berechnungen der NAGRA, dass die Tragfähigkeit der Stützmittel in den Versiegelungsstrecken schon bei einer Tiefe von 400 bis 500m überschritten wird. Bei Anwendung des Ausweichprinzips können nach NAGRA in den Versiegelungsstrecken Tiefen von 600 bis 700 m erreicht werden. Allerdings ist bei dieser Ausbauvariante in den Versiegelungsstrecken und in grossen Tiefen damit zu rechnen, dass unerwünschte Ereignisse weitaus weniger gut zu kontrollieren sind als bei Anwendung des Widerstandsprinzips. Das vorgeschlagene Ausbaukonzept (Stahlbögen und Netze) unter Annahme des Ausweichprinzips wird von den Experten als kritisch erachtet.

Bautechnische Auswirkungen auf die Langzeitsicherheit

Die Nagra bewertet die Auswirkungen der Auflockerungszone auf die Langzeitsicherheit mit dem Indikator 29 (Auflockerungszone im Nahbereich der Untertagebauten). Die Bewertung dieses Indikators beruht auf der Grösse und den Transporteigenschaften der Auflockerungszone, des Selbstabdichtungsvermögens und der Relevanz für den Radionuklidtransport. Die Selbstabdichtung stellt eine phänomenologische Beobachtung der Reduktion der Porosität und hydraulischen Leitfähigkeit in natürlichen (tektonischen Störungen) und künstlichen Schwächezonen (Auflockerungszonen) dar. Die dieser Beobachtung zugrunde liegenden Prozesse (Primär- oder Sekundärkonsolidation, Quellprozesse, Desintegration) sind nach Ansicht der Prüfexperten bis heute nicht genau verstanden. Die Selbstabdichtung wird von der NAGRA als fundamentale wichtige Eigenschaft des Wirtgesteins betrachtet, mit dem Tongehalt korreliert, und in den Bewertungen der Nagra zur Standorteinengung in Etappe 2 sehr stark gewichtet. Ebenso erhält der Radionuklidtransport in der Auflockerungszone durch die von der Nagra geplanten Zwischensiegel und die von der Nagra festgelegten Anforderungen an die Entwurfsindikatoren eine sehr grosse Bedeutung.

Die neuen Konsolidations- und Quellversuche an Proben der Bohrung Schlattingen-1 sind wertvolle Ergänzungen der früheren Datensätze über das Quell- und Konsolidationsverhalten des Opalinustons. Die Quelldrücke entsprechen den Wertebereichen anderer Langzeitversuche und in-situ-Messungen. Die ausgewiesenen Quellhebungen des Opalinustons sind jedoch im Vergleich zu anderen Langzeitversuchen tief. Die wenigen bisherigen in-situ-Versuche zur Selbstabdichtung bestätigen grundsätzlich, dass Konsolidations- und Quellprozesse zu einer signifikanten Reduktion der initial sehr hohen Durchlässigkeit der Auflockerungszone führen können, und dass der Betrag und die räumliche Verteilung der Stützdrücke am Ausbruchrand wesentlich für eine signifikante Reduktion der hydraulischen Durchlässigkeit in einer moderat gestörten Auflockerungszone sind. Die für eine signifikante Reduktion der Durchlässigkeit notwendigen Stützdrücke können vermutlich nicht durch herkömmliche Stützmittel, sondern nur durch den quellenden Bentonit erzeugt werden, insbesondere in den Versiegelungsstrecken (Zwischensiegel) der HAA-Lagerstollen. Die bisher von der NAGRA durchgeführten Untersuchungen beziehen sich fast ausschliesslich auf eine Auflockerungszone mit moderater Gebirgsschädigung und nicht auf die Auswirkungen von grösseren Ausbrüchen und Niederbrüchen. Für die Prüfexperten ist die Verhinderung und Beherrschung von grösseren Ausbrüchen und Schädigungen während Bau und Betrieb von zentraler Bedeutung.

Die neuen in Etappe 2 SGT von der NAGRA verwendeten Modellrechnungen zur Selbstabdichtung der Auflockerungszone tragen nach Ansicht der Prüfexperten keine neuen Erkenntnisse zur Selbstabdichtung bei, da sie auf fragwürdigen numerischen Ansätzen (u.a. Skalen-, 3D-Effekte und Netzeffekte, fehlende HM-Koppelung im Rissimulator; fragwürdiges Kluftschliessungsgesetz im Fliessmodell) basieren. Zudem wurden die Modellparametrisierungen und Annahmen über

Randbedingungen nicht aufgrund von Versuchsergebnissen festgelegt, sondern derart, dass Vorgaben zur maximalen Tunnelkonvergenz oder Selbstabdichtung bei vollständiger Aufsättigung erreicht werden.

Die neuen Modellrechnungen zum Radionuklidtransport in der Auflockerungszone bestätigen grundsätzlich frühere Modellresultate der NAGRA und ihrer Prüfbehörden. Die Berechnungen zeigen, dass die Auflockerungszone um die verfüllten Untertagebauwerke einen unbedeutenden Freisetzungspfad darstellt, solange das hydraulische Leitvermögen kleiner als rund $1\text{E-}7\text{ m}^3/\text{s}$ ist (hydraulische Durchlässigkeit kleiner als $1\text{E-}8\text{ m/s}$). Dieses langfristig geforderte hydraulische Leitvermögen von maximal $1\text{E-}7\text{ m}^3/\text{s}$ sollte bei entsprechenden technischen Massnahmen im Tunnelvortrieb an allen Standortgebieten eingehalten werden können. Das Einhalten dieser Anforderung hängt nach Ansicht der Prüfexperten primär davon ab, ob und mit welchen technischen Mitteln grössere Ausbrüche im Stollenvortrieb verhindert und allenfalls wirksam verfüllt werden können.

Schlussfolgerungen

Die Experten kommen nach Abschluss ihrer Prüfungsarbeiten zum Schluss, dass die von der Nagra eingereichten felsmechanischen Grundlagen, Berechnungen und Festlegungen bezüglich der maximalen Tiefenlage nicht nachvollziehbar sind. Demzufolge ist auch der Schritt der optimierten Abgrenzung der Lagerperimeter in NTB 14-01 bezüglich maximaler Tiefenlage nicht nachvollziehbar. Aus Sicht der Prüfexperten führt die grundsätzliche Beziehung, dass sich die Auflockerungszone und die Verformungen mit zunehmender Tiefe vergrössern (unter der Voraussetzung eines gleich bleibenden Ausbauwiderstandes und Gebirgseigenschaften), zu einer schlechteren relativen Bewertung tieferliegender Standortareale. Allerdings zeigt der Stoffansatz der NAGRA, welcher von den Experten als zutreffend erachtet wird, dass mit einer zunehmenden Festigkeit und Steifigkeit mit zunehmender Tiefe zu rechnen ist. Im relevanten Tiefenbereich zwischen 400 und 900 m wird dieser Effekt von der NAGRA nicht berücksichtigt und kann anhand der vorliegenden Laborversuche nur für die Steifigkeit aber nicht für die Festigkeit quantifiziert werden kann. Der drainierte E-Modul des intakten Opalinuston nimmt in diesem Tiefenbereich deutlich zu (Faktor 3.3), was einen relevanten Einfluss auf die Beurteilung und Schlussfolgerungen bezüglich der Entwurfsindikatoren EI-2, EI-3, EI-4 und EI-5 hat. Die Auswirkungen einer etwaigen Zunahme der Festigkeit im relevanten Tiefenbereich und damit der Beurteilung des Entwurfsindikators EI-1 lassen sich heute nicht quantifizieren.

Auswirkungen der Auflockerungszone auf die Langzeitsicherheit werden im Rahmen von experimentellen Befunden bewertet und mittels Radionuklid-Ausbreitungsrechnungen modelliert. Nach Ansicht der Prüfexperten werden die diesen Ausbreitungsrechnungen zugrunde liegenden wichtigen Annahmen zur Selbstabdichtung durch die bisherigen experimentellen Befunde, nicht aber wesentlich durch die neuen Modellrechnungen gestützt. Die experimentellen Befunde zur Selbstabdichtung beziehen sich nur auf gering bis moderat gestörte Auflockerungszonen, aber nicht auf grössere Ausbrüche. Demzufolge erachten die Experten bautechnisch machbare Konzepte, welche Ausbrüche oder Niederbrüche, insbesondere in den Strecken zur Unterbindung des Längsdurchflusses, verhindern können oder allenfalls wieder eine wirksame Verfüllung mit Bentonit garantieren, als sehr wesentliche Bausteine für den Nachweis der Langzeitsicherheit.

Executive Summary

The maximum depth below the ground surface for high-level (HLW) and intermediate level (ILW) nuclear waste repositories is a key issue for long term safety and for the optimization of the repository perimeters in the proposed siting regions. During stage 2 of the Sectorial Plan Deep Geological Repositories (SGT) ENSI commissioned the Chair of Engineering Geology at ETH Zurich to review both the evaluation and assessment of NAGRA's reports related to the technical indicators No. 1 (Depth below ground surface in terms of technical feasibility) and No. 29 (Excavation damage zone in the near-field of underground excavations). The expert guideline provided by ENSI lists the following key questions:

- 1) Are the rock mechanical fundamentals and scoping calculations for Opalinus Clay provided by NAGRA reproducible, complete and correct?
- 2) Are both the numerical calculations and evidences for defining the maximum depth below ground surface in NAB 14-81 in terms of the expected rock mass behavior reproducible?
- 3) Is the optimized delineation of the disposal perimeter in NTB 14-01 in terms of maximum depth below ground surface and its assessment reproducible?
- 4) Are potential effects of the longer term EDZ development after repository closure covered and assessed by NAGRA? Are these effects reproducible and plausible?

The experts reviewed a large number of reports to answer these key questions posed by ENSI.

Constitutive framework and Geomechanical Properties

The constitutive framework described by NAGRA is in agreement with behavioral aspects that have also been reported in many other studies on clay shales (e.g., Aristorenas 1992). The model is well described and documented with literature and laboratory data. NAGRA introduces a series of simplification to the constitutive framework to account for limitations in the numerical codes used for the engineering feasibility studies. One major simplification is to omit the Roscoe yield surface and to assume a linear-elastic behavior before reaching the Hvorslev yield surface or tension cut-off. The simplifications introduced by NAGRA are reasonable for engineering feasibility studies provided that the consequences of omitting the Roscoe yield surface are considered with adequate elastic properties. In addition, the constitutive models used for analytical and numerical analysis by NAGRA do not account for an increase in effective strength and stiffness with increasing effective stress or depth. Therefore, NAGRA defined effective strength properties and E-Moduli that are either representative for a depth up to 400 m or a depth range between 400 and 900 m. For the relevant depth range between 400 and 900 m the influence of increasing depth on the effective strength properties and stiffness was not considered. This can influence the maximum depth assessment.

All geomechanical test series used by NAGRA for determining elastic properties, effective strength properties, and the undrained shear strength of Opalinus Clay at a depth range < 400m and between 400 and 900m were analyzed by the experts (a detailed summary of the analysis is given in Amann and Vogelhuber, 2015). The analysis reveals that the majority of the test specimens were not saturated prior to differential loading, or saturation could not be demonstrated. Capillary forces caused an apparent strength component and the suggested effective strength properties tend to overestimate the actual strength. The data basis used for establishing the undrained shear strength as a function of the water content is not adequate. The undrained strength values suggested by NAGRA are in addition inconsistent with the suggested effective strength properties, and largely overestimate the actual undrained strength. The suggested elastic properties for the intact rock are in agreement with laboratory data on saturated specimens. The same elastic properties were also assigned to all rock mass models

(i.e. tunnel scale models which consider weakness planes). It is shown that rock mass elastic properties should be reduced compared to intact rock properties.

In-situ Stress

The most common method of predicting the principal stress orientations at depth is through the analysis of borehole breakouts or by conducting hydraulic fracture tests. NAGRA has used both to constrain the stress orientations in the siting regions of Northern Switzerland (using boreholes within or near-by the siting regions). Regional variations in the orientations are examined and carefully discussed. Beyond this NAGRA has also examined paleo-indicators to determine how the stress orientations have changed with time. Stress magnitude analyses are clearly documented and how the reference, minimum, and maximum stress scenarios are derived can be followed. The smaller scale variability in orientation and magnitude for each site has not been addressed. However, the minimum and maximum stress scenarios can be considered conservative estimates of the lower and upper bound stress states, respectively.

Design Criteria

NAGRA's approach to assess the maximum depth below ground surface is primarily based on five design criteria. Three design criteria are related to long term safety, and two design criteria to the technical feasibility. One design criterion utilizes the size of the excavation damage zone (EI-1), three design criteria utilize the calculated diametral tunnel strain averaged over the tunnel circumference (EI-2, EI-3 and EI-4), and one design criterion (EI-5) addresses the structural safety according to the Swiss Standard. The experts assessed design criteria EI-1 and EI-5 as applicable for the maximum depth assessment. Design criteria based on the diametral tunnel strain are not applicable for assessing tunnel depth for the following reasons:

- For design criterion EI-2 NAGRA relates the hydraulic EDZ conductance parallel to the repository tunnels to the diametral tunnel strain. In addition to the fact that relations between hydraulic conductance and tunnel strain have not been experimentally demonstrated by NAGRA, the tunnel strain also depends to a significant degree on the chosen elastic properties. For a reduction of the E-Modulus of 50% the tunnel strain doubles while both the extent and the accumulated plastic volumetric strain within the EDZ remain constant (for the assumption of zero dilatancy). Changes in hydraulic conductivity are, however, only related to the EDZ area and accumulated plastic volumetric strains.
- Design criterion EI-3 relates the averaged diametral tunnel strain to local overbreak which affect the condition for proper bentonite backfill and swelling within the sealing section. In addition to the fact that an averaged diametral tunnel strain is unsuitable for assessing local rock failure problems, the total diametral tunnel strain depends on both elastic and plastic strains in the rock mass, which cannot be fully measured in-situ. In addition, NAGRA derives thresholds for the maximum diametral strain from the results of laboratory strength tests, which typically show that the residual strength is reached at 1% axial strain. However, this axial strain cannot be considered to correspond to the accumulated diametral tunnel strain.
- Design criterion EI-4 was derived by NAGRA based on recommendations given in the literature, which relate tunnel strain to tunneling difficulties. Those recommendations, however, do not allow a quantitative assessment of the maximum depth below ground surface or to establish reliable quantitative design criteria.

As pointed out above, the calculated accumulated tunnel strain depends to a significant degree on the elastic properties. The assessment of the above design criteria is therefore dependent on the elastic properties suggested by NAGRA. Undrained rather than drained elastic properties were used for effective stress analysis, which is not acceptable, and the effects of the simplification of the constitutive model on the choice of elastic properties, and the experimentally confirmed, significant increase in the

drained E-Modulus in the relevant depth range between 400 and 900 m are not considered. This also affects the assessment of design criteria EI-5.

Evaluation of Maximum Repository Depth

Different computational methods including effective stress calculations using FLAC2D / 3D (a finite difference program), ground reaction curve (GRC) approach using effective strength properties, total stress calculations using Phase2 (a finite element program), and a collection of worldwide experience were used by NAGRA to constrain the maximum depth below ground surface.

Several issues were identified which affect the reliability of a quantitative assessment of the maximum depth below ground surface using the reported effective stress calculations: 1) both the used rock mass strength and stiffness tend to overestimate the actual strength and stiffness, 2) the specified rock mass properties used for the effective stress calculations are partly inconsistent with the theory, 3) an increase of the drained E-Modulus and effective strength properties with increasing effective stress or depth are not considered for the relevant depth range between 400 and 900m (e.g. a constant drained E-Modulus is assumed), and 4) a structural analysis of the various support types using FLAC2D is not presented by NAGRA (2014b),

Using the GRC for reliable and quantitative conclusions on the maximum depth is problematic because the deformation characteristics, in-situ stress conditions and the ground behavior deviate significantly from the assumptions for which the GRC concept was developed. Additional assumptions need to be made which add further limitations to the reliability of a quantitative assessment. The reliability of a quantitative assessment of the maximum depth below surface is further affected by the used rock mass properties (i.e. effective strength is overestimated, undrained rather drained elastic properties are used, effective stress dependency of the drained E-Modulus is not considered for the depth range between 400 and 900 m, the effects of the simplified constitutive model on the choice of the E-modulus are not considered, GRCs assuming bedding plane strength may over-predict the displacements). As a consequence of the various assumptions the concept of using the GRC for an anisotropic rock mass and anisotropic in-situ stresses for a quantitative assessment of the maximum depth is largely uncertain.

Two cases for support installation have been considered for the GRC analysis: 1) support installation at a distance of $1 \times D$ (one tunnel diameter, i.e. approx. 3 m) behind the tunnel face (called "Widerstandsprinzip") and 2) installation of yielding support that develops its full support capacity at a distance of $3 \times D$ (three tunnel diameters, i.e. approx. 9 m) behind the tunnel face (called "Ausweichprinzip"). For the most critical intermediate sealing sections the load bearing capacity of a support class utilizing TH25 steel arches is exceeded between 400 and 500 m in case support is installed at a distance of $1 \times D$ behind the tunnel face. For the case of yielding support the load bearing capacity is exceeded at a depth between 600 and 700m. This case or installation of a yielding support that develops its full support capacity at a distance of $3 \times D$ behind the tunnel face (i.e. 9 m) is considered critical (less control on rock mass damage, local failure), at least for rock mass models that contain bedding parallel weaknesses or at greater depths where large accumulated plastic strain may lead to an intense rock mass disintegration. The GRC analysis suggests that with the currently available and considered support measures in the intermediate sealing sections the maximum depth is strongly reduced. Owing to the above mentioned issues, quantitative results to constrain the maximum depth below ground surface are unreliable for both displacements and the depth where the maximum load bearing capacity is exceeded.

The total stress analysis with Phase2 provides tendencies for the EDZ depth and displacements. A quantitative assessment of the maximum depth is, however, not possible. This is mostly due to the strength properties used, which overestimate the strength, and the sensitivity of the model results to the assumptions of joint element persistence.

Based on the material provided by NAGRA, the experts conclude that the quantitative assessment of the maximum depth below ground surface and the optimized delineation of the disposal perimeter in terms of maximum depth below ground surface is not reproducible.

Impacts of Excavation Induced Damaged on Long Term Safety

The work of NAGRA discusses the long term EDZ behavior based on laboratory and in-situ experiments and numerical modelling. The work primarily focuses on empirical evidence from Mont Terri (long term permeability testing; plate loading tests; mega-packer sealing experiments) and numerical modelling.

The results from laboratory experiments and in-situ experiments support the hypothesis of self-sealing in a moderately damaged EDZ in Opalinus Clay. Experiments lasting only a few years and including a passive support pressure suggest a reduction of EDZ transmissivity by several orders of magnitude down to 10^{-8} or 10^{-9} m²/s which is required for long-term safety. Active support pressure further reduces EDZ transmissivity and hydraulic conductance. While the impacts of a moderately damaged EDZ on long-term safety have been studied by several experiments, the effects of large overbreak on long-term safety have not been systematically explored.

Numerical modelling to predict the dimensions of the EDZ, to determine the hydraulic conductivity, and to understand the change in the conductivity with time were conducted by NAGRA. These models include time dependent behavior to capture bentonite swelling, support degradation, and rock mass swelling. The fracture mechanics code, Y-Geo, was used to determine the initial (early time) extent of the EDZ and the fracture apertures. A mechanical load was used to simulate swelling pressure developed during resaturation of the bentonite. The fracture apertures taken after the 'resaturation' phase was considered to be representative for the long term (late time) EDZ properties. These early and late time EDZ properties were used in further hydraulic simulations. A number of assumptions and limitations (many not fully discussed) in the numerical approach for the long term EDZ behavior render the results unreliable for predictions or safety analyses. In particular, the modelled fracture density is significantly over-estimated (in comparison to in-situ observations or measurements at Mont Terri), potential influencing factors on the EDZ properties derived from the Y-Geo code are not discussed and are not reproducible for evaluation, and the relationship between effective stress and fracture aperture (rock mass swelling mechanism) with time is questionable.

The effect of the EDZ on long term safety has also been modelled and assessed by NAGRA based on pipe-flow and radionuclide transport models. Model assumptions are in general agreement with experimental results. These calculations show that the EDZ around backfilled tunnels only provides a significant radionuclide transport path if the hydraulic conductance does exceed $1E-7$ m³/s (corresponding to a hydraulic conductivity of $1E-8$ m/s and a flow cross-sectional area of about 10 m²). These results show that tunnel support systems which allow reliable ground control and EDZ self-sealing are of foremost relevance for the long term safety, in particular in the sealing sections. Of particular relevance are tunnel support measures, which allow to reliably control tunnel overbreak and induce damage, or measures, which enable effective back-filling. The actual tunnel support types in the sealing section may not be adequate to allow a reliable ground control.

Conclusions

Based on the available rock mechanical fundamentals, calculations and conclusions, the maximum depth below ground surface as suggested by NAGRA cannot be supported by the experts. As a consequence, the optimized delineation of the repository perimeter in NTB 14-01 is not reproducible.

The fundamental assumption of an increasing EDZ and tunnel deformations with increasing depth (assuming the same support measures and rock mechanical properties) lead generally to a worse assessment for deeper siting regions. However, the constitutive framework of NAGRA, which is

supported by the experts, suggests an increasing effective strength and stiffness with increasing depth. For the important depth range between 400 and 900 m these effects are not considered by NAGRA, and can only be quantified based on the available experimental data for the drained E-Modulus, but not for the effective strength. The drained E-Modulus of intact Opalinus Clay increases in this depth range by a factor of 3.3, which has a relevant effect on the assessment and conclusion for the utilized design criteria EI-2, EI-3, EI-4 and EI-5. A possible increase of the effective strength properties in the relevant depth range, and its consequences for design indicator EI-1 cannot be quantified.

The influence of the EDZ on the long-term safety has been assessed by NAGRA based on experimental results and radionuclide transport models. The important self-sealing assumptions of these radionuclide transport models are supported by experimental observations, but not by the new numerical models presented by NAGRA. Effective self-sealing mechanisms have mainly been shown to work for weekly to moderately damaged rock masses in the EDZ, but not for larger overbreak. Therefore the experts consider support measures that effectively mitigate overbreak or measures that allow an effective bentonite backfill in sections with overbreak, as very important, in particular in the sealing sections or other cut-off systems.

Table of Contents

Zusammenfassung.....	ii
Executive Summary	vii
Table of Contents.....	xii
List of Figures.....	xiv
List of Tables	xvi
1 Introduction.....	1
1.1 Mandate.....	1
1.2 Reports Reviewed	1
2 Fundamental rock mechanical properties and conditions	3
2.1 Strength and Stiffness of Opalinus Clay	3
2.1.1 Effective strength of the intact rock – NAGRA’s approach and assessment	4
2.1.2 Undrained shear strength of the intact rock – NAGRA’s approach and assessment	5
2.1.3 Elastic properties– NAGRA’s approach and assessment.....	7
2.1.4 Strength and Stiffness of the rock mass – NAGRA’s approach and assessment	7
2.1.5 ETH assessment of intact rock properties.....	10
2.1.6 ETH Assessment of rock mass properties.....	14
2.2 In-situ state of stress.....	16
2.2.1 Stress state – NAGRA’s assessment and approach.....	16
2.2.2 ETH Assessment of Stress state.....	19
3 Maximum depth of the high-level nuclear waste repository.....	20
3.1 Higher-level requirements and design criteria used by NAGRA.....	20
3.1.1 Background	20
3.1.2 Optimization requirements and design criteria for long-term safety	21
3.1.3 Optimization requirements and design criteria for constructability	23
3.2 Rock mechanical calculations and input properties used by NAGRA.....	23
3.2.1 Methods used	23
3.2.2 Input properties for numerical and analytical calculations	25
3.2.3 Findings and conclusions drawn by NAGRA.....	26
3.3 ETH assessment of design criteria selection.....	27
3.3.1 Design Criteria for long-term safety	27
3.3.2 Design criteria for constructability.....	29
3.4 ETH Assessment of methods and results.....	30
3.4.1 Experiences and empirical results.....	30
3.4.2 Effective stress calculations using FLAC 2D	31
3.4.3 Analytical and semi-analytical method.....	34
3.4.4 Total stress calculation using Phase2.....	37

3.4.5	ETH Assessment of NAGRA's Findings and Conclusions	38
4	Assessment of long-term EDZ evolution of HLW waste emplacement drifts.....	39
4.1	Lab and modelling investigations of Opalinus Clay self-sealing by NAGRA.....	40
4.1.1	Intact rock laboratory tests related to consolidation and swelling	40
4.1.2	In-situ observations and measurements related to EDZ self-sealing	41
4.1.3	Numerical simulations of long-term EDZ self-sealing	43
4.2	ETH Assessment of long-term EDZ properties	49
4.2.1	Overview of long-term evolution of HLW repository near field.....	49
4.2.2	Lab and in-situ experiments.....	49
4.2.3	Numerical Simulations.....	50
5	Conclusions.....	53
5.1	Are the rock mechanical fundamentals and scoping calculations for Opalinus Clay provided by NAGRA reproducible, complete and correct?.....	53
5.2	Are both the numerical calculations and evidences for defining the maximum depth below ground surface in NAB 14-81 in terms of the expected rock mass behavior reproducible?.....	54
5.3	Is the optimized delineation of the disposal perimeter in NTB 14-01 in terms of maximum depth below ground surface and its assessment reproducible?.....	54
5.4	Are potential effects of the longer term EDZ development after repository closure covered and assessed by NAGRA? Are these effects reproducible and plausible?	55
6	References.....	55

List of Figures

Figure 1:	a) Conceptual geomechanical framework; b) simplified model (NAGRA 2014a).....	4
Figure 2:	a) Data basis used for establishing unconsolidated undrained shear strength values for various water contents (NAGRA 2014a); b) Fitting of data for establishing the matrix strength of different rock mass types (GM1 to GM6).....	6
Figure 3:	Stress-strain curve for a typical triaxial test on Opalinus Clay (modified from NAGRA 2014a). The blue line represents the behavior of specimen P 109 (Jahns 2013). The green line represents the response of a specimen assuming linear-elastic behavior (i.e. no plastic deformation prior to peak strength) using an E-Modulus obtained from unloading/reloading, which results in a difference of 0.14% from that in the triaxial test.	10
Figure 4:	Calculated unconfined compressive strength for suggested effective strength properties of the matrix (a) and bedding (b) for Opalinus Clay shallow and deep and the various rock mass models as proposed by NAGRA (Nagra 2014a).....	14
Figure 5:	Suggested S_u values versus water content of the matrix (a) and bedding (b) for the rock mass models. The S_u values were calculated from the relations given in NAGRA 2014a.	15
Figure 6:	Stress measurements from hydraulic fracturing in the Benken and Schlattigen-1 boreholes (from Giger and Marschall 2014).	18
Figure 7:	Reference, minimum, and maximum stress scenarios with depth used in the numerical modelling by NAGRA (from Giger and Marschall 2014).	18
Figure 8:	Definition of the maximum vertical extend of the EDZ (green area, with ρ_v being the maximum plastic radius and a being the tunnel radius) and minimum vertical thickness of intact Opalinus Clay ($M_{\min, \text{intakt}}$) for sufficient radionuclide retention. From NAGRA (2014b).....	21
Figure 9:	Radionuclide pathways. Radial / vertical radionuclide pathways (red) and longitudinal migration pathways (blue). Within the sealing section the longitudinal hydraulic conductance is of key relevance (dashed blues arrows). From NAGRA (2014b).	22
Figure 10:	Simplified concept of the EDZ and homogenized hydraulic conductivity ($A_{UZ} = EDZ$). The hydraulic conductance is the product of area, A_{EDZ} , and the hydraulic conductivity, $K_{\text{eff}, EDZ}$, (from NAGRA 2014b), with ρ being the plastic radius and a the tunnel radius.	22
Figure 11:	Definition of the normalized tunnel strain (from NAGRA 2014b).....	22
Figure 12:	Examples for unfavorable or unacceptable situations for sealing sections (from NAGRA 2014b).	22
Figure 13:	Ground reaction curves for GM 3 rock mass properties and two different values for the E-Modulus. The diametrical strain increases substantially and exceeds the allowable limits of design indicator EI-2. The radius of the plastic zone, however, remains constant.	28
Figure 14:	Accumulated plastic shear strains (bedding) at the time of support installation (70% relaxation is assumed) at a depth of 800 m. The calculation is based on GM 3 properties.	29
Figure 15:	Load bearing capacity versus non-uniform load distribution P_A/P_B (Kovári and Staus 1996) for an unreinforced shotcrete, a mesh reinforced shotcrete, steel arches and systematic bolting. A circular tunnel of 6 m diameter was considered. Except for rock bolts the load bearing capacity decreases significantly for even slight non-uniform load distributions. Note that the reduction of the load bearing capacity depends on the ratio P_A/P_B and the ratio of the lining thickness / radius.	34
Figure 16:	Comparison in diametral tunnel strain assuming persistent and non-persistent joint elements in Phase2.	38
Figure 17:	Nuclear waste repository evolution with time (from Bossart 2013).	39

Figure 18:	a) Development of a large structurally controlled overbreak in the EZ-A Niche due to interaction of the excavation damage with pre-existing fault and b) influence of bedding on minor overbreak within the HG-A microtunnel with illustration of maximum convergence measurement cord orientation for excavations parallel to bedding strike (from Lanyon et al. 2014).	41
Figure 19:	Long-term changes in the EDZ bulk transmissivity due to re-saturation for 800 days and from mechanical compaction / consolidation pressures between 1 – 5 MPa (from Alcolea et al. 2014).....	42
Figure 20:	Longer term effective hydraulic conductivity changes during the HG-A experiment at Mont Terri for an equivalent radial EDZ. (from Alcolea et al. 2014)	43
Figure 21:	Relationships between packer pressure (black line), test section fluid pressure (red line) and stress in sealing section (blue line) and sealing section fluid pressure (green line) during constant rate injection tests of the HG-A experiment a) test response under high packer pressure, b) test response under lower packer pressure (from Marschall et al. 2013).	43
Figure 22:	Temporal evolution of simulated equivalent hydraulic conductivity of the EDZ and of the axial flow rate across the abstracted EDZ (from Alcolea et al. 2014).	47
Figure 23:	Profiles of effective porosity (a) and effective hydraulic conductivity (b) for all HLW simulations of the “late times” EDZ with increasing distance from the excavation boundary. The safety case analysis “average” (c) equivalent porosity and (d) conductivity values with distance from the excavation surface taken from the HLW simulations which show values equal to the matrix for a radius of 8 m and illustrations of the averaged (e) porosity and (f) conductivity for safety assessment (from Alcolea et al 2014).	48
Figure 24:	Key processes controlling EDZ short- and long-term properties.	48
Figure 25:	Three fundamental long-term mechanical effects (creep, stress relaxation, strength degradation) on the EDZ expressed in terms of strain-time and principal stress space (after Paraskevopoulou et al. 2015).	50

List of Tables

Table 1:	Effective strength properties established by NAGRA for the matrix and bedding planes for shallow and deep Opalinus Clay (NAGRA 2014a).	5
Table 2:	Suggested values for A, B and calculated S_u for a depth of 500m and 900m (NAGRA 2014a). S_u is calculated based on the expected water content, w , at the two depth (i.e. 3.6-4.3% at 900m and 3.8-5.2% at 500m; NAGRA 2014a).	6
Table 3:	Effective strength properties for the seven rock mass models (GM's) and two depth ranges (NAGRA 2014a). The numbers in brackets are for the case of using a bi-linear failure envelope.	9
Table 4:	Suggested S_u values for A and B for the Matrix (subscript M) and bedding (subscript S). λ is an intrinsic material constant (NAGRA 2014a)	9
Table 5:	Comparison of S_u values calculated from suggested effective strength properties (Opalinus Clay deep) and S_u values suggested for depths of 500 and 900m with related water content w from NAGRA (2014a).	15
Table 6:	Suggested principal stress magnitudes and ratios at reference depths used within the numerical modelling studies of NAGRA (from NAGRA 2014a).	19
Table 7:	Design Criteria ("Entwurfsindikatoren" EI) used for the assessment of geotechnical conditions and maximum depth below ground surface (from NAGRA 2014b).	24
Table 8:	Comparison between E normal to bedding and anisotropy coefficient A for different assumption of joint persistence and joint length.	37
Table 9:	Consolidation and swelling indices summarized from Giger and Marschall (2014), including lower and upper bounds where stated. *NAGRA states (based on personal communication with Favero (EPFL)) that this value should be used with caution as the tests were not designed to examine long-term creep. Note that not all of the sources cited in Giger and Marschall (2014) have been reviewed.	40
Table 10:	The time dependent aspects considered by NAGRA and the associated codes to examine long-term EDZ evolution for HLW repository modelling. Note that the behaviors are categorized based on the dominate influence in reality and not based on how it is implemented in the code (i.e. swelling is the expansion of the bentonite / rock but implemented as an applied pressure to mimic swelling pressure). The symbol '- ' indicates that this aspect was not included in the modelling presented in the reports reviewed.	44
Table 11:	Input parameters (micro-mechanical properties) reported by Geomechanica (2013) and used for sensitivity analysis to the geomechanical properties of the HLW and K09 models.	45

1 Introduction

1.1 Mandate

In 2008 the Federal Council approved the Sectorial Plan “Deep Geological Repository” (SGT), which regulates the site selection process for high and low-level nuclear waste repositories in three consecutive stages. This site selection process is based on pre-defined criteria, which are measured by so-called indicators in all stages.

In the first stage the National Cooperative for the Disposal of Radioactive Waste (NAGRA) suggested in 2008 six potential sites for low- and intermediate-level radioactive waste (SMA), and three sites for high-level radioactive waste (HLW). The aim of the current second stage, is to limit these potential sites to at least two sites per waste type for further in-depth investigations in stage three. The reduction to at least two sites per waste type is based on a comparative assessment of long-term safety and constructability. A site can only be eliminated if, compared to other sites, clear disadvantages exist.

As a result of stage two investigations, NAGRA suggested in January 2015 two potential sites which are suitable both for SMA and HLW repositories. Until the beginning of 2016 the Swiss Federal Nuclear Safety Inspectorate (ENSI) and other expert groups are reviewing the documents and conclusions submitted by NAGRA. The Chair of Engineering Geology at ETH Zurich was commissioned by ENSI to review both the evaluation and assessment of NAGRA related to the following technical indicators:

- 1) Indicator No. 1 “Depth below ground surface in terms of technical feasibility”
- 2) Indicator No. 29 “Excavation damage zone in the near-field of underground excavations”

Whereas indicator 1 is critical for site selection and optimization of the spatial repository configuration in the siting regions, indicator 29 is mainly relevant for long-term safety assessments. The expert guideline provided by ENSI lists the following key questions related to the site selection:

- I. Are the rock mechanical fundamentals and scoping calculations for Opalinus Clay provided by NAGRA reproducible, complete and correct?
- II. Are both the numerical calculations and evidences for defining the maximum depth below ground surface in NAB 14-81 in terms of the expected rock mass behavior reproducible?
- III. Is the optimized delineation of the disposal perimeter in NTB 14-01 in terms of maximum depth below ground surface and its assessment reproducible?

The construction related damage of the host rock, i.e. the formation of an excavation damage zone (including both stress and structurally controlled fracturing and overbreak) can have an impact on the long-term safety of the repository. The related key question of ENSI is:

- IV. Are potential effects of the longer term properties of the Excavation Damage Zone (EDZ) after repository closure covered and assessed by NAGRA? Are these effects reproducible and plausible?

These indicators and questions are addressed in this report. Reference is made to an important companion document (Amann and Vogelhuber 2015), which focusses on the geomechanical properties of intact Opalinus Clay.

1.2 Reports Reviewed

The following reports have been considered for this review:

Alcolea A., Kuhlmann U., Lanyon G.W., Marschall P. (2014) Hydraulic conductance of the EDZ around underground structures of a geological repository for radioactive waste – A sensitivity study for the candidate host rocks in the proposed siting regions in Northern Switzerland. NAB 13-94

- Chiffolleau, S., Robinet, J.C. (1999) HE Experiment: determination of the hydro-mechanical characteristics of the Opalinus Clay. TN 98-36
- Favero V., Ferrari A., Laloui L. (2013) Diagnostic analyses of the geomechanical data bases from the SLA-1 borehole. NAB 13-45
- Ferrari A., Favero V., Manca D., Laloui L. (2012) Geotechnical characterization of core samples from the geothermal well Schlattingen SLA-1 by LMS/EPFL. NAB 12-50
- Geomechanica Inc. (2012) The excavation of a circular tunnel in a bedded argillaceous rock (Opalinus Clay): short-term rock mass response and numerical analysis using FEM/DEM. TN 2012-06.
- Geomechanica Inc. (2013) Extent and shape of the EDZ around underground structures of a geological repository for radioactive waste – A sensitivity study for the Opalinus Clay formation in the proposed siting regions in Northern Switzerland. NAB 13-78
- Giger S., Marschall P. (2014) Geomechanical properties, rock models and in-situ stress conditions for Opalinus Clay in Northern Switzerland. NAB 14-01
- Heidbach O., Hergert T., Reiter K., Giger S.B. (2014) Stress sensitivity analysis – case study of Nördlich Lägern. NAB 13-88
- Heidbach O., Reinecker J. (2013) Analyse des rezenten Spannungsfelds der Nordschweiz. NAB 12-05:
- Jahns E. (2007) RA experiment - Rock strength of Opalinus Clay subject to time of storage. TN 2007-30
- Jahns E. (2010) RA experiment - Opalinus Clay rock characterization. TN 2008-55rev
- Jahns E. (2013) Geomechanical laboratory tests on Opalinus Clay cores from the bore hole Schlattingen SLA-1. NAB 13-18
- Lanyon G.W., Martin D., Giger S., Marschall P. (2014) Development and evolution of the Excavation Damaged Zone (EDZ) in the Opalinus Clay – A synopsis of the state of knowledge from Mont Terri. NAB 14-87
- Leupin O.X., Birgersson, M., Karnland, O., Korkeakoski, P., Sellin, P., Mäder, U., Wersin, P. (2014) Montmorillonite stability under near-field conditions. NTB 14-12
- Madritsch, H., Hammer, P. (2012) Characterization of Cenozoic brittle deformation of potential geological siting regions for radioactive waste repositories in Northern Switzerland based on structural geological analysis of field outcrops. NAB 12-41
- Mathier, J.F., Egger P., Descoedres F. (1999) Sondierbohrung Benken: Felsmechanische Untersuchungen an Bohrkernen (Teil 2). Unpubl. NAGRA Int. Bericht. NAGRA, Wettingen.
- Matter A., Peters T., Isenschmid Ch., Bläsi H.R., Ziegler H.J. (1988) Sondierbohrung Riniken – Geologie. Textband und Beilagenband. NTB 86-03
- NAGRA (2001) Sondierbohrung Benken – Untersuchungsbericht. NTB 00-01
- NAGRA (2010) Standortunabhängige Grundlagen, Anlagen und betrieb SGT Etappe 2, Orientierende felsmechanische Berechnungen für BE/HLW-Lagerstollen in 400m, 650m und 900m im intakten und gestörten Opalinuston. NAB 10-41
- NAGRA (2014a) SGT Etappe 2, Vorschlag weiter zu untersuchender geologischer Standortgebiete mit zugehörigen Standortarealen für die Oberflächenanlage - Geologische Grundlagen - Geomechanische Unterlagen. NTB 14-02, Dossier IV

NAGRA (2014b) Unterlagen zur Anlagenauslegung in Bezug auf maximale Tiefenlage und Platzbedarf. Grundlagen für die Abgrenzung und Bewertung der Lagerperimeter. NAB 14-81

Olalla C., Martin M.E., Saez J. (1999) ED-B experiment – Geotechnical laboratory tests on Opalinus Clay rock samples. TN 98-57

Popp T., Salzer K. (2006) HE-D experiment (influence of bedding planes) - Triaxial deformation tests in a multi-anvil apparatus with ultrasonic monitoring, sampling and rock preparation, adaptation of laboratory techniques. TN 2005-34

Rummel F., Hettkamp T., Weber U. (1999) DM experiment - Laboratory experiments for the determination of deformation mechanisms and a constitutive law for time dependent deformation behavior of the Opalinus Clay. TN 99-35

Rummel F., Weber U. (1999) Sondierbohrung Benken - Felsmechanische Untersuchungen an Bohrkernen. NIB 99-38a

Rummel F., Weber U. (2004) RA experiment - Rock mechanical testing and characterization on drillcores of boreholes BRA-1 and BRA-2. TN 2004-38

Schnier H., Stührenberg D. (2007) LT experiment - Strength tests on cylindrical specimens, documentation and evaluation (Phases 8 & 9). TR 2003-04

Vöggtli, B., Bossart, P. (1998) DT Experiment, swelling experiment on Opalinus Clay drillcores. TN 97-06

2 Fundamental rock mechanical properties and conditions

2.1 Strength and Stiffness of Opalinus Clay

Conceptual geomechanical model and approach

Based on laboratory experiments, borehole logging data and comparisons with other clay rocks NAGRA provides a description of fundamental constitutive aspects of Opalinus Clay (NAGRA 2014a; Giger and Marschall 2014) that includes:

- Effective stress dependency of porosity, water content, density, hydraulic conductivity and elastic properties
- Primary and secondary consolidation, including stress dependent compression index, swelling index and secondary compression index
- Irreversible compression in loading-unloading-cycles (for consolidations pressure beyond an apparent over-consolidation pressure)
- Swelling pressure and heave as a consequence of water uptake
- Transversely isotropic elastic behavior
- Dilatant failure behavior
- Anisotropic compressive and tensile strength
- Strong post-failure stress drop
- Strong dependency of strength and stiffness on capillary forces.

These behavioral aspects lead to a conceptual geomechanical framework for Opalinus Clay that follows basic principles of critical state soil mechanics (Figure 1a. NAGRA 2014a, Giger & Marschall 2014). This model shows how the elastic limits, expressed by the Hvorslev yield surface, the tension cut-off and the Roscoe yield surface, are varying with changes in differential stress (q), effective mean stress (p') and void ratio.

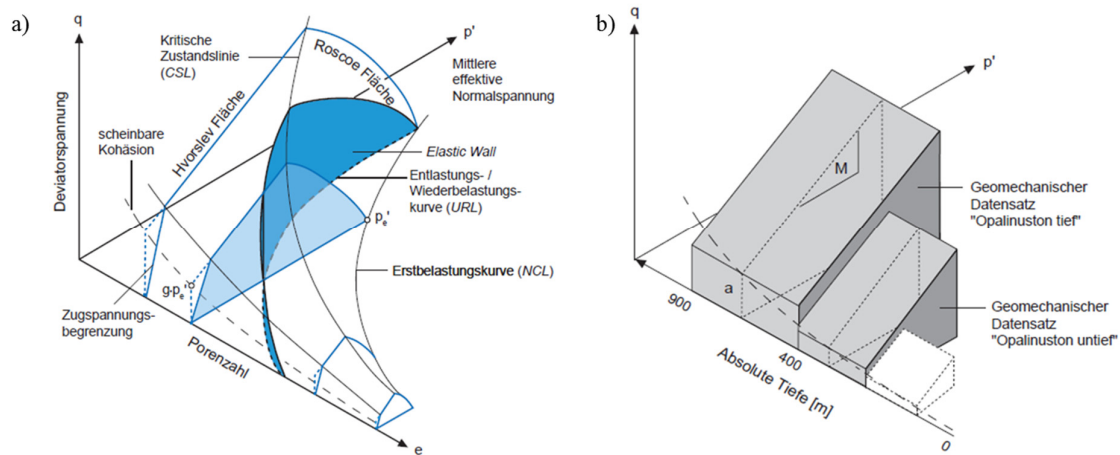


Figure 1: a) Conceptual geomechanical framework; b) simplified model (NAGRA 2014a)

NAGRA states that their analytical and numerical methods for calculating the hydro-mechanical coupled response of Opalinus Clay do not offer constitutive relations that account for all of the above described behavioral aspects. This is in particular true for the stress dependent elastic and strength properties which tend to increase with increasing effective pressure or decreasing porosity (i.e. increasing compaction). In addition, the Roscoe yield surface (Figure 1a) was assessed irrelevant by NAGRA for the engineering feasibility assessment. Owing the latter aspects (i.e. behavioral aspects which were assessed irrelevant for engineering design) of the conceptual geomechanical model, and to overcome limitations in the analytical and numerical methods, a simplified model was established (Figure 1b). This model accounts for the relevant elastic limits (i.e. tension cut-off and shear failure envelope). Since both, the stiffness and strength of Opalinus Clay tend to increase with increasing depth, parameter sets have been established which are either representative for Opalinus Clay at a depth up to 400m (called “shallow”) and a depth range between 400 and 900m (called “deep”) below ground surface.

2.1.1 Effective strength of the intact rock – NAGRA’s approach and assessment

Effective strength properties for the two depth levels have been derived from laboratory test results (uniaxial and triaxial compression tests). Four different samples geometries were utilized: P-samples, where the load axis is parallel to the bedding planes, S-samples, where the load axis is normal to the bedding planes, Z-samples, where the bedding planes are 45° inclined with respect to the load axis, and X-samples, where the bedding planes are 30° inclined with respect to the load axis. P- and S-samples were used to establish the strength properties of the intact matrix, and Z- and X-samples for the bedding planes.

A large series of tests was used, and the quality of the test results were assessed, classified and weighted by NAGRA based on the test protocols and completeness of key parameters being monitored during testing (Giger & Marschall 2014). Four quality classes (A to D) were distinguished. The best assigned quality (B) was attributed to test series, in which the pore pressure was controlled (i.e. measured) during testing and small strain rates were utilized (i.e. $1.0E-6$ to $1.0E-1$ 1/s). In the test series attributed with quality D no pore pressure control (i.e. measurement) was used and the utilized strain rate was fast (i.e. $1.0E-5$ 1/s). The weighing factors for the individual quality classes range linearly between 100% for quality A and 25% for quality D. Usually, the same quality class was assigned to the entire triaxial test series. Only for the triaxial test series carried out by Jahns (2013) the quality classes suggested by Favero et al. (2013) for each individual triaxial test results were utilized by NAGRA.

The weighted data points were further used to establish the effective friction angle and the effective cohesion of Opalinus Clay (i.e. matrix and bedding) at the two depth ranges by a linear-regression

analysis through all data points in q-p' space. For a depth up to 400m, data obtained from specimens at the Mont Terri Underground Research Laboratory (URL) was utilized (Jahns 2010, Jahns 2007, Schnier & Stührenberg 2007, Popp & Salzer 2006, Rummel & Weber 2004, Rummel et al. 1999, Olalla et al. 1999). For a depth range between 400 and 900m, data from the boreholes in Benken and Schlattingen was utilized (Jahns 2013, Rummel & Weber 1999). The regression analysis accounts for the individual weighting factors of the different quality classes. According to Giger & Marschall (2014) some uniaxial compression tests were considered in addition to the above mentioned triaxial compression tests to complement the data set in the low stress range. NAGRA's suggested effective strength properties for shallow and deep intact Opalinus Clay are summarized in Table 1 for the matrix and bedding planes.

Table 1: Effective strength properties established by NAGRA for the matrix and bedding planes for shallow and deep Opalinus Clay (NAGRA 2014a).

	Matrix		Bedding	
	ϕ' (°)	c' (MPa)	ϕ' (°)	c' (MPa)
shallow	29	3.1	19	1.7
deep	33	7.1	24	3.9

2.1.2 Undrained shear strength of the intact rock – NAGRA's approach and assessment

Because of the uncertainties stemming from the predominantly conducted consolidated undrained tests (e.g. representativeness of measured pore pressures during consolidation and shearing, NAGRA 2014a) an alternative interpretation based on total stresses (as opposed to effective stresses) was performed assuming unconsolidated undrained testing conditions. A large series of triaxial compression test results¹ including artificially dried and wetted specimens (Rummel & Weber 1999, Rummel et al. 1999), test results from Mont Terri URL, Benken and Schlattingen (Jahns 2013, Jahns 2010, Rummel & Weber 2004, Rummel & Weber 1999, Rummel et al. 1999, Olalla et al. 1999) were analyzed to establish the undrained shear strength of both matrix and bedding planes (Figure 2a). The undrained shear strength S_u was defined as (NAGRA 2014a):

$$S_u = \frac{\sigma_{1f} - \sigma_{3f}}{2}$$

where σ_{1f} and σ_{3f} are the maximum and minimum principal total stresses at failure. The water content after testing of each specimen was utilized to establish a relationship between the water content w and the undrained shear strength S_u (Figure 2b).

The increase in undrained shear strength with decrease in water content was used as a basis to estimate undrained shear strength values for water content values representative of the actual depth at the potential repository sites. For the derivation of the undrained shear strength of the intact material a regression analysis using peak strength values was conducted for both matrix and bedding. A linear relation in the logarithmic diagram was assumed, which allowed to establish the following equation (NAGRA 2014a):

$$S_u = A \exp(-Bw)$$

where A is the magnitude of S_u for $w = 0$ (intersection of the regression line with the y-axis) and B is the slope of the regression line². The suggested values for A and B for deriving the undrained shear strength of the intact material (for both matrix and bedding planes) are given in Table 2.

¹ Results from uniaxial compressive strength tests were not included due to suction effects (NAGRA 2014a).

² Note that for defining undrained shear strength values for rock mass models GM 2 to GM 6 the slope B was considered constant. These rock mass types are explained in section 2.1.3.

Table 2: Suggested values for A, B and calculated S_u for a depth of 500m and 900m (NAGRA 2014a). S_u is calculated based on the expected water content, w , at the two depth (i.e. 3.6-4.3% at 900m and 3.8-5.2% at 500m; NAGRA 2014a).

	A	B	S_u , 500m (MPa)	S_u , 900m (MPa)
Matrix	61.5	23.5	18.1-25.2	21.4-26.4
Bedding	42.4	28.9	9.4-14.1	11.5-15.0

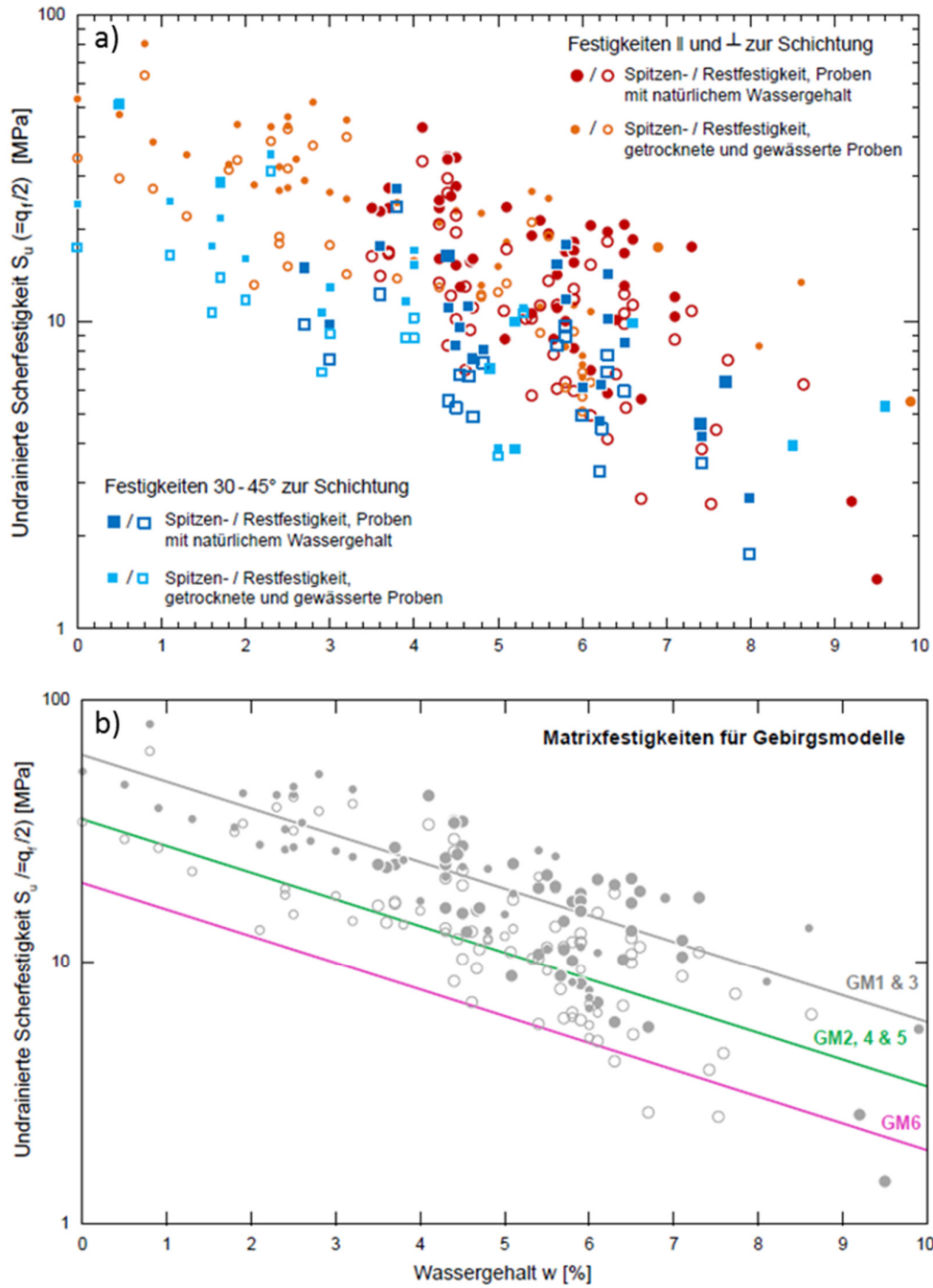


Figure 2: a) Data basis used for establishing unconsolidated undrained shear strength values for various water contents (NAGRA 2014a); b) Fitting of data for establishing the matrix strength of different rock mass types (GM1 to GM6).

2.1.3 Elastic properties– NAGRA’s approach and assessment

The elastic properties (drained and undrained) were determined based on results of uniaxial and triaxial compression tests, oedometer tests and permeameter tests (Giger & Marschall 2014). Therefore, the test results from Mont Terri URL, Benken and Schlattingen were compiled to constrain the elastic properties representative for Opalinus Clay at a depth range $\leq 400\text{m}$ (shallow) and 400 to 900m (deep). Concerning the uniaxial and triaxial compression tests, the E-Modulus was either determined as tangent modulus at 50% of the maximum differential stress (i.e. from the primary loading curve), or as secant modulus from unloading/reloading cycles at approximately 30-70% of the maximum differential stress. The E-Modulus from oedometer tests was determined indirectly from the oedometer modulus assuming a linear elastic material behavior.

For constraining the undrained E-Modulus of Opalinus Clay shallow, results from triaxial compression tests compiled by Bock (2009) between 2000 and 2009 were used. Results from S- and P-samples within a particular stress interval were averaged. Drained E-values for Opalinus Clay shallow were taken by NAGRA from oedometer tests on S-samples of three test series (Peron et al. 2009, Horseman et al. 2006 and Chiffolleau & Robinet 1999). For constraining the undrained E-Modulus of Opalinus Clay deep, results of uniaxial and triaxial compression tests from Jahns (2013), Rummel & Weber (1999), Mathier et al. (1999) and Klee & Rummel (2000) were used. Drained E values for Opalinus Clay deep were taken by NAGRA from the two test series by Ferrari et al. (2012; oedometer tests on S-samples) and Horseman & Harrington (2000; long-term permeameter test on a S-sample).

According to Giger & Marschall (2014) the test results suggest that 1) the ratio between the undrained E-Moduli (E_u) of P-samples and those of S-samples derived in both cases from triaxial tests is in the range of 2:1, 2) the undrained E-Moduli for unloading/reloading cycles increase with increasing effective confining stress, 3) the undrained E-Moduli obtained from the primary loading curve at 50% of the peak strength are lower compared to the values for unloading/reloading cycles and they do not show a clear dependency on the effective confining stress, and 4) the drained E-Moduli (E) for unloading/reloading cycles obtained from oedometer tests also increase with increasing effective confining stress. The absolute values are approximately 50% of the undrained E-Moduli obtained from unloading/reloading cycles during triaxial tests.

The results of the undrained Poisson’s ratios (ν_u) obtained from triaxial tests are considered unreliable (Giger & Marschall 2014) because in many cases the results strongly differ from the theoretically derived value of $\nu_u = 0.50$ which is expected for a linear elastic and isotropic material behavior under undrained conditions. Since only undrained triaxial tests and no drained triaxial tests exist, the drained Poisson’s ratios (ν) were estimated from the results of uniaxial compression tests.

The drained E-Modulus (based on oedometer tests on S-specimens) suggested by NAGRA (2014a) is $E = 2 \text{ GPa}$ for Opalinus Clay shallow and $E = 4 \text{ GPa}$ for Opalinus Clay deep. The undrained E-Modulus (based on uniaxial and triaxial compression tests on S- and P-specimens) suggested by NAGRA (2014a) is $E_u = 4/8 \text{ GPa}$ (normal/parallel to bedding) for Opalinus Clay shallow and $E_u = 9/18 \text{ GPa}$ (normal/parallel to bedding) for Opalinus Clay deep. The related values of the drained Poisson’s ratio are $\nu = 0.25$ or 0.35 for Opalinus Clay shallow and $\nu = 0.27$ or 0.27 for Opalinus Clay deep (NAGRA 2014a).

2.1.4 Strength and Stiffness of the rock mass – NAGRA’s approach and assessment

Scale effects stemming from heterogeneities due to sedimentation and tectonic structures are expected to alter the strength and stiffness of the Opalinus Clay at the tunnel scale. Heterogeneities associated with sedimentary structures are considered less important than tectonic structures since they are captured in laboratory experiments (NAGRA 2014a). The tectonic overprint in the different siting regions is difficult to predict and therefore conceptual rock mass models (“Gebirgsmodelle GM”) have been established by Giger and Marschall (2014). These GM’s are based on different structural

conditions which likely occur in the siting regions and are related to strength reductions of the matrix, the bedding or both matrix and bedding.

The structural analysis performed by NAGRA includes surface outcrop mapping, analysis of cores taken from the boreholes Gösgen, Oftringen, Riniken, Schaffisheim, Weiach and Schlattigen-1, structural interpretation of the new 2D-seismic survey, kinematic analysis of geological cross sections, and structural analysis in the Mont Terri Underground Research laboratory. The key findings of NAGRA are:

- 1) Rock mass degradation increases towards fault cores
- 2) Tectonically disturbed rocks were only locally observed in cores from boreholes at the potential siting areas. Large sections of the Opalinus Clay do not contain tectonic structures. The latter holds true for the boreholes Benken and Weiach, which are located in the Tafeljura and Vorfaltenzone.
- 3) Within the lower 20-30m of the boreholes Riniken (Vorfaltenzone) and Schaffisheim (Subjurassische Zone) larger disintegrated sections of Opalinus Clay have been found and interpreted as bedding parallel tectonic shear zones.
- 4) Disking-type structures occur occasionally and have been interpreted to be associated with weakness planes (i.e. they correlate with clay content). These types of structures may have frequencies of 10-20 m⁻¹.
- 5) According to NAGRA the structural analysis of cores is consistent with the general assumption of the tectonic overprint in the Northern Switzerland. The deformation increases from the Tafeljura in the East (Benken) towards the Vorfaltenzone (Weiach and Riniken) and the Subjurassische Zone (Schaffisheim) in the West.

According to these findings and the recommendations given in SIA 199, discontinuities were classified as effective discontinuities (i.e. complete loss of coherence) and potential discontinuities (i.e. weakness zones). In a further step NAGRA established seven rock mass models, i.e. GM's, which account for various scenarios of structural weaknesses, and are represented by homogenized continua with smeared discontinuity properties. Strength degradation of the homogenized continua may be associated with a degradation in the matrix strength, bedding strength or both. The GM's represent typical borehole sections and have been established as follows (Giger and Marschall 2014):

GM1: Represents the bulk intervals of the boreholes Benken and Weiach. The peak strength of both matrix and bedding strength were obtained from laboratory tests on intact rock (i.e. peak strength of the matrix and bedding).

GM2: Represents borehole intervals with isolated discontinuities of moderate to steep inclination. The strength of the matrix is reduced due to potential discontinuities (i.e., properties were taken from the lower limits of laboratory tests on intact rock; i.e. lower limit of the 95% confidence interval)

GM 3: Represents borehole intervals with isolated bedding-parallel discontinuities. The peak strength was considered equal to the intact rock strength (i.e., GM1 matrix strength) and the bedding strength was reduced by approximately two standard deviations (i.e. lower limit of the 95% confidence interval; standard deviation from laboratory tests results on specimens with a bedding orientation inclined by 30-45 degrees with respect to the loading axis (X- and Z-samples)).

GM4: Represents zones in the vicinity of major slip surfaces (i.e., fault cores) containing discontinuities of various orientations. Both, the matrix and bedding strengths were reduced by approximately two standard deviations (i.e. lower limits of the 95% confidence intervals)

GM5 and GM6: Represents tectonized zones at the base of Opalinus Clay in boreholes Schaffisheim and Riniken. For GM5 the matrix strength was reduced by approximately two standard deviations. The bedding strength was considered to be the post-peak strength obtained from laboratory tests on X- and

Z-samples. For GM6 the residual strengths of both matrix and bedding obtained from laboratory tests was assumed.

GM7: Represents fault core material. Further reduction of the strength without considering a strength anisotropy.

For the siting regions, GM1, 2, 3, 4 are considered representative (NAGRA 2014b) and are used in the comparative engineering feasibility analysis (i.e. numerical and analytical calculations).

2.1.4.1 Effective rock mass strength

Following the above approach NAGRA suggested effective strength properties for the seven rock mass models, which are summarized in Table 3.

2.1.4.2 Unconsolidated undrained shear strength of the rock mass

A similar approach was used to establish undrained shear strength properties for six rock mass models (for the general approach see section 1.1.1.1 and Figure 2b). A linear regression analysis through peak S_u data of the matrix and bedding was used to constrain GM1 (see also section 1.1.1.1). The slope of the regression analysis B was considered constant (Figure 2b). The lower 95% confidence interval was further used to establish y-axis intercepts (i.e., the A -value) for reduced peak strength fits (GM1, 4, 5 for the matrix and GM 3 and 4 for bedding). Post-peak intercepts with the y-axis were constrained by regression analysis through the lower boundary of experimental data (GM6 for matrix and GM5 and 6 for bedding). Following this procedure the values (Table 4) for A and B were suggested by NAGRA.

Table 3: Effective strength properties for the seven rock mass models (GM's) and two depth ranges (NAGRA 2014a). The numbers in brackets are for the case of using a bi-linear failure envelope.

Gebirgsmodell	Opalinuston untief (< 400 m)				Opalinuston tief (400 – 900 m)			
	Matrix		Schichtung		Matrix		Schichtung	
	C' [MPa]	φ' [°]	C' [MPa]	φ' [°]	C' [MPa]	φ' [°]	C' [MPa]	φ' [°]
GM1	3.1	29	1.7	19	7.1 (14.5)	33 (18)	3.9 (7.5)	24 (17)
GM2	2.6	28	1.7	19	6.0 (13.4)	32 (17)	3.9 (7.5)	24 (17)
GM3	3.1	29	1.3	18	7.1 (14.5)	33 (18)	2.9 (5.8)	21 (18)
GM4	2.6	28	1.3	18	6.0 (13.4)	32 (17)	2.9 (5.8)	21 (18)
GM5	2.6	28	1.0	17	6.0 (13.4)	32 (17)	2.3 (2.3)	20 (20)
GM6	2.3	22	1.0	17	5.2 (5.2)	22 (22)	2.3 (2.3)	20 (20)
GM7	0.3	17	0.3	17	0.5 (0.5)	17 (17)	0.5 (0.5)	17 (17)

Table 4: Suggested S_u values for A and B for the Matrix (subscript M) and bedding (subscript S). λ is an intrinsic material constant (NAGRA 2014a)

Gebirgsmodell	Materialparameter für die Ableitung von undrainierten Scherfestigkeiten S_u *					
	Festigkeit der Matrix			Festigkeit der Schichtung		
	A_M [MPa]	B_M [-]	λ_M [-]	A_S [MPa]	B_S [-]	λ_S [-]
GM1	61.5	23.5	0.12	42.4	28.9	0.09
GM2	35.0	23.5	0.12	42.4	28.9	0.09
GM3	61.5	23.5	0.12	30.0	28.9	0.09
GM4	35.0	23.5	0.12	30.0	28.9	0.09
GM5	35.0	23.5	0.12	18.0	28.9	0.09
GM6	20.0	23.5	0.12	18.0	28.9	0.09

2.1.4.3 Elastic rock mass properties

The influence of structural variations was considered for the rock mass strength and not the rock mass stiffness (i.e. no reduction of rock mass stiffness due to discontinuities) with the following justifications:

- 1) Re-loading cycles in the post failure region of triaxial tests suggest a reduction of the E -modulus of 20%
- 2) The suggested undrained E -modulus is based on E -moduli taken from samples loaded normal to bedding (i.e. the E -Modulus of specimens loaded parallel to bedding is typically higher) and considered conservative by NAGRA (i.e. the difference in E -moduli between post- and pre-peak is smaller than the difference between E -moduli from P- and S-specimens).
- 3) Dilatometer tests in Mont Terri and Benken suggest that the E -modulus parallel to bedding is consistent with the E -Modulus obtained from laboratory tests.
- 4) The influence of large stiffness anisotropies is covered by numerical analysis (Lanyon et al. 2014)

2.1.5 ETH assessment of intact rock properties

2.1.5.1 Simplified geomechanical model

The constitutive framework and the behavioral aspects described by NAGRA, in particular the effective stress dependent strength and stiffness of the tested rock, are in agreement with many other studies on clay shales (e.g. Aristorenas 1992) and are well described and documented in the literature. Laboratory studies conducted for NAGRA (e.g. Ferrari et al. 2012; data of Jahns 2013 reported in Favero et al. 2013) support the conceptual framework. The introduced simplified elastic-plastic model (i.e. with the Mohr-Coulomb failure envelope corresponding to the Hvorslev yield surface for different depth ranges; with a tension cut-off; without a Roscoe yield surface) might be reasonable for engineering feasibility studies. The simplifications, in particular the modification of the tension cut-off and the omission of the Roscoe yield surface, have some consequences, which need to be considered.

The stress-strain curves of Opalinus Clay obtained from triaxial tests suggest a highly non-linear stress-strain behavior in the pre-failure region. The non-linearity is most probably related to plastic deformations that occur far before reaching the peak strength. Ignoring the Roscoe yield surface this non-linearity is not explicitly included in the simplified model and the elastic properties for loading and reloading are exactly the same (i.e. the E -Modulus obtained from first loading at 50% of the peak strength is exactly the same as the E -Modulus obtained from unloading/reloading cycles). Figure 3 shows a typical stress-strain curve from a triaxial test on an Opalinus Clay specimen (NAGRA 2014a).

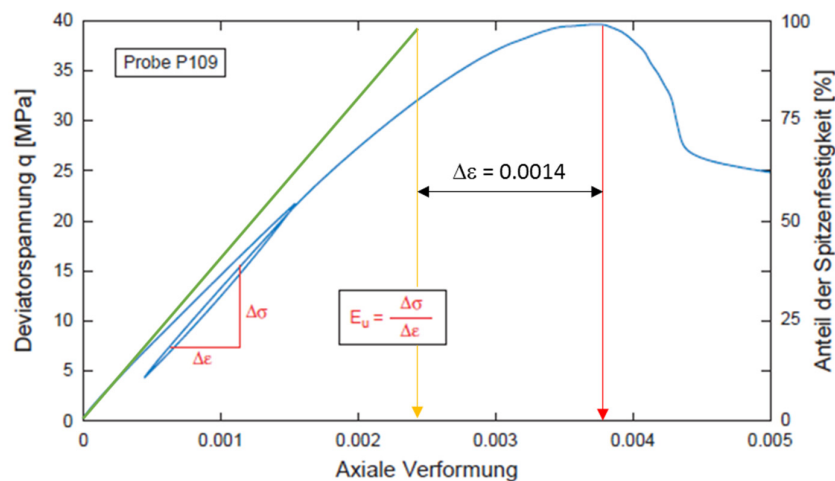


Figure 3: Stress-strain curve for a typical triaxial test on Opalinus Clay (modified from NAGRA 2014a). The blue line represents the behavior of specimen P 109 (Jahns 2013). The green line represents the response of a specimen assuming linear-elastic behavior (i.e. no plastic deformation prior to peak strength) using an E -Modulus obtained from unloading/reloading, which results in a difference of 0.14% from that in the triaxial test.

The blue line represents the behavior of specimen P 109 (Jahns 2013). The green line represents the response of a specimen assuming linear-elastic behavior (i.e. no plastic deformation in the pre-peak region) using an E-Modulus obtained from an unloading/reloading cycle. The axial strain at failure in the model (at 0.24%) differs by 0.14% from that in the actual triaxial test (at 0.38%). This means that the value in the model corresponds to only 64% of the value in the actual triaxial test. Thus, the simplification may lead to a relevant underestimation of the pre-peak deformation and therefore to a relevant overestimation of the stiffness of Opalinus Clay which needs to be considered in numerical and analytical engineering design calculations.

The definition of effective strength properties and E-Moduli by NAGRA for the two different depth ranges is in general agreement with the constitutive framework and was introduced by NAGRA to overcome limitations in the utilized numerical and analytical calculation tools. Two depth ranges were introduced: a depth range up to 400m (Opalinus Clay shallow) and a depth range between 400 and 900m (Opalinus Clay deep). The depth range from 400 – 900m covers the relevant depth at the siting regions. For this depth range, a single set of effective strength properties (i.e. effective friction and effective cohesion) and a single E-Modulus were assigned. Thus, the effective strength properties and E-Modulus do not change within the relevant depth range, which may have relevant consequences on the assessment of the maximum depth below ground surface as discussed in the following sections

The simplified model is reasonable for engineering feasibility studies, providing that the consequences of omitting the Roscoe yield surface are considered for the choice of the elastic properties and the dependency of the effective strength properties and E-Modulus with increasing depth (effective confining stress) is considered for Opalinus Clay deep. For quantitative engineering design calculations more advanced constitutive models are required.

2.1.5.2 Effective strength of the intact rock

Amann and Vogelhuber (2015) assessed the data basis (i.e. triaxial test results) used by NAGRA to establish effective strength properties for the depth range < 400m and between 400 and 900m. The analysis shows that the majority of the results were obtained from specimens which were not saturated prior to loading, or saturation could not be demonstrated.

Only 8 specimens representative for the depth range 400-900m were most probably saturated prior to loading, but 6 of them were likely loaded too fast in order to provide a reliable basis for effective strength analysis, i.e. only 2 specimens may be considered appropriate for effective strength analysis. For Opalinus Clay shallow none of the triaxial tests considered by NAGRA fulfill the requirements of a reliable triaxial test (Amann and Vogelhuber 2015). The current data basis for defining reliable effective strength properties is too small, and the weighting of data points based on the quality assessment used in Giger and Marschall (2014) is not reproducible (Amann and Vogelhuber 2015). Based on qualitative considerations, Amann and Vogelhuber (2015) show that the suggested effective strength properties tend to overestimate the actual strength. This overestimation is associated with the unsaturated state of the majority of specimens (i.e. capillary forces) and, in case of the bedding plane strength, with the sample geometry. The degree of overestimation cannot be quantified. Results from triaxial tests using Z-samples (i.e. bedding planes are 45° inclined with respect to the load axis) overestimate the bedding plane strength. In this case the degree of overestimation can be quantified.

As discussed in the previous section, the depth range that is considered for defining effective strength properties for Opalinus Clay deep is 400 – 900m. According to NAGRA's constitutive framework, the effective strength tends to increase with an increase in depth. The limited amount of reliable triaxial test results does not allow to quantify the increase of effective strength with increasing depth. The two valid triaxial data are representative for a depth of approximately 900m and it remains unclear if these triaxial test results can be used to characterize the strength in the entire depth range for Opalinus Clay deep.

2.1.5.3 Undrained shear strength

The data basis used to establish the unconsolidated undrained shear strength S_u is largely not appropriate. As shown by Amann and Vogelhuber (2015), the majority of specimens were not saturated and the resulting S_u values overestimate the actual S_u due to capillary forces (suction). A consistency test revealed that the suggested S_u values for the intact matrix and bedding planes are between 1.2 – 2.0 times larger than the S_u values calculated by Amann and Vogelhuber (2015) from the related effective friction angles and effective cohesions suggested by NAGRA. For the calculation, Amann & Vogelhuber (2015) assumed zero volumetric strain and a linear-elastic, isotropic material behavior (i.e. the same assumption as for the effective stress calculations utilizing FLAC2D). Valid consolidated undrained (CU) triaxial test results from Jahns (2013), Aristorenas (1992) and Wild et al. (2015) were used by Amann and Vogelhuber (2015) to develop a relationship between S_u values obtained from P- and S-specimens and the effective stress. A linear increase of S_u with increasing effective confining stress was assumed. This analysis shows that the S_u values suggested by NAGRA are significantly larger than the S_u values obtained from valid triaxial tests. Owing the inappropriate data base and the above described inconsistencies, the suggested S_u values, as proposed by the NAGRA, overestimate (partly significantly) the actual undrained shear strength of the intact matrix and the bedding planes.

2.1.5.4 Elastic properties

Amann and Vogelhuber (2015) found that for the majority of the triaxial tests the specimens were not saturated or saturation could not be demonstrated. For the case of Opalinus Clay deep only 8 CU tests reported by Jahns (2013) were probably conducted on saturated specimens with completeness of the consolidation phase. Therefore, the corresponding triaxial test results (2 S-samples, 2 P-samples and 4 X-samples) can be used to define reliable values for the undrained E-Modulus. According to Giger & Marschall (2014) the suggested values for analytical or numerical analyses are $E_u = 9/18$ GPa (normal/parallel to bedding) and were derived from unloading/reloading cycles on S- and P-samples. For the 2 saturated S-samples (specimens 03 and 05) values of $E_u = 8.8$ and 8.9 GPa representative for an effective confining stress of 13.0 MPa in both cases were identified by Jahns (2013). For the 2 saturated P-samples (samples P109 and P115) values of $E_u = 15.4$ and 13.8 GPa with an effective confining stress of 7.6 and 4.6 MPa respectively were identified by Jahns (2013). Therefore, the values suggested by NAGRA are in reasonable agreement with laboratory results for both S- and P-samples when considering that the undrained E-Modulus for unloading/reloading cycles increases with increasing effective confining stress. For the case of Opalinus Clay shallow none of the triaxial test results analyzed by NAGRA allows to define reliable values for the undrained E-Modulus since probably none of the specimens was fully saturated.

The drained E-Modulus was derived from oedometer tests and a long-term permeameter test (NAGRA 2014a, only S-samples). According to Giger & Marschall (2014) the suggested values for analytical or numerical analyses are $E = 2$ GPa for Opalinus Clay shallow and $E = 4$ GPa for Opalinus Clay deep irrespective of the orientation of the load axis (normal/parallel to bedding). For Opalinus Clay shallow, the relevant effective confining stress is in the range of $\sigma'_3 = 1.0$ to 6.0 MPa. The data basis from the Mont Terri URL shown in Giger & Marschall (2014) suggests that for the relevant effective confining stress range a drained E-Modulus of $E = 0.2$ to 2.3 GPa was determined. A value of 2 GPa for Opalinus Clay shallow, as suggested by NAGRA, is on the upper limit of the experimental data. For Opalinus Clay deep, the relevant effective confining stress is in the range of $\sigma'_3 = 6.0$ to 14.0 MPa. The data basis from the Mont Terri URL shown in Giger & Marschall (2014) suggests a drained E-Modulus of $E = 0.7$ to 5.2 GPa for the relevant effective confining stress range. However, the oedometer tests on samples from the borehole Schlattigen by Ferrari et al. (2012) and the permeameter test on a sample from the borehole Benken by Horseman & Harrington (2000) are considered to be more relevant for the case of Opalinus Clay deep. These data suggest a drained E-Modulus obtained for unloading/reloading cycles which is strongly dependent on the effective confining stress and increases from $E = 2.4$ GPa for approximately $\sigma'_3 = 6.0$ MPa to $E = 8.0$ GPa for approximately $\sigma'_3 = 14.0$ MPa

(with evaluation of the oedometer tests according to Favero et al. 2013). The value suggested by NAGRA, for the drained E-Modulus for Opalinus Clay deep ($E = 4$ GPa) is within the range of experimental data. However, for the depth range between 500 and 900m (Opalinus Clay deep) the data suggest a major increase of the E-Modulus with increasing effective confinement (i.e. from 2.4 GPa to 8 GPa). This may have a relevant effect on numerical and analytical calculations which address the maximum depth below ground surface.

As shown in the previous sections, for the majority of the triaxial tests the specimens were not saturated or saturation could not be demonstrated. For the case of Opalinus Clay deep only 8 CU tests reported by Jahns (2013) were probably conducted on saturated specimens with completeness of the consolidation phase. Therefore, the corresponding triaxial test results (2 S-samples, 2 P-samples and 4 X-samples) can be used to define reliable values for the undrained E-Modulus. According to Giger & Marschall (2014) the suggested values for analytical or numerical analyses are $E_u = 9/18$ GPa (normal/parallel to bedding) and were derived from unloading/reloading cycles on S- and P-samples. For the 2 saturated S-samples (specimens 03 and 05) values of $E_u = 8.8$ and 8.9 GPa representative for an effective confining stress of 13.0 MPa in both cases were identified by Jahns (2013). For the 2 saturated P-samples (samples P109 and P115) values of $E_u = 15.4$ and 13.8 GPa with an effective confining stress of 7.6 and 4.6 MPa respectively were identified by Jahns (2013). Therefore, the values suggested by NAGRA are in reasonable agreement with laboratory results for both S- and P-samples when considering that the undrained E-Modulus for unloading/reloading cycles increases with increasing effective confining stress. For the case of Opalinus Clay shallow none of the triaxial test results analyzed by NAGRA allows to define reliable values for the undrained E-Modulus since probably none of the specimens was fully saturated.

The drained E-Modulus was derived from oedometer tests and a long-term permeameter test (NAGRA 2014a, only S-samples). According to Giger & Marschall (2014) the suggested values for analytical or numerical analyses are $E = 2$ GPa for Opalinus Clay shallow and $E = 4$ GPa for Opalinus Clay deep irrespective of the orientation of the load axis (normal/parallel to bedding). For Opalinus Clay shallow, the relevant effective confining stress is in the range of $\sigma'_3 = 1.0$ to 6.0 MPa. The data basis from the Mont Terri URL shown in Giger & Marschall (2014) suggests that for the relevant effective confining stress range a drained E-Modulus of $E = 0.2$ to 2.3 GPa was determined. A value of 2 GPa for Opalinus Clay shallow, as suggested by NAGRA, is on the upper limit of the experimental data. For Opalinus Clay deep, the relevant effective confining stress is in the range of $\sigma'_3 = 6.0$ to 14.0 MPa. The data basis from the Mont Terri URL shown in Giger & Marschall (2014) suggests a drained E-Modulus of $E = 0.7$ to 5.2 GPa for the relevant effective confining stress range. However, the oedometer tests on samples from the borehole Schlattingen by Ferrari et al. (2012) and the permeameter test on a sample from the borehole Benken by Horseman & Harrington (2000) are considered to be more relevant for the case of Opalinus Clay deep. These data suggest a drained E-Modulus obtained for unloading/reloading cycles which is strongly dependent on the effective confining stress and increases from $E = 2.4$ GPa for approximately $\sigma'_3 = 6.0$ MPa to $E = 8.0$ GPa for approximately $\sigma'_3 = 14.0$ MPa (with evaluation of the oedometer tests according to Favero et al. 2013). The value suggested by NAGRA, for the drained E-Modulus for Opalinus Clay deep ($E = 4$ GPa) is within the range of experimental data. However, for the depth range between 500 and 900m (Opalinus Clay deep) the data suggest a major increase of the E-Modulus with increasing effective confinement (i.e. from 2.4 GPa to 8 GPa). This may have a relevant effect on numerical and analytical calculations which address the maximum depth below ground surface.

As discussed in section 2.1.5.1 the simplification introduced by NAGRA for the geomechanical behavior ignores plastic deformations in the pre-failure region. As a consequence, numerical calculations based on a linear-elastic model with elastic properties obtained from unloading/reloading may underestimate the strain at failure. This was not considered by NAGRA for the recommended values for numerical and analytical models.

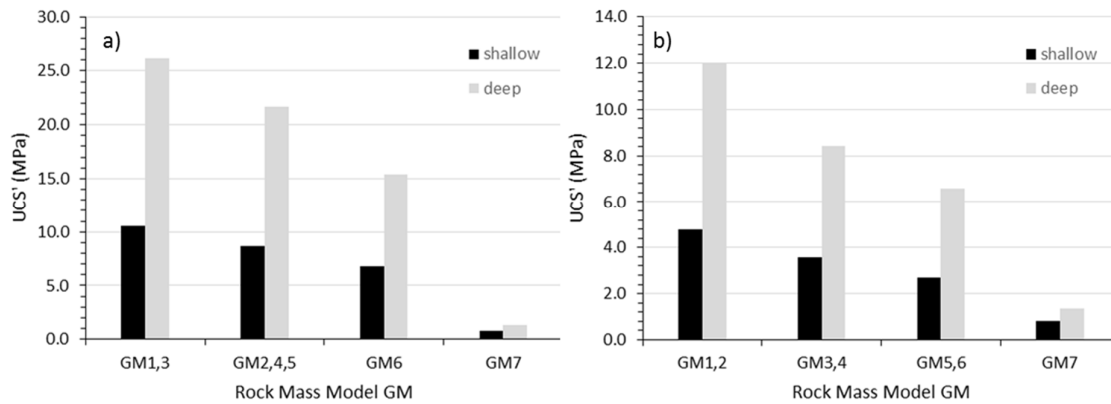


Figure 4: Calculated unconfined compressive strength for suggested effective strength properties of the matrix (a) and bedding (b) for Opalinus Clay shallow and deep and the various rock mass models as proposed by NAGRA (Nagra 2014a)

As shown above, the drained E-Modulus in the depth range between 400 to 900 m increases from 2.4 GPa to 8.0 GPa based on reliable laboratory test results (i.e. by a factor of 3.3). In the same depth range, the effective overburden stress increases by a factor of 2.25. Bobet et al (1998) performed a numerical feasibility analysis for a nuclear waste repository in Opalinus Clay assuming an advanced constitutive model that explicitly accounts for an increase in stiffness with increasing octahedral mean stress (i.e. this increase is consistent with NAGRA's constitutive framework). Both, the short- and long-term behavior were considered. The analysis of repository scenarios, which assume a depth of 400 m, 700 m and 1000 m, and various in-situ stress ratios showed that "the liner stress increases only slightly with depth". According to Bobet et al. (1998) this is related to an increase in stiffness with increasing depth. The assumption of a single E-Modulus for the depth range between 400 and 900 m may have relevant consequences on the assessment of the maximum depth below ground surface. Thus, the increase in stiffness in the depth range between 400 and 900m needs to be considered by NAGRA based on reliable laboratory test results.

2.1.6 ETH Assessment of rock mass properties

The strength degradation concept used by NAGRA to establish rock mass strength properties is well described and based on observations in several boreholes and laboratory test results. Seven rock mass models (GM) were distinguished. It was, however, not shown how these rock mass models are related to the different siting regions which may have different tectonic overprints.

2.1.6.1 Effective rock mass strength

The degradation of matrix and bedding strength is shown in Figure 4 based on the unconfined compressive strength (UCS) calculated from the effective friction and effective cohesion suggested by NAGRA for each GM. The calculated strength degradation with respect to the intact matrix strength (GM1,3) for shallow/deep are 18/17% for GM2,4,5, 35/41% for GM6 and 92/95% for GM7. The calculated strength degradation with respect to the intact bedding strength (GM1,2) for shallow/deep are 25/30% for GM3,4, 43/45% for GM5,6 and 83/89% for GM7.

As shown by Amann and Vogelhuber (2015), the suggested effective strength properties of the intact Opalinus Clay, which form the basis for strength reduction, tend to overestimate the actual strength. As a consequence, the suggested rock mass properties also tend to overestimate the actual rock mass strength.

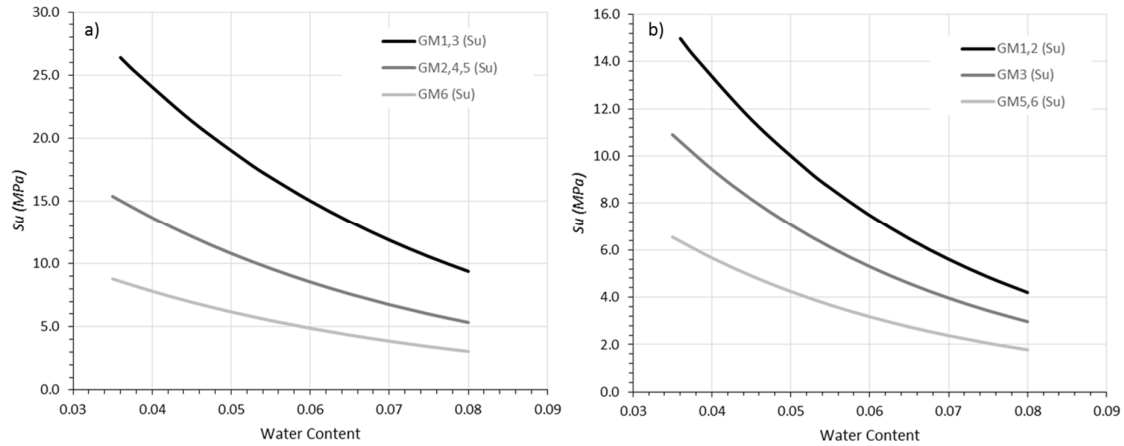


Figure 5: Suggested S_u values versus water content of the matrix (a) and bedding (b) for the rock mass models. The S_u values were calculated from the relations given in NAGRA 2014a.

Table 5: Comparison of S_u values calculated from suggested effective strength properties (Opalinus Clay deep) and S_u values suggested for depths of 500 and 900m with related water content w from NAGRA (2014a).

	S_u , calc	S_u , suggested		Suggested/Calculated	
	(MPa)	w	w	w	w
Matrix					
500m		0.038	0.052	0.038	0.052
GM1,3	12.3	25.2	18.1	2.1	1.5
GM2,4,5	11.0	14.3	10.3	1.3	0.9
GM6	3.0	8.2	5.9	2.8	2.0
900m		0.04	0.043	0.038	0.052
GM1,3	16.3	26.4	22.4	1.6	1.4
GM2,4,5	14.9	15.0	12.7	1.0	0.9
GM6	4.9	8.6	7.3	1.8	1.5
Bedding					
500m		0.038	0.052	0.038	0.052
GM1,2	4.5	14.1	9.4	1.8	1.2
GM3,4	4.0	10.0	6.7	1.6	1.1
GM5,6	3.5	6.0	4.0	1.1	0.8
900m		0.036	0.043	0.038	0.052
GM1,2	10.5	15.0	12.2	1.4	1.2
GM3,4	8.6	10.6	8.7	1.2	1.0
GM5,6	7.7	6.4	5.2	0.8	0.7

2.1.6.2 Unconsolidated undrained shear strength of the rock mass

The S_u values suggested by NAGRA for the various rock mass models depend on the water content (Giger and Marschall 2014) and are shown in Figure 5 for both matrix and bedding strength. The strength degradation with respect to the intact matrix strength (GM1,3) is independent of the water content and is 43% for GM2,4,5 and 67% for GM6 (S_u for GM7 was not defined). The strength degradation with respect to the intact bedding strength (GM1, 2) is 39% for GM3, 4, and 57% for GM5, 6. The quantity of strength degradation to account for rock mass weaknesses is largely inconsistent between S_u and the effective strength. In addition, calculated S_u values from effective strength properties should be consistent with the suggested S_u values. Table 5 shows S_u values calculated from

effective strength properties (Opalinus Clay deep) for the various rock mass models for an effective stress at 500m and 900m depth compared with suggested S_u values calculated for water contents representative for the two depths (NAGRA 2014a). Major inconsistencies exist which are associated with two aspects: 1) the majority of data points used for establishing S_u values for both intact and rock mass strength stem from unsaturated specimens and therefore the undrained shear strength is overestimated, and 2) the degradation of S_u is generally inconsistent compared to the degradation of effective strength properties.

Consistency between suggested and calculated S_u values only exists for the matrix strength of GM 2,4,5, and the bedding plane strength of GM 3,4 for water content at 900 m depth, and the bedding plane strength of GM 5,6 for water content at 500 m depth. As a consequence, the suggested S_u values are considered unreliable because of the following points: 1) the inappropriate data basis used for establishing S_u , and 2) the inconsistency in strength degradation between effective strength properties and undrained shear strength.

2.1.6.3 Elastic properties of the rock mass

Elastic moduli have been established for drained conditions (only S-samples) and undrained conditions (P- and S-samples).

For the rock mass, these properties were not further reduced to account for weaknesses based on several arguments (see section 2.1.4). These arguments are not reproducible because:

- 1) E -Moduli obtained from post-peak un-/reloading cycles (i.e., 20% E -Moduli reduction were observed; NAGRA 2014a) do not represent a layered rock mass with bedding parallel weaknesses that is loaded normal to bedding. An E -Modulus equal to the intact rock might be justified for GM 2 (i.e., moderate to steep inclined fractures rather than bedding parallel structures) but not for GM 3, 4, 5, 6 and 7. For the former (GM 2) laboratory test results would, however, also suggest a reduction of 20%.
- 2) E -Moduli obtained with in-situ tests (dilatometer tests in Benken and Schlattigen) are consistent with laboratory tests on specimens which were loaded parallel to bedding, but not normal to bedding. The majority of rock mass models contain, however, weaknesses parallel to bedding which do not (or only slightly) affect the E -modulus parallel to bedding but significantly affect it normal to bedding. This has also been shown by Lanyon et al. (2014).
- 3) The choice of E -Modulus has a major impact on the assessment of the maximum depth below ground surface since tunnel strain based criteria were used (for details see below). These tunnel strains were calculated using various computational tools and concepts and the assessment is not limited to results obtained from numerical calculations in Lanyon et al. (2014), which consider a stiffness anisotropy and strongly reduced rock mass E -Moduli.
- 4) The components of strength (i.e., matrix and bedding) underpinning the rock mass strength degradation are reduced between 17 and 45% with respect to the intact matrix / bedding strength for GM1 to GM4. For such a significant strength degradation a significant degradation of the stiffness need to be anticipated.

2.2 In-situ state of stress

2.2.1 Stress state – NAGRA's assessment and approach

Since 2008 NAGRA has added 107 new measurements and estimates to the world stress map in northern Switzerland. Of the 107, 71 are new measurements of high quality (A to C ranking according to Heidbach and Reinecker (2013)). 15 of these new measurements come from 11 new boreholes with depths up to 2.5 km. Previous records from 7 old boreholes were re-analyzed to ensure a consistent evaluation criteria was applied to all the data sources.

To assess the stress state in the different siting regions, NAGRA has used data from the world stress map (version 2012), in-situ measurements and estimates from borehole breakouts and earthquake focal mechanisms. Limit estimates have also been based on indirect indicators and material properties. The work of NAGRA (Giger and Marschall 2014, NAGRA 2014a, Heidbach and Reinecker 2013) concludes the following, with respect to the available stress data and analysis:

- The stress orientation of the maximum horizontal stress (SH) has been derived from borehole breakout and earthquake focal mechanism analysis, which indicate a NNW-SSE direction or $160^\circ (\pm 21^\circ)$, when considering all the data in Northern Switzerland.
- If only deep borehole breakout measurements are considered the orientation is similar, but with less deviation: $166^\circ (\pm 12^\circ)$. This mean orientation is most consistent in the siting regions and deviates in the North-East and West of the siting regions. In the NE the orientation becomes NS, within the $\pm 12^\circ$ deviation of the dominate orientation in the siting regions. In the West the orientation becomes WNW-ESES, a $\sim 40^\circ$ rotation from the dominate orientation in the siting regions.
- The relative stress magnitudes have been estimated from earthquake focal mechanisms, which indicates a transpressive to transtensive stress regime. In a transpressive regime the minimum horizontal stress (Sh) would be less than the vertical (Sv) and maximum horizontal (SH) stresses, which would be similar (i.e. $Sh < Sv \sim SH$). In a transtensive regime $Sh \sim Sv < SH$. This has been used to constrain the potential relationship between the magnitudes of the principal stresses.
- Paleo-stress orientation evidence suggests that the SH orientation has not changed since the Late Miocene. Evidence includes:
 - Kinematic indicators on fracture planes (Madritsch and Hammer 2012).
 - Stylolite formation processes from core analysis at Schaffisheim (Matter et al. 1988) and Benken (NAGRA 2001).
- Paleo-slip analysis (Madritsch and Hammer 2012) shows an abundance of thrust fault indicators from the past which suggests that the magnitudes of the horizontal stresses have decreased.
- The vertical stress has been estimated using a constant density of 2500 kg/m^3 for the overlying rock mass.
- The minimum horizontal stress, Sh, has been constrained by hydraulic fracture tests, two of which were conducted in the Opalinus Clay in the Benken borehole, and by semi-empirical relationships.
 - Measurements indicate generally Sh is close to or less than Sv (closer to Sv in clay-rich formations), with the exception of two measurements in the upper Malm which indicate Sh slightly greater than Sv.
 - Range of Sh /Sv ratios between 0.6 and 0.95
 - Sh has also been estimated using a semi-empirical over consolidation approach which yields Sh/Sv ratios below 1.1 at depths greater than 250 m decreasing to 0.85 at 900 m.
 - This approach neglects lateral tectonic loading and therefore represents a lower bound estimate of the Sh magnitude.
- The maximum horizontal stress, SH, has been constrained by borehole breakout analysis and based on the magnitude of Sh measured in the Benken borehole in combination with the evidence from Bure in France.
 - Borehole break estimations yield SH/Sh ratios between 1.1 and 1.6.
 - Reported estimate of Sh/SH from the hydraulic fracturing in the Benken borehole was 1.35.
 - Estimating SH magnitudes from hydraulic fracture tests is stated to have larger errors than Sh values due to assumptions in the mechanics of hydraulic fracturing.
 - SH/Sh ratios from Bure range from 1.0 to 1.2.

- An upper bound SH magnitude can be assumed based on the rock strength, which assuming residual strength values ($\phi = 20^\circ$, $c = 0.5 \text{ MPa}$) give an upper bound SH/Sh of 1.7 to 1.8.
- Numerical analysis using elasto-plastic rock mass behavior indicates that the Sh/Sv and SH/Sv ratios are not sensitive to applied stress boundary conditions due to the relatively low stiffness of the Opalinus Clay (Heidbach et al. 2014).

At the present time there are only two measured horizontal stress values within the Opalinus Clay from the Benken borehole, at approximately 630 m depth, which were obtained from hydro fracture tests. These measured values fit the trend observed from other measured values in clay rich (>35% clay minerals) formation above and below the Opalinus Clay within the Benken borehole. The measurements from the Benken and Schlattigen-1 boreholes are shown (Figure 6) for reference to the measured and estimated magnitudes of the stresses up to 1450 m depth.

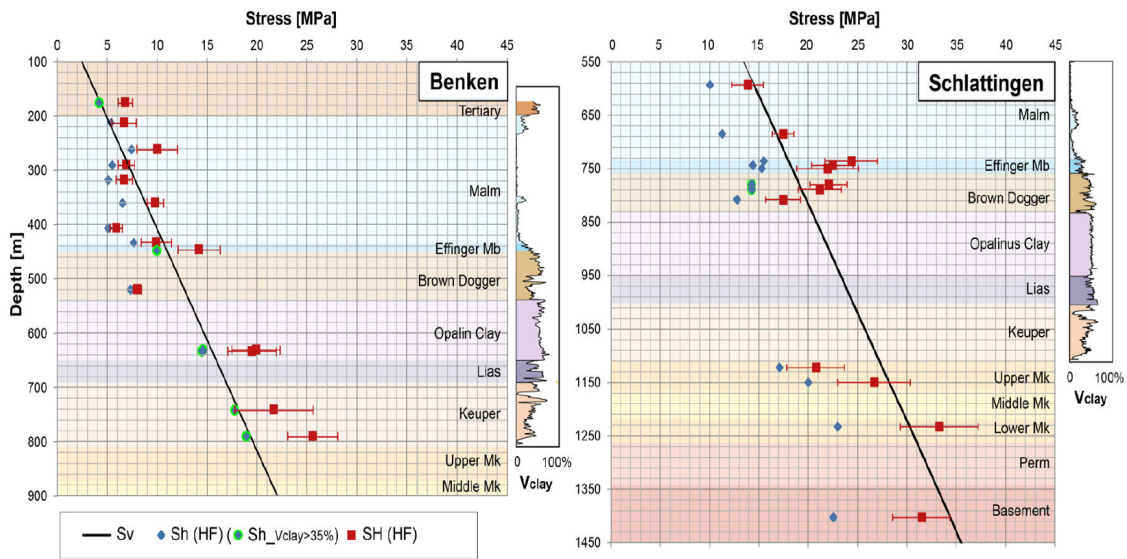


Figure 6: Stress measurements from hydraulic fracturing in the Benken and Schlattigen-1 boreholes (from Giger and Marschall 2014).

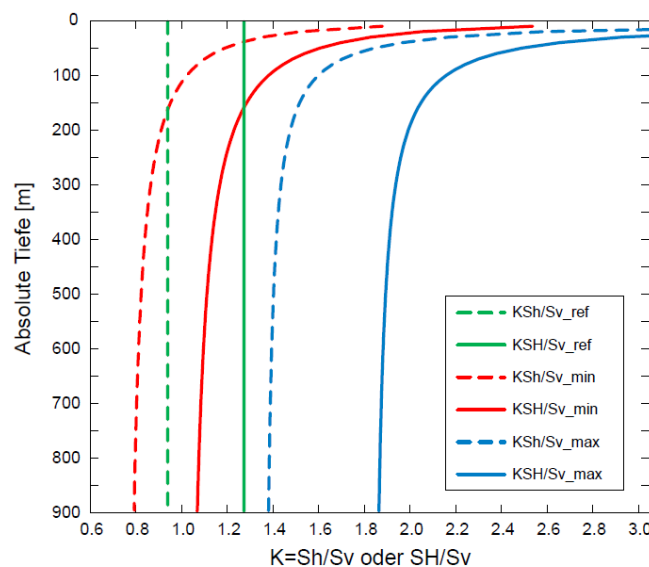


Figure 7: Reference, minimum, and maximum stress scenarios with depth used in the numerical modelling by NAGRA (from Giger and Marschall 2014).

Table 6: Suggested principal stress magnitudes and ratios at reference depths used within the numerical modelling studies of NAGRA (from NAGRA 2014a).

Spannungsmagnituden	Einheit	Werte für spezifische Tiefen in [m]			
		300	500	700	900
Vertikalspannung S_v ($\rho = 2500 \text{ kg/m}^3$)	[MPa]	7.4	12.3	17.2	22.1
Horizontale Spannungen					
<i>Referenzwerte (RSR_{ref})</i>					
minimale horizontale Spannungsmagnitudo ($S_{h,ref}$)	[MPa]	7.0	11.6	16.3	21.0
maximale horizontale Spannungsmagnitudo ($S_{H,ref}$)	[MPa]	9.4	15.7	22.0	28.3
K_{Sh/Sv_ref}	[-]	0.95	0.95	0.95	0.95
K_{SH/Sv_ref}	[-]	1.28	1.28	1.28	1.28
<i>Alternativwerte bei geringen tektonischen Spannungen (RSR_{min})</i>					
minimale horizontale Spannungsmagnitudo ($S_{h,min}$)	[MPa]	6.4	10.1	13.8	17.5
maximale horizontale Spannungsmagnitudo ($S_{H,min}$)	[MPa]	8.6	13.7	18.7	23.7
K_{Sh/Sv_min}	[-]	0.87	0.83	0.81	0.79
K_{SH/Sv_min}	[-]	1.17	1.12	1.09	1.07
<i>Alternativwerte bei hohen tektonischen Spannungen (RSR_{max})</i>					
minimale horizontale Spannungsmagnitudo ($S_{h,max}$)	[MPa]	10.6	17.2	23.8	30.5
maximale horizontale Spannungsmagnitudo ($S_{H,max}$)	[MPa]	14.2	23.2	32.2	41.1
K_{Sh/Sv_max}	[-]	1.43	1.40	1.39	1.38
K_{SH/Sv_max}	[-]	1.94	1.89	1.87	1.86

The suggested stress ratios are shown in Figure 7, which have been used in the numerical modelling for maximum depth estimation and impact on long-term safety (EDZ extent). The depth specific magnitudes are listed in Table 6, including the minimum, reference, and maximum values for 300, 500, 700, and 900 m depths.

Site specific (SMA and HLW sites) data and estimates are found from boreholes within the potential siting regions Jura Ost (Riniken), Nördlich Lägern (Weiach), Zürich Nordost (Benken). With the exception of Zürich Nordost, where hydraulic fracture tests were conducted in the Benken borehole, the other site observations related to stresses within the Opalinus Clay are limited to borehole breakouts and paleo observations. Other boreholes close to the siting regions are also used in the stress analysis, with hydraulic fracture testing being conducted in the Schlattingen borehole. Stresses are also analyzed above and below the Opalinus Clay where data is available. An extensive report on the stress state of Northern Switzerland was published by Heidbach and Reinecker (2013).

2.2.2 ETH Assessment of Stress state

The most common method of predicting the principal stress orientations at depth is typically through borehole breakout analysis or by conducting hydraulic fracture tests. As mentioned above NAGRA has used both methods to constrain the orientations from boreholes within or near the siting regions. Variations in the orientations are stated clearly and discussion is presented on how the orientation is relatively consistent across northern Switzerland, with a rotation NE of the Bodensee and in the west of Switzerland. Beyond this NAGRA has also examined paleo-indicators to determine how the stress orientations have changed with time.

The stress magnitude analysis of NAGRA is clearly documented and the derived reference, minimum, and maximum stress scenarios can be followed. The minimum and maximum stress scenarios can be

considered conservative estimates of the lower and upper bound stress states, respectively. Some points for future consideration are discussed below.

As the vertical stress is difficult to measure it is typically estimated by the density of the overlying rock mass. NAGRA has considered a generic unit weight or density for all the rock formations to estimate the vertical stress component. This is a reasonable first pass, however, the average density for each formation and a range should be used for site specific studies to gain a better estimate of the vertical stress and the associate uncertainty. The error in the approach of NAGRA is largest near surface where the density is less due to limited consolidation (Valley 2007). The error could be estimated following the method detailed by Valley (2007), where densities can be estimated from geophysical borehole measurements where specific measurements are lacking.

The uncertainty of the stress magnitudes is better constrained and discussed for the horizontal stresses. Here NAGRA's suggested maximum principal stresses at the reference depths (500, 700, 900 m) exceed the measured values from the Benken and Schlattigen-1 boreholes. Since the maximum stress magnitude is based on the residual strength properties (GM7 deep values), the actual stress magnitudes at the specific sites may differ from those used in the maximum stress regime scenario. Carrying the maximum stress scenario forward, for example for predictive numerical models for maximum EDZ extent or convergence, would yield higher estimates. This may not be the case for all design criteria where stresses are incorporated, however, not all aspects where stresses are used have been evaluated in this review. The minimum horizontal stress measurements are more reliable than those of the maximum horizontal stress and therefore less uncertain, as reported by NAGRA. Because there is less uncertainty in S_h , there is less increase in the stress ratios from the minimum, reference, to maximum scenarios for the S_h/S_v ratio than for the SH/S_v ratio (dashed vs solid lines in Figure 7 and scenarios defined in Table 6).

Assuming a constant ratio for SH/S_h (equal 1.35) based on hydro fracturing measurements from the Benken borehole represents a reasonable assumption, however some uncertainty exists since Giger and Marschall (2014) state that the SH/S_h ratio could be as high as 1.6 based on borehole breakout analysis. The uncertainty of this assumption and the variability of the stress magnitudes on a site specific basis are not discussed and whether new interpretations replace previous findings.

3 Maximum depth of the high-level nuclear waste repository

3.1 Higher-level requirements and design criteria used by NAGRA

3.1.1 Background

The maximum depth below ground surface is of high relevance for the potential siting regions and their optimized repository perimeter and thus a very important aspect for narrowing down the potential siting regions in stage two of the Sectorial Plan. Repository depth influences the geotechnical conditions (i.e. in-situ stress and rock mass properties) and the damage of the geological barrier in vicinity of the repository excavations. For the assessment of the maximum depth below ground surface the following higher-level requirements ("*übergeordnete Anforderungen*") have been considered by NAGRA: 1) Warranty for safe construction, operation and closure of the underground facilities, 2) limited use of construction material (i.e. support measures) that may cause damage to the technical barriers (i.e. bentonite backfill and seals) and the geological barrier, 3) limitation of perturbation and prevention for exceeding the allowable damage of the geological barrier around HLW emplacement tunnels and sealing sections (i.e. limitation of geological barrier damage and fluid flow along emplacement tunnels), and 4) appropriate conditions for the construction of technical barriers (bentonite) and self-sealing of the host rock.

Because all these requirements are more difficult to be achieved with increasing repository depth, and at the same time, the repository shall be placed as deep as possible to prevent host rock destruction

during future uplift and erosion scenarios, the repository depth needs to be optimized. Therefore the higher level requirements need to be translated into optimizing requirements (“Optimierungsanforderungen”) for constructability and long-term safety.

For the delineation of the optimized disposal perimeter a depth with favorable geotechnical conditions is targeted. According to NAGRA (2014b) favorable conditions exist, when the requirements are satisfied in a robust and reliable way considering uncertainties and variability. These requirements were therefore converted into five design criteria (“Entwurfsindikatoren EI”) which are quantitatively assessed by NAGRA using a large variety of empirical, analytical and numerical approaches. Table 7 summarizes these design criteria which are described in the following sections.

3.1.2 Optimization requirements and design criteria for long-term safety

For the long-term safety three requirements were defined: 1) Limited extent of the excavation damage zone to maintain a sufficient thickness of the intact geological barrier (vertical radionuclide migration distance), 2) Limitation of the hydraulic conductance of the EDZ parallel to the HLW repository tunnels and sealing sections (longitudinal radionuclide migration pathways), and 3) Assure appropriate conditions for emplacing the bentonite buffer.

3.1.2.1 Vertical radionuclide migration distance

According to NAGRA (2014b) Opalinus Clay is a very effective barrier against radionuclide transport and an intact vertical thickness of 35m ($M_{min,intakt}$) is sufficient for radionuclide retention of a HLW repository (Figure 8). Assuming an irregular layer thickness of the Opalinus Clay ranging around 100m, and the possibility of having repository tunnels not exactly in the center of the host rock layer, the maximum vertical extension of the EDZ for a HLW repository $p_{v,HLW}$ (Figure 8) shall not exceed 5m. This maximum vertical extend shall not be exceeded during construction, operation and after repository closure.

3.1.2.2 Radionuclide migration in EDZ

Numerical and analytical radionuclide transport models used for safety analysis revealed that the hydraulic conductivity of the EDZ, in particular around sealing sections, is relevant for the long-term radionuclide migration longitudinal to the emplacement tunnels, as illustrated in Figure 9. To ensure that the majority of radionuclide migration occurs radially through the intact geological barrier rather than longitudinally along the emplacement drifts, the product of the cross sectional area of the EDZ in Figure 10 and the hydraulic conductivity needs to be smaller than $1E-7 \text{ m}^3/\text{s}$.

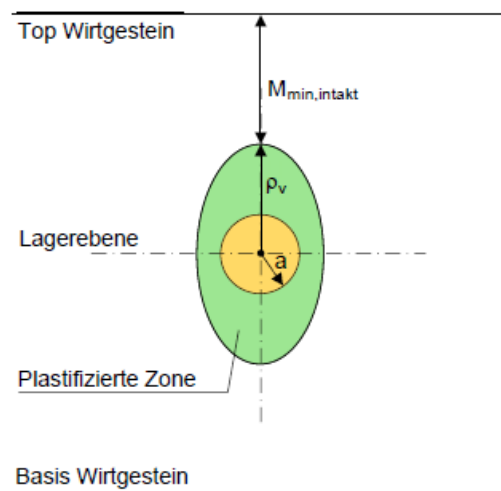


Figure 8: Definition of the maximum vertical extend of the EDZ (green area, with p_v being the maximum plastic radius and a being the tunnel radius) and minimum vertical thickness of intact Opalinus Clay ($M_{min,intakt}$) for sufficient radionuclide retention. From NAGRA (2014b).

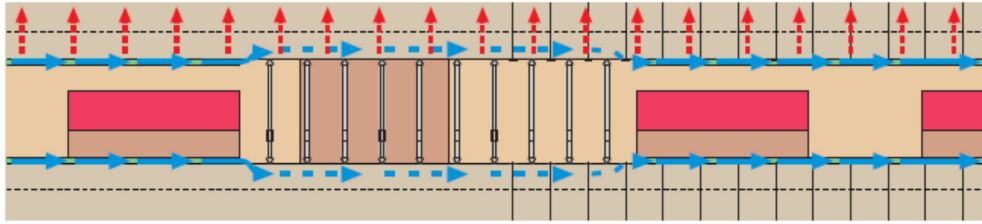


Figure 9: Radionuclide pathways. Radial / vertical radionuclide pathways (red) and longitudinal migration pathways (blue). Within the sealing section the longitudinal hydraulic conductance is of key relevance (dashed blues arrows). From NAGRA (2014b).

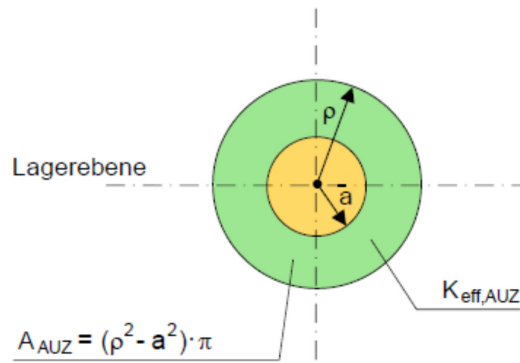


Figure 10: Simplified concept of the EDZ and homogenized hydraulic conductivity (AUZ = EDZ). The hydraulic conductance is the product of area, A_{EDZ} , and the hydraulic conductivity, $K_{eff,EDZ}$, (from NAGRA 2014b), with ρ being the plastic radius and a the tunnel radius.

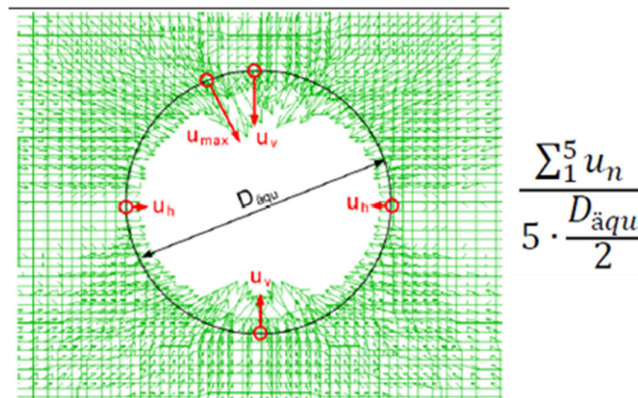


Figure 11: Definition of the normalized tunnel strain (from NAGRA 2014b)



Figure 12: Examples for unfavorable or unacceptable situations for sealing sections (from NAGRA 2014b).

According to NAGRA (2014b) a series of HM-coupled simulations using a simplified conceptual model of the EDZ (i.e. circular EDZ), and various scenarios for fracture networks were performed and suggest that the requirements for longitudinal radionuclide transport are fulfilled for normalized tunnel strains $< 4\%$ (the definition of the normalized tunnel strain is given in Figure 11).

3.1.2.3 Favorable conditions for emplacing the bentonite buffer

Favorable conditions are required for the bentonite buffer, backfill installation and functionality. This includes the following requirements: 1) Reduction of shotcrete and/or cementitious material to minimize geochemical bentonite transformation and its long-term influence on the pH plume (i.e. shotcrete thickness $< 30\text{cm}$), 2) Reduction of steel (e.g. for reinforcement, steel arches, rock bolts) and organics (e.g. shotcrete additives, GDF rock bolts) to minimize gas formation, 3) Avoid local overbreak and loose material (i.e. ground loosening) along the tunnel circumference (Figure 12) which may compromise the development of sufficient swelling pressures or cause local, inappropriate porosities within the bentonite and/or near the excavation boundaries, and 4) Use of linear support elements such as steel arches in the sealing sections to ensure direct contact between bentonite and host rock and avoid retreat of support elements.

For estimating ground loosening along the tunnel circumference the normalized tunnel strain before support installation was utilized. The stress-strain response obtained from compression tests on P- and S-specimens shows a typical failure strain of $0.3 - 0.8\%$ (0.5% on average). The residual strength is typically reached at 1% strain³ which is converted by NAGRA into 1% normalized tunnel strain. Thus, NAGRA considers normalized tunnel strain $< 1\%$ favorable, and normalized tunnel strain $> 2.5\%$ unfavorable.

3.1.3 Optimization requirements and design criteria for constructability

For the constructability assessment it is essential that underground structures can be built, operated and sealed in a safe and robust way for the given boundary conditions and comply with the higher-level requirements. This requires that both structural safety (during excavation and operation) and serviceability (during operation) are demonstrated. In addition, damage of the host rock must be limited to reduce technical difficulties and the influence on long-term safety. The approaches for structural safety and serviceability are defined in SIA 197 and SIA 267.

For the constructability two requirements were defined in NAGRA (2014b): 1) Limitation of rock damage and ground loosening during excavation, and 2) Ensure rock mass and structural safety during construction and service life.

3.1.3.1 Limitation of rock damage and ground loosening

NAGRA's requirements for limiting rock damage and ground loosening are based on normalized tunnel strains following the recommendations given in Hoek and Marinos (2000). These recommendations suggest that for normalized tunnel strains $< 1\%$ constructability is favorable and for normalized tunnel strains $> 2.5\%$ construction is increasingly challenging.

3.1.3.2 Rock mass and structural safety

The requirements are defined in SIA 260. The support must have a sufficient load-bearing capacity and the global stability must be demonstrated for all states of construction.

3.2 Rock mechanical calculations and input properties used by NAGRA

3.2.1 Methods used

Various calculation methods have been used for assessing the design criteria defined in Table 7 (EDZ size and tunnel convergence).

³ Note that it is not specified which strain was considered (i.e. axial, radial, shear, or volumetric strain)

Table 7: Design Criteria (“Entwurfsindikatoren” EI) used for the assessment of geotechnical conditions and maximum depth below ground surface (from NAGRA 2014b).

Übergeordnete Anforderung	Entwurfsindikator (Kriterium)	Referenzprofil		
		F	K09	K04
Ungestörte vertikale Migrationsdistanz im Wirtgestein (Langzeitsicherheit): HAA-Lagerstollen: ≥ 35 m SMA-Lagerkaverne: ≥ 20 m Versiegelung: ≥ 20 m	EI-1: Normierte vertikale Ausdehnung der plastifizierten Zone $2 \cdot \rho / D_{\text{äqu}}$ [-] (Kurz-/Langzeitverhalten und ohne/mit Ausbau) auf X_4 -Niveau unter Berücksichtigung einer Abweichung der Solllage des Hohlraums von ± 10 m ¹⁾ HAA-Lagerstollen: ≤ 4.0 SMA-Lagerkaverne: ≤ 3.5 Versiegelung / LMA-Lagerkaverne: ≤ 4.0 Angestrebt: erfüllt ohne Ausbau; Geprüft: mit Ausbau	×	×	×
Beschränkung der Durchlässigkeit der Auflockerungszone (Langzeitsicherheit) Äquiv. hydr. Leitvermögen: 7×10^{-8} m ³ /s ($A_{\text{AUZ}} \approx 7$ m ² , $K_{\text{eff,AUZ}} = 1 \times 10^{-8}$ m/s).	EI-2: Normierte mittlere Konvergenz u_v/a [%] (Kurz-/Langzeitverhalten und mit/ohne Ausbau) auf X_4 -Niveau: angestrebt: ≤ 4 % ohne Ausbau geprüft: ≤ 4 % mit Ausbau	×		×
Qualität der Einbaubedingungen (Ausbruch, Ausbau) für die technischen Barrieren	EI-3: Normierte Konvergenz $u(e)/a$ [%] (Kurzzeitverhalten und ohne Ausbau) X_4 -Niveau angestrebt: ≤ 1 % (ohne Ausbau) geprüft: $1\% < \dots \leq 2.5$ % (vor Einbau des Ausbaus)	×		×
Beschränkung der Beanspruchung des Gebirges Gewährleistung der Gebrauchstauglichkeit (Funktionstüchtigkeit, Dauerhaftigkeit, Verformungen während der Nutzungsdauer)	EI-4: Normierte Konvergenz $u(e)/a$ [%] (Kurzzeitverhalten und ohne Ausbau) X_4 -Niveau angestrebt: ≤ 1 % (ohne Ausbau) geprüft: $1\% < \dots \leq 2.5$ % (vor Einbau des Ausbaus)	×	×	×
Hohlraumstabilität im Grenzzustand während Bau und Nutzungsdauer (Tragsicherheit technische Machbarkeit)	EI-5: Beurteilung der Gebirgstragfähigkeit (Grenz Zustand III) und des Tragwiderstands des Ausbaus (Grenz Zustand II) in Anlehnung an SIA 267 (2013a) auf X_4 -Niveau (Kurzzeitverhalten und bis zum Verschluss sowie mit Ausbau) Mindestanforderung: - Tragwiderstand Ausbau: Verwendung von nominalen Ausbauwiderständen auf Basis orientierender Vordimensionierung - Gebirgstragfähigkeit: Gleichgewicht unter Verwendung nomineller Ausbauwiderstände	×	×	×

The methods include:

Experience gained from existing tunnels

In addition to computational methods, experience gained from tunnels in Opalinus Clay and a worldwide collection of experience in weak rocks was compiled (NAGRA 2014b).

Semi-empirical considerations

Semi-empirical considerations are based on the ratio between the unconfined compressive strength (UCS) and the vertical overburden stress according to SIA 198. In addition, empirical data from a series of underground excavations in clay rocks (i.e., Mont Terri, Bure, Mol and Site C) were collected. These data relate the ratio of UCS/maximum tangential stress with the measured radial strains that accumulated within 100 days after excavation. This relation was further used to predict the diametral strains at a depth range between 400 and 900m based on UCS test results obtained from cores taken from the borehole Benken (NAGRA 2014b).

Analytical and semi-analytical method

Ground reaction curves were used to estimate tunnel deformation, the extent of the plastic zone and the required support pressure with increasing depth using various support models (i.e. ranging from steel arch to concrete segments). Two support installations were assumed: 1) installation at a distance of one tunnel diameter ($1 \times D$) behind the tunnel excavation face and 2) installation at a distance of 3 tunnel diameters ($3 \times D$) behind the tunnel excavation face. The latter is considered as an approximation for a yielding support that develops full support capacity $3 \times D$ behind the face. To account for anisotropic stress and strength conditions (i.e. non-uniform radial displacements) reduction factors for the support capacity were considered according to Kovári (1998). A total stress analysis with effective strength properties has been performed assuming that the calculated displacements represent long-term deformation. A Mohr-Coulomb failure criterion with a linear-elastic, brittle-plastic behavior was assumed that allows to consider the typically observed post-failure stress drop in compressive strength tests on Opalinus Clay.

Effective stress calculations using FLAC 2D

2-dimensional finite difference calculations have been performed using the numerical code FLAC2D. The code allows modelling anisotropic stress states and introduces a rock mass strength anisotropy using a constitutive model (SUBI; strain softening ubiquitous joint model) which considers smeared weakness planes within a continuum. The utilized constitutive model allows modelling strain softening to reproduce the post-failure stress drop that is typically observed in compressive strength tests on Opalinus Clay. The stiffness anisotropy of the rock mass cannot be reproduced. The approach is based on effective stresses and allows to model both the short and long-term rock mass response with and without support measures.

Total stress calculation using Phase2

The influence of elastic anisotropy has been analyzed using the finite element code Phase2. An anisotropy was introduced by distributed joint elements with variable spacing, distribution, persistence and normal / shear stiffness. The matrix and bedding strength are assumed equal (homogeneous strength). The analysis is based on total stresses using undrained shear strength for various rock mass models (i.e. short-term response). Support measures are not included.

3.2.2 Input properties for numerical and analytical calculations

3.2.2.1 Properties for effective stress calculations and ground reaction curves

The effective intact rock and rock mass properties (i.e., GM1 – GM4⁴) recommended by NAGRA were used and reduced to three parameter levels (Appendix B, NAGRA 2014b): The Xm level describes the expected properties and is equal to mean values (note that Xm values were not used for numerical and analytical rock mechanical calculations). The Xk level describes characteristics properties (i.e. the lower limit of the 68% confidence interval was used for GM1). For GM2 characteristic values were established assuming that the peak strength of the matrix is reduced to the residual strength, for GM3 it was assumed that the peak strength of bedding is reduced to the residual strength and for establishing characteristics values for GM4 both strength components were reduced to residual values. The tensile strength was reduced by a factor of 2. The Xd level represents design properties. Xd properties were defined according to SIA 267 using partial factors of safety (i.e. 1.5 for cohesion, tensile strength and E-Modulus, and 1.2 for the friction coefficient).

⁴ GM1 – GM4 were used for effective stress calculations. For calculations with the ground reaction curve GM1 – GM3 were used.

The E -Modulus used for effective stress calculation and ground reaction curves is based on the undrained E -Modulus normal to bedding ($E_u = 9.0\text{GPa}$, NAGRA 2014b). For the Xm level $E = 8.16\text{GPa}$, the Xk level $E = 6.12\text{GPa}$ and for the Xd level $E = 4.08\text{GPa}$ were assumed.

3.2.2.2 Properties for total stress calculations (Phase2)

For total stress calculations the S_u values suggested by NAGRA were not reduced to the above described levels. S_u was assumed to be the same in the matrix and the bedding planes (i.e. isotropic strength). The stiffness anisotropy was introduced through compliant, non-persistent and statistically distributed joint elements. Both, the density of joint elements and the joint stiffness (i.e. the joint normal and shear stiffness) were varied. A range of anisotropy coefficients A between $1 < A < 7$ was considered relevant (anisotropy coefficient $A = (E_G / E)^{-1/2}$; with E_G being the Young's modulus normal to bedding and E the Young's Modulus parallel to bedding). The anisotropy coefficient was calculated according to Duncan and Goodman (1968) using the following equations:

$$E_G = \frac{1}{1/E + \Lambda/k_n}$$

with Λ being the number of bedding planes per meter normal to bedding and k_n being the normal stiffness.

3.2.3 Findings and conclusions drawn by NAGRA

NAGRA concludes that the used methodology which combines analytical and numerical calculations and experience gained from tunneling in clay rocks provides a robust basis for predicting the anticipated rock mass and system behavior with increasing depth. NAGRA's main findings of the analysis are (summary from NAGRA 2014b):

- 1) The different methods lead to comparable results and tendencies in terms of convergences and EDZ depth with increasing overburden.
- 2) Even though limitations exist in support measures a HLW repository can be built in a safe way even at a depth of 900m.
- 3) With increasing depth, however, the rock mass perturbation or damage increases disproportionately, although support measures were considered. More support is required to control rock mass damage at greater depth. This is, however, unfavorable for the long-term safety.
- 4) For the available support types and a support installation close to the tunnel face (i.e., "Widerstandsprinzip") HLW repository construction is possible to a depth of 600-700m. For greater depths, yielding support elements are required which do not allow proper control of rock mass damage. For the small diameter HLW tunnels a tunnel boring machine (TBM) is preferred which allows support installation behind the TBM shield. This is considered disadvantageous for squeezing conditions which are anticipated for depths greater than 700m.
- 5) With increasing depth the required technical effort increases, the flexibility is limited and the sensitivity of the system to variations in geotechnical boundary conditions increases. In addition, the reliability of performance decreases and a significant damage of the host rock is anticipated. As a consequence, unexpected rock mass characteristics such as a fault zone at greater depths may cause major technical problems and the likelihood for giving up individual repository sections increases.
- 6) The above points are not valid for the sealing sections without a shotcrete liner or concrete segments. Analytical calculations showed that steel arches (i.e., the preferred support type in sealing sections) are only technically feasible to a depth range of 600-700 m when installed 3 diameters behind the face. Support installation behind the face (1 diameter distance) in sealing sections is already reaching the load bearing capacity in a depth range of 400-500 m.

- 7) Even with support measures rock mass damage cannot be avoided. With respect to long-term safety an optimized maximum depth below ground surface is sought, for which the requirements for long-term safety are met with “minor support measures” (i.e., “ohne grösseren Ausbau”).
- 8) Considering limitations in support measures outside the sealing sections the most critical design criteria (EI-1 and EI-2) are not violated for a depth between 600-700m depending on the analysis method and assumption for rock mass models and stress states.

NAGRA’s conclusions are:

- 1) Squeezing conditions can be coped with in a safe way with appropriate support design and construction methods to large depths. Thus, the maximum depth below ground surface is primarily associated with the requirements for long-term safety (i.e., design criteria EI-1, 2, 3).
- 2) Even though all available information and various analysis methods were used, uncertainties remain (i.e., variations of the results). Therefore, the maximum depth below ground surface was chosen with caution.
- 3) The analysis suggests that for HLW repositories at depth > 700m the design criteria for EDZ depth and EDZ conductance are possibly violated. Thus, the higher level requirements cannot be fulfilled in a robust and reliable way.
- 4) The maximum depth below ground surface of 700m for the HLW repository is primarily valid for siting regions with increased tectonic overprint.
- 5) Considering the geological variability in the siting regions the analysis allows clear conclusions with respect to the maximum depth below ground surface: for the HLW repository the minimum requirement on the maximum depth is $\leq 900\text{m}$, the optimized requirement is $\leq 700\text{m}$. The latter requirement does not differentiate between the various rock mass models (GM). For GM 4 the maximum depth tends to be less. A depth between 600 and 700m is considered “favorable”, a depth $\leq 600\text{m}$ “very favorable”.

3.3 ETH assessment of design criteria selection

3.3.1 Design Criteria for long-term safety

Design criteria EI-1, EI-2 and EI-3 address long-term safety issues associated with the vertical and longitudinal radionuclide migration path and the effectiveness of the bentonite barrier.

The vertical migration criterion EI-1 is based on a clearly defined limit of the vertical extent of the EDZ. The vertical extend is defined as the normalized vertical extend (i.e., $2p/D_{\text{aqu}}$; where p is the vertical extend of the plastic zone and D_{aqu} the equivalent diameter) which should not exceed 4 for a HLW repository tunnel. The vertical extend of the plastic zone can be directly obtained from numerical and/or analytical models.

The design criterion for the maximum allowable vertical extent of the EDZ is reasonable and can be readily applied.

The longitudinal migration criterion EI-2 is defined by limiting the normalized accumulated (i.e., elastic plus plastic) tunnel strain (no support) in both the short and long-term to a maximum value of 4%. This limitation implies 1) that the longitudinal hydraulic conductivity and conductance of the excavation damage zone is related to the tunnel strain and 2) that the maximum allowable, longitudinal hydraulic conductance of $1\text{E-}7 \text{ m}^3/\text{s}$ is reached at 4% tunnel strain. Despite the fact that these relations are material specific and need to be established for Opalinus Clay, the attempt to link accumulated tunnel strains to hydraulic properties of the excavation damage zone is not acceptable for the following reason: Because elastic deformations are not considered critical for EDZ hydraulic conductance (see also NAGRA 2014b, p. 51), the use of a tunnel strain criterion, that considers both accumulated elastic and plastic strains, likely leads to erroneous assessments, in particular in cases where the deformability of the rock mass is high. For otherwise constant stress and strength properties, but decreasing stiffness, the tunnel

convergence increases, but the plastic zone dimensions remain unchanged (a finding that is also reported by NAGRA 2014b). This is illustrated by the following example of a ground reaction curve (GRC) utilizing GM 3 effective rock mass strength properties and two cases for the E -Modulus. In the first case an undrained E of 8.16 GPa was used (Xk level NAGRA 2014b), for the second case an E -Modulus of 4 GPa (drained E -Modulus for Opalinus Clay between 400-900m suggested by NAGRA 2014b). The radius of the plastic zone remains constant while the tunnel convergence in case 1 would be assessed uncritical in terms of longitudinal migration path, but critical for case 2.

In the theory of the GRC (i.e., assumptions are an infinite long circular tunnel, rotation symmetry, a hydrostatic stress state, an elasto-plastic constitutive law) the radial displacements are indirectly proportional to the E -Modulus. Assuming zero dilation, a reduction of 50% of the E -Modulus leads to a duplication of radial displacements; the radius of the plastic zone, and the accumulated volumetric plastic strain in the EDZ, however, remain constant (see Figure 13).

A similar example based on complex hydro-mechanical calculations is given by NAGRA (2014b). These hydro-mechanical coupled calculations confirm that the EDZ extent is independent of the E -Modulus.

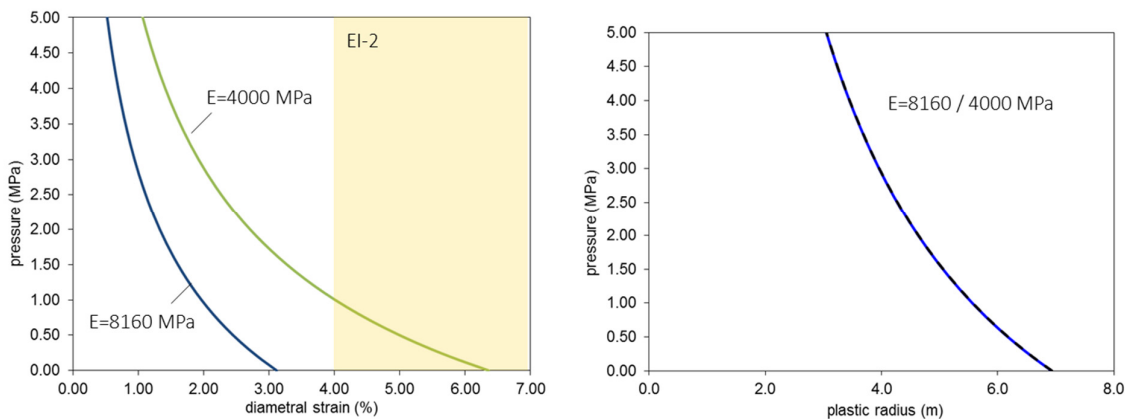


Figure 13: Ground reaction curves for GM 3 rock mass properties and two different values for the E -Modulus. The diametral strain increases substantially and exceeds the allowable limits of design indicator EI-2. The radius of the plastic zone, however, remains constant.

The use of a tunnel strain criterion to assess the hydraulic conductivity and conductance of the excavation damage zone is not acceptable, in particular because robust relationships between hydraulic conductivity of the EDZ, EDZ area and tunnel strain have not been established and the assessment is significantly dependent on the E -Modulus used in numerical analysis.

Conditions for sealing installation were assessed using an accumulated, averaged tunnel strain criterion. An accumulated tunnel strain before support installation $u(e)/a < 1\%$ was targeted for an unsupported tunnel (i.e. classified as “favorable”), and the maximum allowable accumulated strain before support installation was defined to be $u(e)/a < 2.5\%$ (classified as “less favorable”). The derivation of these limits are based on stress-strain curves from compressive strength tests in the laboratory, where the residual strength is typically reached for strains in the order of 1%. The axial strain measured in triaxial compression tests in the laboratory cannot be directly compared to a tangential tunnel strain and thus cannot be directly converted into a diametral tunnel strain criterion NAGRA (2014b) also provides examples of unfavorable or unacceptable situation for sealing installations (Figure 12). All examples show local failure phenomenon rather than global failures, which questions the use of an average tunnel strain criterion as defined in Figure 11. Locally the strain around the excavation may exceed the strain required to reach the residual strength, but the average tunnel strain can still be moderate or low. This

is illustrated using the example⁵ shown in Figure 14. A circular repository tunnel with a radius of 1.6 m was assumed in an isotropic effective stress field representative for a depth of 800 m. GM3 rock mass properties were utilized as defined by NAGRA (2014b). The residual strength is assumed to be reached for an accumulated plastic shear strain $\gamma_{plast} = 0.01$ for the matrix, and $\gamma_{plast} = 0.005$ for the bedding planes (NAGRA 2014b).

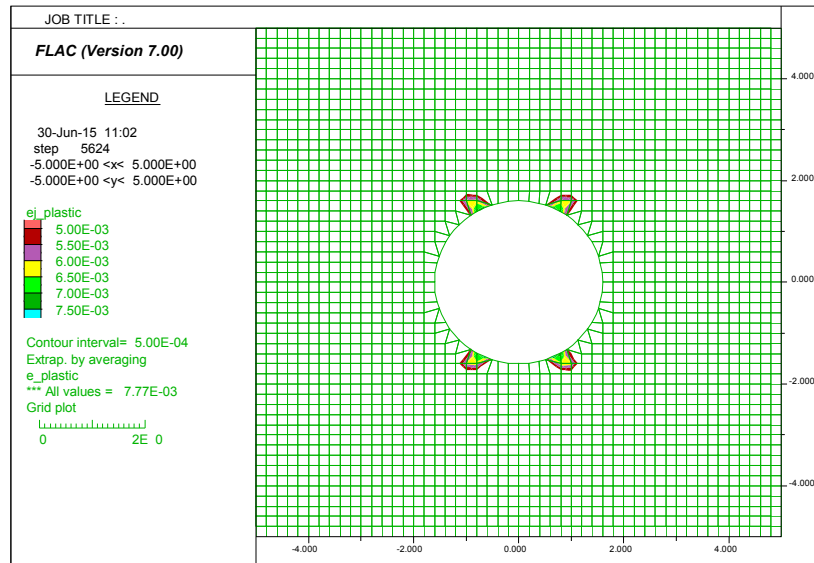


Figure 14: Accumulated plastic shear strains (bedding) at the time of support installation (70% relaxation is assumed) at a depth of 800 m. The calculation is based on GM 3 properties.

The example shows that the tunnel strain (in this case the maximum strain that accumulates without support measure) is 0.32% at support installation (70% relaxation was assumed). Within the rock mass, however, the residual strength for the bedding is reached locally indicated by the colored areas. Even though the tunnel strain criterion suggests favorable conditions at support installation (i.e., $u(e)/a = 0.32\%$), the residual strength in the bedding planes is reached. Note that the assessment of $u(e)/a$ depends on the assumption of the amount of deformations which occur ahead of the tunnel face or before support installation. For the FLAC2D calculations of NAGRA (2014b) it is not clear which assumptions have been made.

The derived and used averaged tunnel strain criterion (accumulated elastic and plastic strain) for assessing the conditions for sealing conditions is not appropriate. The residual strength in the rock mass can be reached far before the diametral tunnel strain exceeds the specified limit of 1%. If it is considered that the residual strength should not be reached (i.e., at 1% axial strain derived from compression tests in the laboratory) the maximum allowable diametral tunnel strain would be significantly lower than 1%.

3.3.2 Design criteria for constructability

Design criteria EI-4 and EI-5 address the serviceability and structural safety during construction, operation and closure.

For limiting rock mass damage, normalized tunnel strain criteria were established. Short-term accumulated normalized tunnel strains $< 1\%$ are considered favorable (classified as “günstig”) for unsupported tunnels, i.e. tunnel performance is not sensitive to small deviations from the expected

⁵ For the numerical analysis FLAC2D was utilized. The constitutive model and the constitutive properties were exactly the same as for numerical models reported by NAGRA (2014b). The model size is 80×80m. Stress boundary conditions were assumed at all four model boundaries.

strength and stress conditions). Accumulated normalized tunnel strains at support installation between 1 and 2.5% are classified as acceptable (“bedingt günstig”), i.e. tunnel performance is moderately sensitive to small deviations from the expected strength and stress conditions. Note that this criterion is quantitatively the same as EI-3 (conditions for sealing installation).

The derivation of the criterion is based on recommendations given in Hoek and Marinos (2000). For assessing the degree of expected difficulties during tunnel construction Hoek and Marinos (2000) integrated measured radial displacement data obtained from a series of tunnels in Taiwan (Chern et al. 1998), the observed tunnel performance (i.e., support damage and stability; Chern et al. 1998), and a closed form solution for calculating the tunnel strain. Monte Carlo analyses were used to determine tunnel displacements for a wide range of conditions⁶. Chern et al. (1998) relate the uniaxial compressive rock mass strength with the measured tunnel strains (i.e., obviously derived from measurable deformations in supported tunnels; no notion could be found at which distance to the tunnel face displacement measurements were initiated). Hoek and Marinos (2000) relate the tunnel strains obtained from the closed form solution to the ratio of the rock mass compressive strength and the maximum principal in-situ stress component.

The applicability of the recommendations given by Hoek and Marinos (2000) are problematic because of the following reasons: 1) the recommendations are primarily based on observed support damage reported by Chern et al. (1998). Thus, the recommendations rely on the interaction between rock mass and support measures which depends on the stiffness and load bearing capacity of the support system. In case of no support, or an infinitely stiff support, the behavior would have been assessed uncritical. 2) The approach does not consider absolute stress magnitudes. For a tunnel strain of, for example, 2% at shallow depth the tunnel can most probably be supported with standard support measures (e.g., shotcrete and rock bolts). For the same strain at larger depth standard support measure may not be sufficient. 3) The calculations performed by Hoek and Marinos (2000) yield total tunnel strains that accumulate in an unsupported tunnel. This is in contrast to the measurable tunnel strains in supported tunnels reported by Chern et al. (1998). For the latter, displacements that occurred ahead of the tunnel face are unknown (note that numerical 3D calculations considering various scenarios for rock properties and support measures revealed that 5-20% of the total crown displacement occur ahead of the tunnel face, and 60-90% of the total displacement accumulate at $1 \times D$ behind the face (NAGRA 2010)). As a consequence, the empirical (measured) tunnel strain data cannot be directly compared with analytically derived total tunnel strains.

The use of an averaged tunnel strain criterion (accumulated elastic and plastic strain) as an indicator for rock mass damage is not appropriate and does not allow a quantitative assessment of the maximum depth below ground surface.

Design criterion EI-5 follows the Swiss tunneling norm SIA 267 and is not put in question. Both global and structural safety with various support options need to be assessed.

3.4 ETH Assessment of methods and results

3.4.1 Experiences and empirical results

The experience from two experimental drifts excavated in the Mont Terri URL was summarized NAGRA (2014b) (i.e., the MB and the FE Experiment; both excavated parallel to bedding). The experience in terms of short- and long-term deformation, EDZ extent and EDZ mechanism are of great value for repository design considerations, even though the in-situ stress state in Mont Terri is more anisotropic (but the effective mean stress is lower compared to the siting regions) and the rock mass is

⁶ The in-situ hydrostatic stress was varied between 2 and 20 MPa, the tunnel radius between 4 and 16 m, the UCS between 1 and 30 MPa, the Hoek-Brown constant m_i between 5 and 12, the Geological Strength Index between 10 and 35, and the dilatation angle between 0 and 10° (Hoek and Marinos 2000).

tectonically more disturbed than expected in the siting regions). Further important information and experience such as the typical short round length (i.e., in the order of 1 m), support installation close to the tunnel face (i.e., 1 m behind the face) and local overbreak associated with tectonic features are not reported in NAGRA (2014b), but can be found in Lanyon et al. (2014).

Additional considerations were based on an empirical diagram from Czaikowski et al. 2005, which relates the depth below ground surface to the rock mass compressive strength. Conditions for tunnel construction are considered favorable when only little support is required (i.e., rock bolts and wire mesh). For the unconfined compressive strength of Opalinus Clay (Benken) the diagram suggests favorable conditions for a matrix strength of 21.5 MPa (i.e., GM1, Xk level, Opalinus Clay deep) to a depth of 680 m. Other rock models such as GM 2, 4 (degraded matrix strength) or the bedding strength were not considered. The reliability of the diagram is problematic. For Opalinus Clay shallow, for example, with a suggested rock mass compressive strength of 10.5 MPa (GM1, Xm level), the diagram suggests unfavorable conditions for a depth greater than 250 m. This is not consistent with experience in the Mont Terri URL. The empirical diagram is of minor value and cannot be used to quantify the maximum depth below ground surface.

3.4.2 Effective stress calculations using FLAC 2D

3.4.2.1 General comments

A large number of numerical realizations are reported by NAGRA (2014b) which systematically address both the long- and short-term rock mass response with increasing depth. The calculations account for important aspects of the Opalinus Clay rock mass such as the anisotropic strength and in-situ state of stress, the excess pore pressure that develops in the short term and dissipates in the long-term, and associated pressures on the support. Various rock mass properties (GM3 at Xk and Xd level) and stress states were utilized. The approach is described in detail and is largely reproducible except for some assumptions which remain unclear: 1) assumption of pre-deformation before support installation, 2) N-M diagrams for the structural safety analysis and 3) the convergence criterion of the numerical code used to assess structural safety. As mentioned by NAGRA (2014b), the latter is not an established criterion. In continuum mechanics the disintegration of a rock mass due to large plastic deformation and associated overbreak or unravelling problems cannot be analyzed explicitly. This is especially true for buckling failure modes which likely occur at the roof and floor of tunnels in horizontally layered rock types such as Opalinus Clay at large depth when unsupported or the support fails (Lanyon et al. 2014). These buckling zones are local, clearly delimited zones (Kupferschmied et al. 2015). Thus, the structural safety analysis needs to deal with a local failure phenomenon rather than global failure.

The major findings are in agreement with common knowledge in tunneling in general and more specifically with tunneling in low permeability rock types (e.g., increasing deformation and plastic zone with depth; long-term displacements due to excess pore pressure dissipation). Long-term lining loads increase according to NAGRA (2014b) by 12% within 4 years⁷. This may depend on the choice of properties for the lining stiffness, the hydraulic and poro-elastic properties of the rock mass. Measurements conducted by Neerdael et al. (1999) at the Tournemire test site suggest a much larger lining load (pressure) increase (i.e., by a factor of 7 within 20 days after excavation). The calculated radial displacements reported by NAGRA (2014b) increase within 4 years by 60% and are, in general agreement with measurements made in the Mont Terri URL.

The majority of the calculations are based on effective strength properties representative for GM3 at the Xk level. As pointed out in section 2.1.6 the strength properties suggested by NAGRA overestimate the actual strength and the degree of overestimation cannot be quantified. Even though general

⁷ Lining loads are only reported at $t = 4$ years. It is not clear if these loads are the most critical loads.

qualitative conclusions on the EDZ depth and the tendency for an increasing EDZ depth with increasing overburden can be done.

For the effective stress calculations effective strength and stiffness properties are required. In NAGRA (2014b) effective rock mass properties have been used for the strength, but not for the stiffness. For the latter, the properties derived from the undrained E -Modulus normal to bedding have been utilized (i.e.; $E_u = 8.16$ GPa at the Xm level, 6.12 GPa at the Xk level and 4.08 GPa at the Xd level; the suggested drained E -Modulus is $E_d = 4.0$ GPa). In addition, the undrained E -Modulus were determined from unloading / reloading cycles (E_{ur}). Considering the simplifications of the geomechanical model introduced by NAGRA (i.e. plastic deformation prior to failure are not considered) the suggested values for E_{ur} are too stiff. Despite the issue of using an E -Modulus derived from unloading/reloading cycles, a mixture between drained and undrained rock properties (i.e. drained strength, undrained E -Modulus and drained Poisson's ratio) is not acceptable and impacts the results, in particular the magnitudes of tunnel displacements which are further used in tunnel strain based criteria for the maximum depth assessment. The choice of a single value for the drained E -Modulus for the depth range between 400 and 900m is not in agreement with laboratory data, which suggest a substantial increase. As shown by Bobet et al. (1998), an increase in stiffness with increasing effective confining stress can substantially affect the results of numerical calculations, in particular the lining loads the accumulate in the short and long-term. Ignoring the stress dependent increase in stiffness can lead to wrong conclusions and needs to be considered in numerical calculations.

Effective stress calculations in FLAC2D are based on the theory of poro-elasticity for an isotropic linear-elastic medium and require quantifying the Biot-Modulus M defined as:

$$M = \frac{K_f}{n + (\alpha - n)(1 - \alpha) K_f / K}$$

Where K_f is the bulk modulus of water, n the porosity, K the drained bulk modulus of the rock and α the Biot coefficient. For the elastic properties assumed by NAGRA (2014b) for the Xm, Xk and Xd level the calculated Biot Moduli are 12.8, 11.6 and 9.8 GPa using the above equation ($K_f = 2$ GPa; $\alpha = 0.8$, $n = 0.11$ for Opalinus Clay deep). The actual used values for M (Table B.4-1 in NAGRA 2014b) are 6.9, 6.5 and 5.9 GPa and are not in agreement with the theory.

M , α and K are related to the Skempton's coefficient B by the following equation:

$$B = \frac{\alpha M}{K + \alpha^2 M}$$

For the poro-elastic properties used by NAGRA (2014b), the Skempton's coefficient ranges between 0.53 for the Xm level, 0.61 for the Xk level, and 0.70 for the Xd level. These values of B are actually used by the numerical code for short-term undrained loading situations. Using values for M calculated with the above equation and the elastic properties used by NAGRA (2014b), Skempton's B ranges between 0.73 (Xm), 0.78 (Xk) and 0.85 (Xd). Despite the inconsistencies of the M -values reported by NAGRA (2014b), the suggested drained E is 4 GPa for Opalinus Clay deep. This suggestion is in agreement with reliable laboratory test results. For the suggested drained E -Modulus for Opalinus Clay deep, the above equation yields $B = 0.85$. This B -value is in reasonable agreement with actual measured B -values for Opalinus Clay (Jahns 2013). The consequence of using too small B -values is that the pore pressure changes Δu associated with changes in mean stress $\Delta \sigma_m$ ($\Delta u = \Delta \sigma_m B$) or volumetric strain are underestimated and can affect both short- and long-term deformations and plastic zone dimensions.

For the isotropic poro-elasticity assumed in FLAC2D the undrained E_u can be calculated from the drained E and Poisson's ratio using the following equation:

$$E_u = \frac{1 + \nu_u}{1 + \nu} E$$

Where ν_u is the undrained Poisson's ratio expressed as (Rice and Clearly 1967):

$$\nu_u = \frac{3\nu + B(1 - 2\nu)\alpha}{3 - B(1 - 2\nu)\alpha}$$

For the Poisson's ratio ν of 0.27, a Biot coefficient α of 0.8 and the values given for M by NAGRA (2014b), the modelled undrained E-Moduli can be calculated to be 9.2 GPa (at the Xm level), 6.6 GPa (at the Xk level) and 4.5 (at the Xd level). Using the suggested drained E-Modulus (i.e. $E = 4\text{GPa}$ ⁸), and the above equations to derive the undrained Poisson's ratio and undrained E-Modulus E_u based on the properties suggested for the Poisson's ratio and the Biot coefficient in NAGRA (2014b), the actually modelled E_u overestimates the undrained E-Modulus by a factor of approximately 1.5 for the case of the Xk level. The poro-elastic properties used for the calculations and specified by NAGRA (2014b) have several consequences on the results of the analysis: 1) Pore pressures during undrained loading are underestimated because B for the case (Xk) is smaller than B values measured for Opalinus Clay (Jahns 2013), 2) the modelled rock mass is significantly stiffer (by a factor of 1.5 for the case of the Xk level), 3) calculated tunnel displacements and thus tunnel strains are underestimated and 4) calculated lining loads are unreliable for both the short- and long-term.

3.4.2.2 Conclusions

Several issues were identified which affect the reliability of a quantitative assessment of the maximum depth below ground surface using the reported effective stress calculations: 1) both the used rock mass strength and stiffness overestimate the actual strength and stiffness, 2) the specified rock mass properties used for the effective stress calculations are partly inconsistent with the theory, 3) an increase of the drained E-Modulus with increasing effective stress (i.e. depth) is not considered for the depth range between 400 and 900 m (i.e. a constant E-Modulus is assumed), and 4) a structural analysis of the various support types using FLAC2D is not presented by NAGRA (2014b).

The above mentioned issues 1 and 2 affect the calculated displacements and the EDZ depth which are further used in design criteria for a quantitative assessment of the technical feasibility and long-term safety. Issue 3 affects the diametral tunnel strain and therefore the maximum depth assessment. In addition, the increase in drained E-Modulus between 400 and 900 m need to be considered for engineering feasibility calculations utilizing support elements (see Bobet et al. 1998).

The above mentioned issue 4 is of foremost importance since depth limitations are to a considerable extend related to limitations in support measures, which may not allow to control the rock mass behavior within specified limits at larger depth. This is especially true for the intermediate sealing sections ("Zwischensiegel") between two sections of HLW repository tunnels. These sections have been identified by the reviewers as the most critical sections of a HLW repository (NAGRA 2014b). Within these sealing sections the tunnel circumference needs to be controlled (i.e. no overbreak) in such a way as to provide optimal conditions for bentonite placement with direct contact to the host rock. The basic design in these sealing sections considers steel arches and wire mesh for rock fall protection. From Figure 5.3-2 in NAGRA (2014b) it seems that full shear-bond was assumed between the support element and the rock mass. At least for the case of steel-arches this assumption is not appropriate. For a quantitative assessment of the maximum depth it is required to 1) assess the depth at which the load bearing capacity of the rock support is exceeded and 2) address the question at which depth the selected support measure will not allow a reliable ground control.

⁸ For the example it is assumed that the drained E-Modulus is 4GPa for the Xm, Xk and Xd level.

3.4.3 Analytical and semi-analytical method

3.4.3.1 General comments

Ground reaction curves (GRC) have been used for estimating the long-term displacements, the extent of the plastic zone and for preliminary structural analysis, i.e. the depth at which the load bearing capacity of the support is exceeded.

The limitations of the ground reaction curve are discussed by NAGRA (2014b) (i.e., the anticipated ground behavior and boundary conditions deviate significantly from the assumption of an isotropic stress state and uniform radial displacements/pressure distribution). Reduction factors for the maximum load bearing capacity of the lining were introduced according to Kovári (1998) to account for the anticipated ground conditions that leads to non-uniform displacements (i.e. non-uniform distribution of rock pressure due to anisotropic rock mass strength, deformability, and in-situ state of stress). A factor of 1.3 was assumed for the non-uniform pressure distribution (i.e. P_A/P_B , Figure 15, Kovári and Staus 1996).

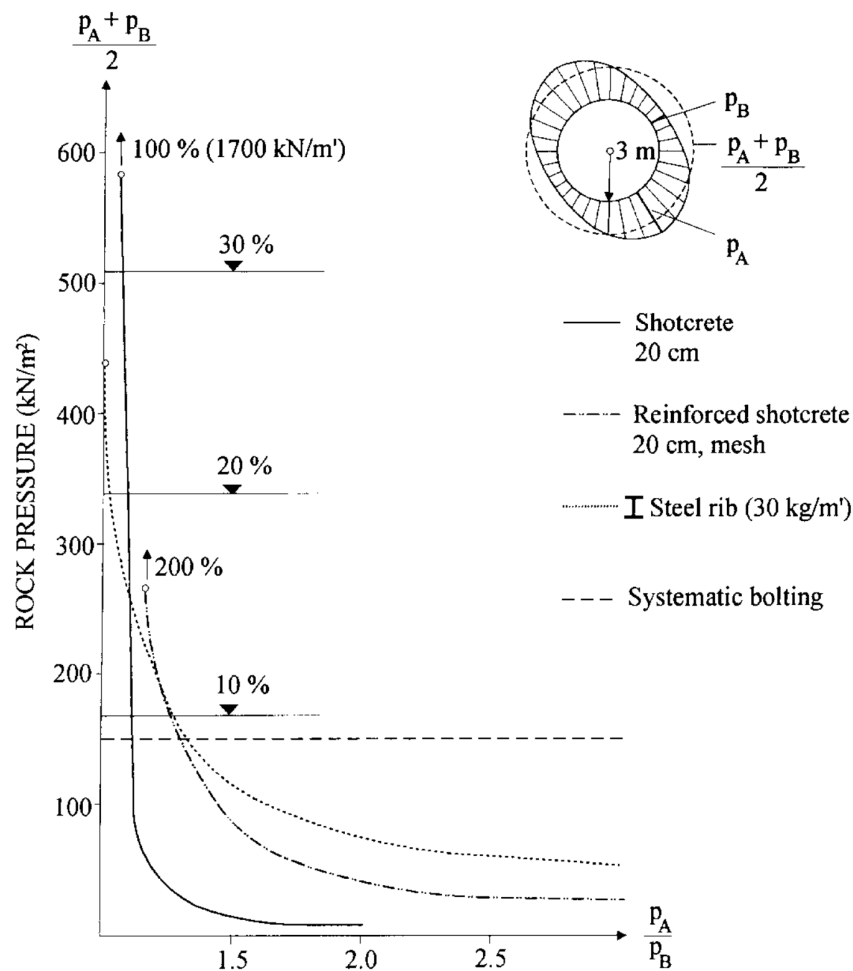


Figure 15: Load bearing capacity versus non-uniform load distribution P_A/P_B (Kovári and Staus 1996) for an unreinforced shotcrete, a mesh reinforced shotcrete, steel arches and systematic bolting. A circular tunnel of 6 m diameter was considered. Except for rock bolts the load bearing capacity decreases significantly for even slight non-uniform load distributions. Note that the reduction of the load bearing capacity depends on the ratio P_A/P_B and the ratio of the lining thickness / radius.

The maximum load bearing capacity for both shotcrete and steel arches was reduced by a factor of 2, and for concrete segments a factor of 0.66 (due to the low bending stiffness) was assumed. For the structural analysis GM3 rock mass properties at the Xk level were used (bedding plane strength).

Kovári (1985) states that for non-uniform load distributions the GRC is not directly applicable and more or less arbitrary assumptions have to be introduced, which are not further discussed in Kovári (1985). In these cases finite element codes with advanced constitutive relations should be used for a correct analysis.

Total stress calculations have been utilized using effective strength properties. The approach was considered to yield long-term deformations and EDZ extends. Anagnostou (2009) shows that this approach is sufficiently exact when the ground is drained/consolidated ahead of the tunnel face prior to excavation. In case the ground is not drained, pore pressure gradients during excavation arise, which significantly influence the total displacements and the extent of the EDZ. The consideration made by Anagnostou (2009) assumes isotropic stress and strength conditions and an elasto-plastic material behavior with zero dilation.

Displacements and EDZ extent calculated with both FLAC2D and the ground reaction curve are compared by NAGRA (2014b) with the aim to demonstrate that both methods yield comparable results. Displacements obtained from unsupported numerical simulations are compared with results from GRCs considering support pressures between 0 and 1.0 MPa, and strength properties either representative for bedding planes or the matrix (i.e. the strength properties for the GRCs are isotropic. Thus, either only the bedding plane strength or only the matrix strength was considered for GRCs in NAGRA (2014b)). In addition short- and long-term results are compared. Long-term displacements predicted with the ground reaction curve for an unlined repository tunnel (assuming bedding plane strength) are significantly larger than predicted with FLAC2D, which is in contrast to the findings of Anagnostou (2009) and maybe related to two reasons: 1) long-term effective stress calculations for HLW repositories used for the comparison were performed for a limited amount of dissipation time, and excess pore pressures are not entirely dissipated (from the description in NAGRA 2014b it is not clear which dissipation time was considered) and 2) the assumption of bedding plane strength is not representative and the calculated displacements are overestimated (note that GRCs using matrix strength properties estimate displacements which are smaller than displacements calculated with FLAC2D). The above comparison shows, however, a reasonable agreement between FLAC2D and the GRC in the extent of the plastic zone. Considering that three tunnel strain based criteria are used (EI-2, 3, 4) for the analysis of the maximum depth below ground surface, and the calculated displacements are uncertain, quantitative conclusions on the maximum depth below ground surface are unreliable.

In addition, similar to the effective stress calculations using FLAC2D, effective rock mass properties have been used for the strength, but not for the stiffness. Note that for an isotropic poro-elastic medium the maximum ratio between $E_u/E_d = 1.2$ (for a Poisson's of 0.25 and the assumption of an incompressible fluid). Thus, the difference is small and can be neglected for engineering design. In case of a transversal isotropic medium such as Opalinus Clay the ratio E_u/E_d is larger (i.e. this ratio is approximately 2 as shown in NAGRA (2014a)). The difference between undrained and drained E -Moduli is large and cannot be neglected for engineering design⁹. Selecting a too high E -Modulus (see also section 2.1.5.1) affects the magnitudes of both elastic and radial tunnel deformations estimated with the ground reaction curve (see equations Appendix D-2 in NAGRA 2014b). Thus, the deformations are underestimated by a factor of 2 in GRCs that utilize undrained rather than drained E -Moduli (the radius of the plastic zone remains, however, constant). Further, the consequences of the simplifications of the constitutive model introduced by NAGRA, and the increase in drained E -Modulus with increasing effective stress in the depth range between 400 and 900 m need to be considered for the choice of the drained E -Modulus.

⁹ Note that a reduction in E by a factor of 2 used in the GRC doubles the radial displacements while the radius of the plastic zones remains constant.

Experimental data provided by NAGRA suggest that the drained E-Modulus of the intact Opalinus Clay increase by a factor of 3.3 between 400 m and 900 m depth. This has a significant influence on the tunnel displacements and thus the assessment of the maximum depth below ground surface using tunnel strain criteria.

Two cases for support installation have been considered by NAGRA: 1) Installation of support at a distance of one tunnel diameter ($1 \times D$) behind the tunnel excavation face (called “Widerstandsprinzip”) and 2) Installation of support at a distance of three tunnel diameters ($3 \times D$) behind the tunnel excavation face (called “Ausweichprinzip”¹⁰). The ground reaction curve predicts uniform radial displacements stemming from elastic and plastic deformations (i.e. shear failure of the rock mass). The observed behavior in the Mont Terri URL consists of a combination of shear and extensional type failure modes around and ahead of excavations (Lanyon et al. 2014). Borehole measurements using extensometers show strongly localized deformations normal to bedding and distributed deformation along bedding (see summary in Lanyon et al. 2014). In addition, borehole observations suggest that overbreak associated with deep, delineated buckling zones may develop within few days in boreholes drilled parallel to bedding (Kupferschmied et al. 2015, Labious and Vietor 2014). Overbreak was also reported by Steiner (2014) for the Bözberg Tunnel (in the folded Jura section), and rapidly developing overbreak in the Mont Russeline exploratory tunnel (tunnel radius 1.77 m; open TBM excavation in folded Jura). Thus, non-uniform deformations and local overbreak within an unsupported span need to be anticipated (at least in tectonically overprinted sections and/or at larger depths) unless support measures are installed early (i.e. close to the tunnel face). Thus, the case considering yielding support that deforms to approximately 9 m behind the excavation face in case of a HLW emplacement tunnel is assessed critical, since yielding support is not as effective in supporting the rock mass from overbreak as compared to a rigid, early installed support. This is especially true when the rock mass contains weaknesses as described for GM 2, 3 and 4 or at greater depths where the rock may disintegrate due to intense accumulated plastic straining. This is of particular relevance for the assessment of the installation conditions in intermediate sealing sections of HLW emplacement tunnels (with design indicator EI-3), where the assumed tunnel support consists of TH25 steel arches with wire mesh only. For these sealing sections the ground reaction curve suggests that the load bearing capacity of TH25 steel arches installed one tunnel diameter ($1 \times D$) behind the tunnel excavation face will be exceeded already between 400 and 500 m.

In addition, the pre-deformations (i.e. deformations that occur ahead of the tunnel face, or before support installation) were estimated following Panet in NAGRA (2014b), but the corresponding quantities are not reported. From Figure 5.4-2 in NAGRA (2014b) it is obvious that the pre-deformations are dependent on the location of support installation and depth (e.g. assuming support installation $1D$ behind the tunnel face, the pre-deformations are 25% for 900m depth and 70% for 400m depth. Assuming support installation $3D$ behind the tunnel face, the pre-deformations are 50% for 900m depth and 90% for 400m depth). These values are difficult to reproduce and need to be explained in greater detail. Further, different angles of dilatancy were assumed (i.e. $0, 5, 10^\circ$ for the matrix and $0, 1, 2^\circ$ for the bedding planes). From the description in NAGRA (2014b) it is not clear in which calculation which dilatancy was assumed.

3.4.3.2 Conclusions

Using the method of ground reaction curve (GRC) for reliable and quantitative conclusions on the maximum depth is problematic, because the deformation characteristics, in-situ stress conditions and the ground behavior deviate significantly from the assumptions for which the GRC concept was developed. Additional assumptions need to be made, reducing the reliability of a quantitative

¹⁰ Note that for the GRCs all support types are installed at different distances from the tunnel face and are rigid. For the case of support installation $3 \times D$ behind the tunnel face a flexible support type (yielding support) is assumed which is usually installed close to the tunnel face and deforms with the rock to a certain limit (as shown in Appendix A3, NAGRA 2014b). The calculation does not explicitly account for the support closure phase.

assessment. The reliability of a quantitative assessment of the maximum depth below surface is further affected by the used rock mass properties (i.e. effective strength is overestimated, undrained rather than drained elastic properties are used, effective stress dependency of the drained E-Modulus is not considered for the depth range between 400 and 900 m, the effects of the simplified constitutive model on the choice of the E-modulus are not considered, GRCs assuming bedding plane strength may over-predict the displacements). As a consequence, a quantitative assessment of the maximum depth is largely uncertain.

For the most critical intermediate sealing sections of HLW emplacement tunnels the load bearing capacity of a support class utilizing TH25 steel arches is exceeded between 400 and 500 m when the support is installed at a distance of one tunnel diameter ($1 \times D$, i.e. 3 m) behind the tunnel excavation face.

For the case of yielding support the load bearing capacity is exceeded at a depth between 600 and 700 m. A yielding support that develops its full support capacity at $3 \times D$ behind the tunnel excavation face (i.e. 9 m) is considered critical due to less control on rock mass damage or local failure, at least for rock mass models that contain bedding parallel weaknesses or at greater depths where the rock may disintegrate due to intense accumulated plastic straining. The GRC analysis suggests that with the currently available/considered support measures in the intermediate sealing sections the maximum depth is strongly reduced. Owing the above mentioned issues, quantitative results to constraint the maximum depth below ground surface are unreliable for both displacements and the depth where the maximum load bearing capacity is exceeded. The conclusions of NAGRA (2014b), p. 101, which state that the constructability is given and the maximum depth below ground surface is solely associated with the long-term safety, contradicts with the GRC analysis and is not reproducible.

3.4.4 Total stress calculation using Phase2

3.4.4.1 General comments

Total stress calculation using Phase2 in Lanyon et al. 2014 utilize undrained shear strength (S_u) values which partly significantly overestimate the strength for both matrix and bedding (see section 2.1.5.3). In addition, distributed joint elements were considered discontinuous (the assumptions used for the joint element distribution and persistence / joint length could not be found in Lanyon et al. (2014) while the rock mass anisotropy was calculated according to Duncan and Goodman (1968). Duncan and Goodman (1968) assumed fully persistent joints. This has an influence on the actual modelled rock mass stiffness.

Table 8 shows the E -moduli normal to bedding for different assumptions of the joint persistence and joint length. The values were derived from an axially loaded block model in Phase2 which consists of an elastic matrix ($E = 18$ GPa) with embedded joint elements with a normal and shear stiffness of 8000 MPa/m). The joint frequency was 20 1/m and the same for all models. The model shows reasonable agreement with the analytical solution for fully persistent joints. For non-persistent joints E normal to bedding increases and A decreases significantly. The spectrum of the anticipated anisotropy coefficient of $1 < A < 7$ was, therefore, not addressed.

Table 8: Comparison between E normal to bedding and anisotropy coefficient A for different assumption of joint persistence and joint length.

	Duncan and Goodman (1968)	Case 1	Case 2	Case 3
Persistence (%)	100	100	50	25
Joint Length (m)	infinite	infinite	5	10
E normal to bedding (GPa)	392	422	970	1570
Anisotropy coefficient A	6.8	6.5	4.4	3.4

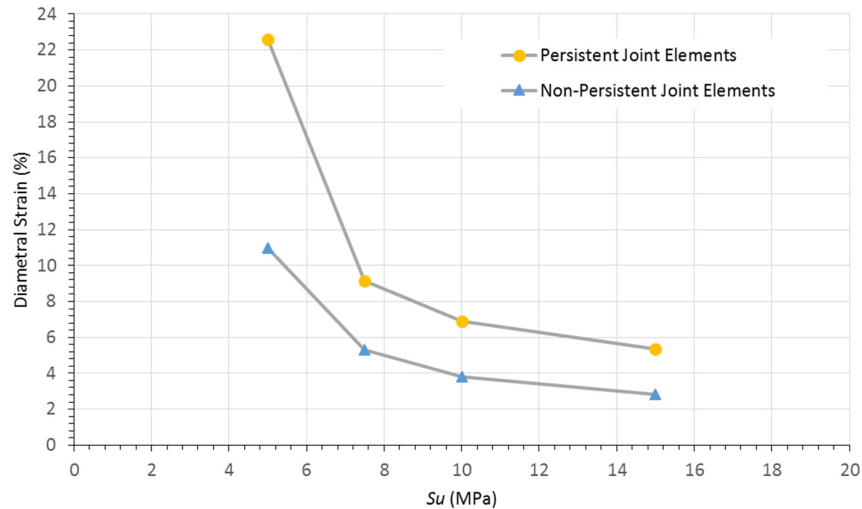


Figure 16: Comparison in diametral tunnel strain assuming persistent and non-persistent joint elements in Phase2.

The impact of joint element persistence on the calculated diametral tunnel strains is shown in Figure 16¹¹. The calculated tunnel strains differ between models assuming non-persistent (50%) and persistent joints depending on the S_u by 2.5 % to 11 %.

For each calculation by Lanyon et al. (2014) an elastic calculation was performed. Half (50%) of the elastic deformations were subtracted from the total deformations assuming that these deformations occur ahead of the tunnel face. This assumption stems from experience gained from the mine-by experiment at the Mont Terri URL. Beside the fact that deformations ahead of the tunnel phase may depend on depth, the rock mass strength and stiffness, the support measures and support installation time as shown by NAGRA (2010), the calculation of normalized tunnel strains is not consistent with the design criteria.

Three design criteria are based on normalized tunnel strains calculated from total deformations at the time of support installation ($u(e)/a$) or at the end of the excavation (ua/a). Thus, the reported results of the Phase2 calculation cannot, in principle, be used with the suggested design criteria EI-2, 3 and 4 unless the elastic deformations are very little and can be ignored. This, however, is not shown.

Despite the discussion of the applicability of tunnel strain based criteria suggested by NAGRA, tunnel strains calculated with Phase2 are based on rock mass properties which overestimate the strength.

3.4.4.2 Conclusions

The total stress analysis with Phase2 provides tendencies for the EDZ depth and displacements. A quantitative assessment of the maximum depth is, however, not possible. This is mostly due to the used strength properties which overestimate the strength, and the sensitivity of the model results to the assumptions of joint element persistence.

3.4.5 ETH Assessment of NAGRA's Findings and Conclusions

The findings and conclusion given by NAGRA (2014b) are inconsistent. In some sections it is stated that even with limitations in support measures the construction of a HLW emplacement drift is feasible in a safe way down to a depth of 900 m. In other sections it is stated that for the available support types and for support installation close to the tunnel face (i.e., considering the so called "Widerstandsprinzip")

¹¹ The same tunnel geometry and the reference stress states at a depth of 900 m according to Lanyon et al. (2014) were used for the calculations by means of Phase2. For the matrix an elastic modulus E of 18 GPa was assumed and a normal and shear stiffness of 8000 MPa/m. The considered joint frequency was 20 1/m.

HLW repository construction is only possible to a depth between 600 and 700 m or that the analysis suggests that for HLW repositories at depths greater than 700 m the design criteria for EDZ depth and EDZ conductance may be violated.

It was shown by NAGRA that the load bearing capacity of the steel sets in the sealing sections is critical for the maximum depth assessment and is exceeded at a depth of 400 to 500m assuming support installation at a distance of one tunnel diameter ($1 \times D$) behind the excavation face. For the assumption of a yielding support the load bearing capacity of this support type is exceeded at a depth between 600 and 700 m. Yielding support is considered critical at large depths or in tectonically overprinted sections, where large and systematic overbreak may have to be expected.

As discussed in section 3.4.3 the depth range (where the load bearing capacity is exceeded) is unreliable because of the various assumptions used in the GRC analysis, and no quantitative conclusion can be made.

In summary, the quantitative conclusions and classifications of the maximum depth provided by NAGRA are not reproducible based on the reported results. This is primarily related to the selection of inappropriate design criteria (strain based criteria EI-2, 3, 4), the rock mass strength properties which overestimate the strength, and the elastic properties used in effective stress calculations. The discussion of the maximum depth below ground surface should be closely related to the expected geological hazards, depth dependent rock mass properties and the limitations in support measures, especially in the intermediate sealing sections.

4 Assessment of long-term EDZ evolution of HLW waste emplacement drifts

The short term EDZ properties are discussed in Chapter 3 and used for the determination of maximum repository depth. They are valid for the period before Bentonite buffer and EDZ re-saturation start to become effective, before the heat generated from the waste packages, geochemical alterations and gas generation start to influence significantly the Opalinus Clay properties. This short-term period is assumed to last a few years and corresponds to the time until backfilling of individual waste emplacement drifts (Figure 17).

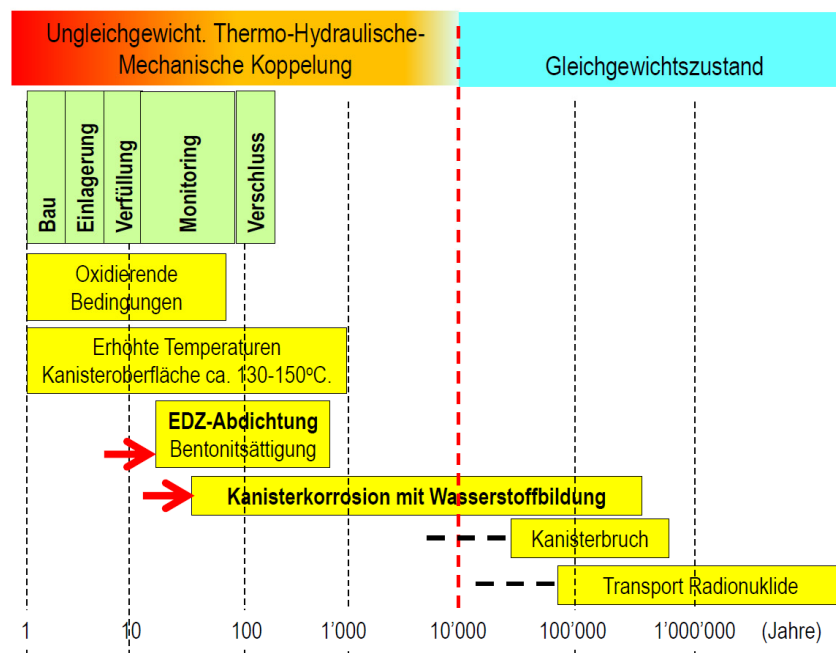


Figure 17: Nuclear waste repository evolution with time (from Bossart 2013).

In the longer term, i.e. the first few thousand years of the HLW repository lifetime, many interacting (coupled) thermo-hydro-mechanical-chemical processes alter the properties of the near field including the bentonite buffer, rock support and EDZ. This alteration is assumed to lead to a strong reduction of EDZ hydraulic conductance, a phenomenon which is called self-sealing. While it is important to understand the individual processes and interactions during this transformation of the repository near-field, the repository near field properties at the time when the waste canisters are corroded to such a degree, that radionuclides are released, is of highest relevance. This time is assumed to correspond to many thousands of years after repository sealing, i.e. at a time when the transient near-field processes have again reached a thermal-hydro-mechanical steady-state situation.

NAGRA's approach to investigate the evolution of the EDZ includes laboratory experiments, observations and in-situ experiments in underground excavations (traffic tunnels in Jura Mountains, Mont Terri, Bure, Tournemire) and numerical simulations. These are summarized and discussed in the following sections. The impact of long-term EDZ properties on long-term safety is discussed in NTB 14-10. One major conclusion from this report is that radionuclide transport along the EDZ of emplacement tunnels only becomes relevant when the hydraulic conductance is bigger than $1E-7 \text{ m}^3/\text{s}$.

*Table 9: Consolidation and swelling indices summarized from Giger and Marschall (2014), including lower and upper bounds where stated. *NAGRA states (based on personal communication with Favero (EPFL)) that this value should be used with caution as the tests were not designed to examine long-term creep. Note that not all of the sources cited in Giger and Marschall (2014) have been reviewed.*

Value	Lower Bound	Upper Bound	Sources cited in Giger and Marschall (2014)
C_c	0.02	0.09	Ferrari et al. 2012, Chiffolleau and Robinet 1999
C_s	0.007	0.017	Chiffolleau and Robinet 1999, Horseman and Harrington 2002 (unpublished)
C_a		0.001*	NAGRA – Favero personal communication
S_e (%)	1.4	9	Mathier et al. 1999, Vöggtli and Bossart 1998
P-orientation			
p_s (MPa)	0.1	0.2	Vöggtli and Bossart 1998, Ferrari et al. 2012
P-orientation			
S_e (%)	0.7	11	Mathier et al. 1999, Ferrari et al. 2012
S-orientation			
p_s (MPa)	0.4	1.4	Vöggtli and Bossart 1998, Ferrari et al. 2012
S-orientation			

4.1 Lab and modelling investigations of Opalinus Clay self-sealing by NAGRA

4.1.1 Intact rock laboratory tests related to consolidation and swelling

The laboratory tests related to long-term behavior summarized by Giger and Marschall (2014) focus on intact samples of Opalinus Clay. Consolidation and swelling tests were conducted to determine the compression index (see equation 1 below), swelling index (see equation 2 below), secondary compression index or creep (see equation 3 below), swelling strain and swelling pressure. Typical values summarized by Giger and Marschall (2014) are shown in Table 9. Also reported are swelling pressures p_s and swelling strains S_e conducted with free and confined boundary conditions. The supporting equations and test type from which the values come from are listed below:

$$C_{c=-\Delta e/\Delta \log \sigma'_v} \quad (\text{during loading in a consolidation test}) \quad (1)$$

$$C_{s=-\Delta e/\Delta \log \sigma'_v} \quad (\text{during unloading in a consolidation test}) \quad (2)$$

$$C_{a=\Delta e/\Delta \log t} \quad (\text{secondary compression during re-loading in a consolidation test – creep rate}) \quad (3)$$

Where Δe is the change in void ratio, $\Delta \log \sigma'_v$ is the change in log of the applied (vertical) effective stress and t is time.

4.1.2 In-situ observations and measurements related to EDZ self-sealing

Longer term observations and in-situ experiments related to EDZ evolution have been recorded at the Mont Terri URL up to a maximum of 3500 days and include visual documentation, convergence and pore pressure measurements, measurements of deformation with extensometers, resistivity surveys, and hydraulic packer testing.

Observations of the EDZ at the Mont Terri URL (Lanyon et al. 2014) are typically related to short-term excavation and borehole behavior during construction or shortly after drilling. The underground excavations are supported by shotcrete, systematic bolting or steel sets soon after excavation. The observations document the influence of structural control on the initial development of the EDZ, both related to tectonic features (Figure 18a) and bedding (Figure 18b). Convergence monitoring at Mont Terri has been and continues to be conducted at many locations throughout the URL. Measurements have been summarized by Lanyon et al. (2014). Typical measurements are in the order of 1 to 2 % diametral strain, with maximum long-term diametral strain of 1.7% being measured in an excavation, with support, along the strike of the bedding. In unsupported excavations local diametral strains of approximately 4% (EZ-B tunnel) have been measured. Local diametral strains in supported tunnels have reached 3 to 4% (Mine-By & FE experiments) and have been attributed to bedding normal displacements and a thin fault zone. Typically convergence is larger for excavations with a heading parallel to bedding and for monitoring points perpendicular to the bedding plane, as illustrated in Figure 18b – right.

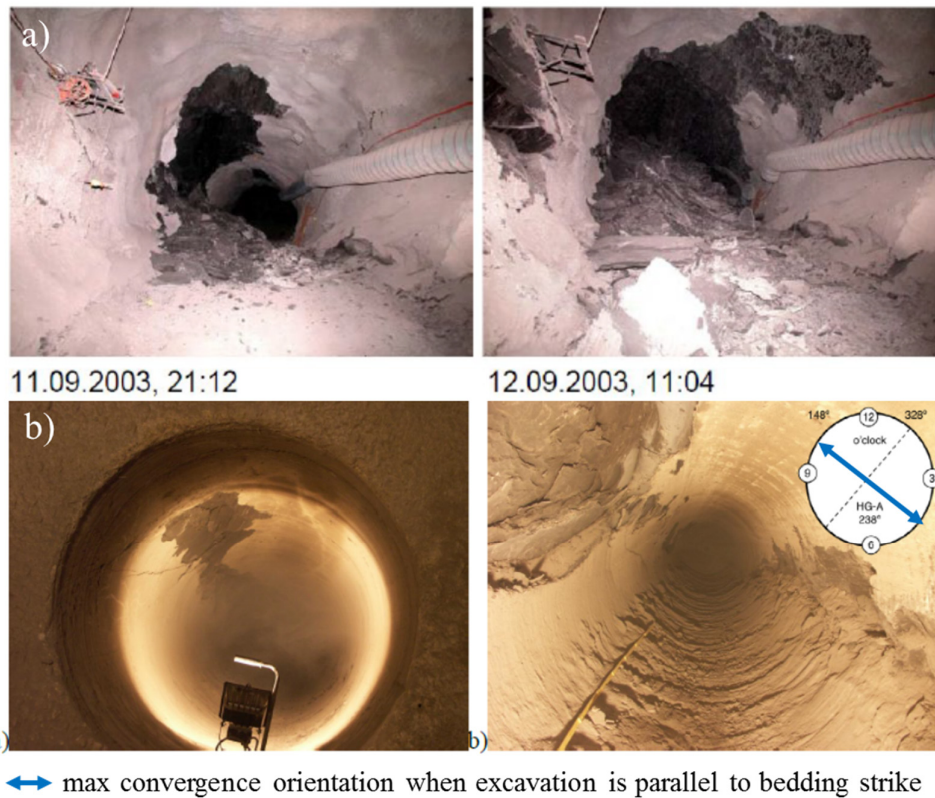


Figure 18: a) Development of a large structurally controlled overbreak in the EZ-A Niche due to interaction of the excavation damage with pre-existing fault and b) influence of bedding on minor overbreak within the HG-A microtunnel with illustration of maximum convergence measurement cord orientation for excavations parallel to bedding strike (from Lanyon et al. 2014).

The most notable long-term experimental measurements, in terms of duration of measurements and in relation to long-term EDZ evolution include:

- An EDZ transmissivity experiment (EH) with 800 days of saturation followed by 100 days of pressure build up from a plate loaded by 1 – 5 MPa (Figure 19)
- The sealing index for the HG-A experiment with a saturation phase of approximately 365 days, followed by multiple phases of hydraulic testing up to 8 years after the start of the experiment (Figure 20).

Figure 19 and Figure 20 both show that the hydraulic parameters, transmissivity and effective hydraulic conductivity respectively, of the EDZ substantially reduce with time. During the re-saturation phase of the plate loading test the EDZ transmissivity is reduced from about $2\text{E-}7 \text{ m}^2/\text{s}$ to $2\text{E-}9 \text{ m}^2/\text{s}$ and with the application of a plate load of up to 5 MPa onto the excavation wall a further transmissivity reduction to about $2\text{E-}11 \text{ m}^2/\text{s}$ is observed, demonstrating empirically the role of bentonite swelling pressure on an excavation in the Opalinus Clay.

The HG-A experiment consists of a 6 m long steel-lined section, a 3 m long packed-off sealing section and 3 m long test interval in a micro-tunnel with a diameter of 1 m (Marshall et al. 2013). The sealing section included overbreak (Figure 18) which were completely backfilled with cement prior to packer installation. Injections with water and gas behind the packer have been used to study gas and water flow and permeability in the EDZ under variably saturated and pressurized conditions (Figure 21).

EDZ effective hydraulic conductivity in the sealing section (normalized to an EDZ area of 1 m^2) is a function of time, fluid and packer pressure. Under elevated packer pressures ($> 3 \text{ MPa}$) fluid pressure in the test section continuously increases under constant injection rates, suggesting reduction in hydraulic conductance with time by self-sealing. When the packer pressure drops to about 2 MPa (under elevated fluid pressures), a significant but reversible increase in effective hydraulic conductivity is observed and explained by re-opening of closed fractures in the EDZ by normal dilation.

These in-situ measurements have been used to support the modelling concepts presented by Alcolea et al. (2014) described in the next section.

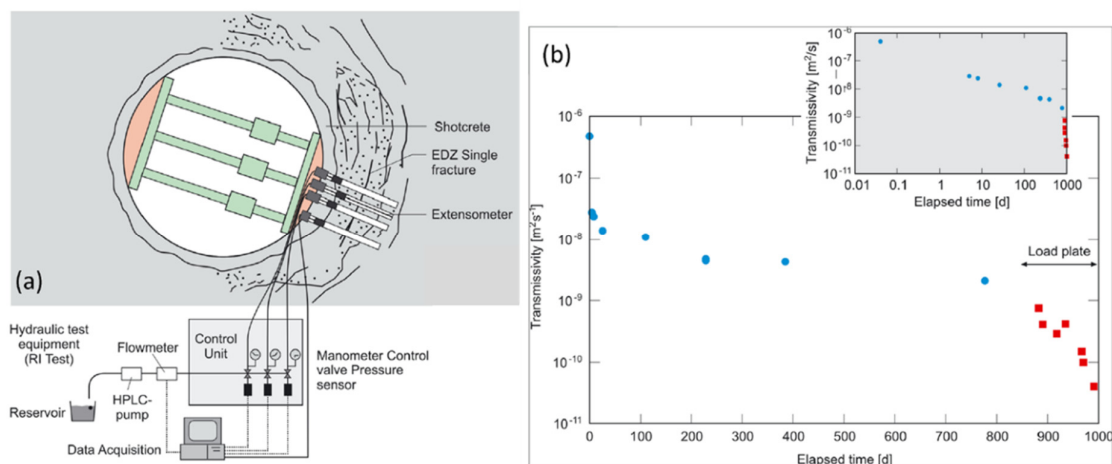


Figure 19: Long-term changes in the EDZ bulk transmissivity due to re-saturation for 800 days and from mechanical compaction / consolidation pressures between 1 – 5 MPa (from Alcolea et al. 2014).

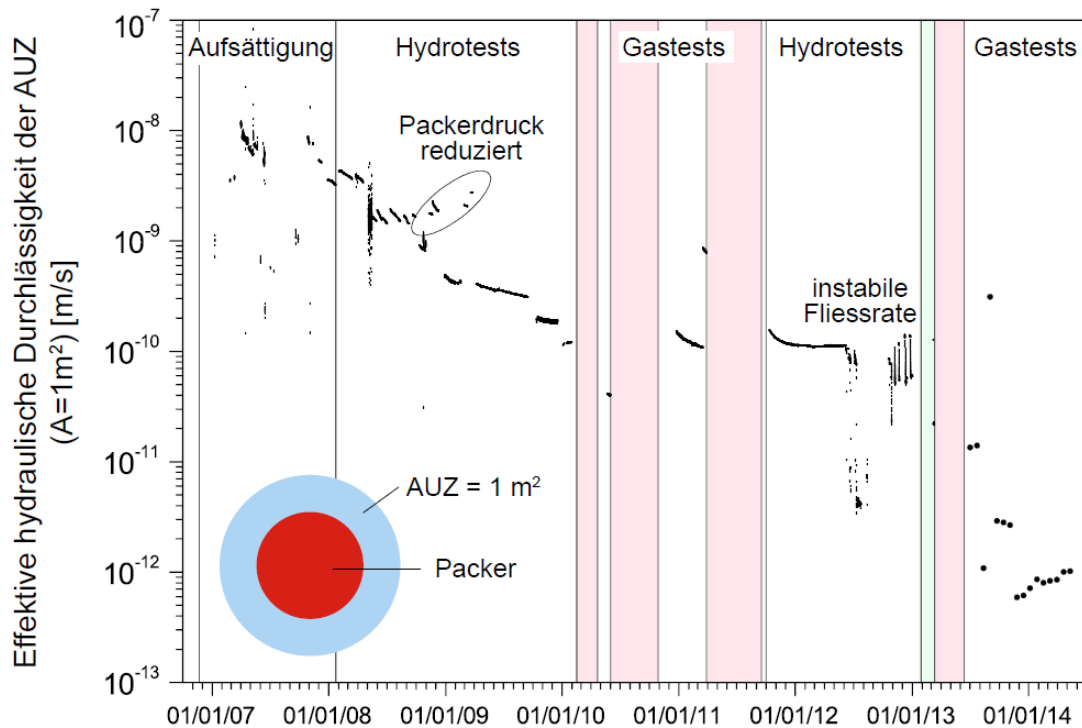


Figure 20: Longer term effective hydraulic conductivity changes during the HG-A experiment at Mont Terri for an equivalent radial EDZ. (from Alcolea et al. 2014)

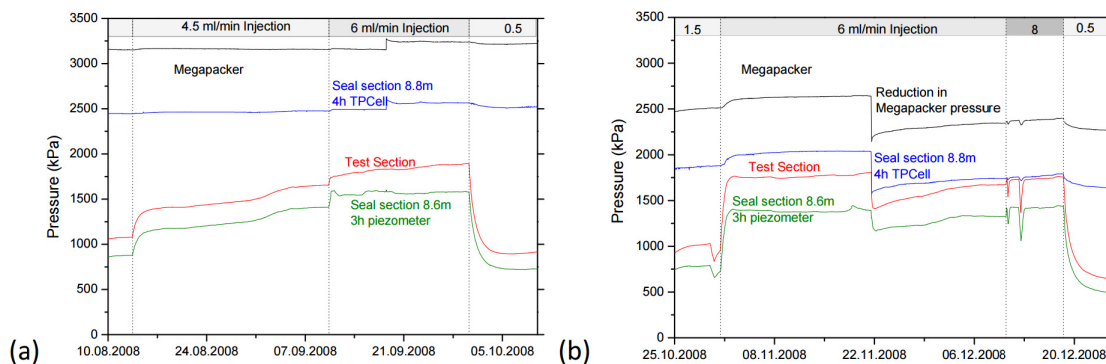


Figure 21: Relationships between packer pressure (black line), test section fluid pressure (red line) and stress in sealing section (blue line) and sealing section fluid pressure (green line) during constant rate injection tests of the HG-A experiment a) test response under high packer pressure, b) test response under lower packer pressure (from Marschall et al. 2013).

4.1.3 Numerical simulations of long-term EDZ self-sealing

Fracture mechanical numerical simulations of the EDZ evolution from Geomechanica (2013) include construction evolution (2D representation of 3D tunnel advance), bentonite swelling, and shotcrete support degradation. Rock mass swelling, pore pressure equilibrium and the influence on the fracture network is simulated and analyzed by Alcolea et al. (2014). Other numerical simulations have been conducted that deal with time dependent evolution of the repository near-field, such as thermal and gas pressure evolution, however these are beyond the scope of this review. The numerical simulation type and the time dependent aspects considered are shown in Table 10. The individual aspects of the reports by Geomechanica (2013) and Alcolea et al. (2014) are summarized in the following sub-sections.

Table 10: The time dependent aspects considered by NAGRA and the associated codes to examine long-term EDZ evolution for HLW repository modelling. Note that the behaviors are categorized based on the dominate influence in reality and not based on how it is implemented in the code (i.e. swelling is the expansion of the bentonite / rock but implemented as an applied pressure to mimic swelling pressure). The symbol '-' indicates that this aspect was not included in the modelling presented in the reports reviewed.

Time Dependent Behavior	Numerical Code and Reference	
	Geomechanica (2013)	Alcolea et al. (2014)
Deformation	Bentonite swelling	Bentonite swelling Swelling of rock
Stress changes	-	Effective stress changes (pore pressure)
Strength degradation	Shotcrete degradation	-

4.1.3.1 Results of Y-Geo Simulations Presented by Geomechanica (2013)

In Geomechanica (2014) the main time dependent mechanisms are bentonite swelling pressure buildup and shotcrete liner degradation. Numerical modelling was conducted to determine the extent of excavation induced fracturing and to input the fracture network properties (location and fracture aperture) into hydromechanical simulations (Alcolea et al 2014). A range of stress conditions, influence of faults and input properties for HLW, SMA, and shaft model geometries were considered. This review focuses on the modelling results for HLW sections only.

Model Inputs

Stress conditions with vertical stresses of 15.9 to 19.6 MPa (650 – 800 m depth) and horizontal to vertical stress ratios (K_0) of 0.8 to 1.3 were considered for HLW model simulations.

Since the modelling software is for distinct elements, where each element edge represents a potential fracture pathway, the properties of the element edges or micro-mechanical properties govern the mechanical response of the model. In order to determine the micro-mechanical properties the code must be calibrated to known laboratory or in-situ behaviors.

Calibration was conducted on laboratory scale models simulating both tensile and compressive strength tests, which included anisotropic strength and stiffness. A constant stiffness was considered with a Young's modulus of 11.4 and 5.5 GPa parallel and perpendicular to bedding, respectively. The resulting calibration determines the input values (micro-mechanical values called OPA, as shown in Table 11) to be used as rock mass properties for excavation scale models. A sensitivity analysis of the input values was conducted using a multiplication factor, OPAx2 through OPAx5, for each micro-mechanical input value, since explicit excavation scale responses for calibration are only available for Mont Terri. Calibration to in-situ convergence measurements for the FE tunnel was discussed by Geomechanica (2012), but not included as part of this review. ¹²

¹² A comparison of the average field convergence values with those predicted by Y-Geo models for the FE experiment was recently published by Lisjak, A et al. (2015) The excavation of a circular tunnel in a bedded argillaceous rock (Opalinus Clay): Short-term rock mass response and FDEM numerical analysis. *Tunnelling and Underground Space Technology*; 45: 227-248.

Table 11: Input parameters (micro-mechanical properties) reported by Geomechanica (2013) and used for sensitivity analysis to the geomechanical properties of the HLW and K09 models.

Parameter	OPA	OPA x 2	OPA x 3	OPA x 4	OPA x 5
Tensile strength parallel to bedding, $f_{t,max}$ (MPa)	2	4	6	8	10
Tensile strength perpendicular to bedding, $f_{t,min}$ (MPa)	0.32	0.64	0.96	1.28	1.6
Cohesion parallel to bedding, c_{min} (MPa)	0.95	1.9	2.85	3.8	4.75
Cohesion perpendicular to bedding, c_{max} (MPa)	17.2	34.4	51.6	68.8	86
Mode I fracture energy parallel to bedding, $G_{Ic,max}$ (Jm ⁻²)	14	28	42	56	70
Mode I fracture energy perpendicular to bedding, $G_{Ic,min}$ (Jm ⁻²)	5	10	15	20	25
Mode II fracture energy parallel to bedding, $G_{IIc,min}$ (Jm ⁻²)	40	80	120	160	200
Mode II fracture energy perpendicular to bedding, $G_{IIc,max}$ (Jm ⁻²)	140	280	420	560	700

Modelling Stages

The modelling stages used capture the 3-dimensional influence of tunnel advance in 2-dimensional software (core softening), installation of rock support (concrete liner), and EDZ reconsolidation (simulation of bentonite swelling pressure and liner stiffness reduction). The core softening technique is a standard method used in 2-dimensional modelling to capture the 3-dimensional stress influences and to develop a ground reaction curve for simulation of the support installation timing.

The maximum allowable displacement for support installation timing was set to 0.1 m (total excavation closure). Support installation timing was tested in a sensitivity analysis with core softening ratios at support installation ranging between 0.01 and 0.008. Sensitivity of the support stiffness was also tested for different elastic moduli (32 GPa, 16 GPa, and 3.2 GPa).

The EDZ reconsolidation considered two aspects: the simulation of bentonite swelling by applying an internal pressure on the liner and the degradation of the liner stiffness with model time. The internal simulated swelling pressure began to increase once the mechanical (short-term) response reach equilibrium and increased in a stepwise manner from 0 to 10 MPa. Once the internal pressure reached 10 MPa the liner stiffness was decreased in a stepwise manner from 32 GPa to 0.32 GPa to simulate crushing of the shotcrete with time.

Conclusions of Geomechanica (2013)

Geomechanica (2013) concluded the following with respect to the EDZ evolution of a HLW repository:

- Lab-calibrated micro-mechanical input parameters, based on Opalinus Clay lab results, had to be increased 2 to 5 times the originally calibrated values to avoid an excessively large fracture zone. It is stated that excessively large amounts of fracturing are not consistent with in-situ observations in tunnels at Mont Terri.
- Back analysis of the FE tunnel excavation behavior using the lab scale micro-mechanical properties had to be increased 2.75 times in order to capture the rock mass deformations measured in the experimental excavation at Mont Terri.
- The EDZ yield equivalent radius is generally between 6 and 8 m deep (created in the short-term, but still existing in the long-term)

- The total EDZ fracture void volume is significantly reduced by a factor of 2 to 3 times in response to the long-term reconsolidation process simulated with an internal pressure increase up to 10 MPa.

It is stated by Geomechanica (2013) that the final EDZ fracture geometries with the associated stress states were used as input for subsequent hydraulic modelling of the EDZ re-saturation process in the report by Alcolea et al (2014).

4.1.3.2 Simulations presented by Alcolea et al (2014)

The simulations presented by Alcolea et al. (2014) examine “early” (short-term) and “late” (long-term) processes and are distinguished as follows:

- Simulation of short-term processes using early time hydraulic EDZ properties derived from initial Y-Geo fracture network models (without re-consolidation)
- Simulation of long-term processes using late time hydraulic EDZ properties derived from Y-Geo fracture network models) and simulating the resaturation process in the software TOUGH2 (representing swelling and/or mechanical stress changes on fracture apertures) until steady state pore pressure conditions are reached.

Model Inputs

The main inputs used by Alcolea et al. (2014) are the fracture networks derived from Geomechanica (2013), i.e. Y-Geo model results for the circular model simulations (HLW and shaft models), including the following parameters

- Fracture failure mode
- Fracture aperture
- Fracture inclination with respect to the x-axis and measured counter-clockwise
- Fracture area

These inputs are used together with assumed values discussed in the following section.

Modelling Stages

The stages reported by Alcolea et al. (2014) refer to both calculations based on the results presented by Geomechanica (2013) and two phase flow simulations for scoping calculations. The calculations take the early and late time EDZ network values (the abstraction process reported by Alcolea et al. 2014) and determine the specific flux (m/s) within the EDZ based on the fracture aperture and area. The EDZ properties have been abstracted from all HLW and shaft models produced by Geomechanica (2013) to compare the changes in the EDZ properties with ‘time’ for a variety of stress and strength scenarios.

In separate calculations, simulations by means of the software TOUGH2 were conducted for scoping calculations, in order to understand if long-term safety assessment models can start from a fully saturated condition within the whole domain (rock and sealing materials). For this, swelling induced fracture closure (fracture aperture with time, $\alpha(t)$) is simulated as a function of pore pressure buildup (Δp) and calculated from the following equation:

$$\alpha(t) = \alpha_0 - \frac{\Delta p(t)}{\alpha_0 K_{n0} \Delta p(t)^\alpha + \Delta p(t)}$$

This equation has been set up based on the classical fracture normal closure law formulated by Bandis et al. (1983), where K_{n0} is the fracture normal stiffness and α controls the velocity of fracture closure. This equation is dimensionally incorrect, as already stated by Alcolea et al (2014). These hydro-mechanical coupled fracture model parameters were defined in such a way, that full EDZ restoration (to about 8 MPa fluid pressure) leads to complete closure of most fractures and an equivalent continuum hydraulic conductivity of the EDZ, which is close to the intact Opalinus Clay conductivity (Figure 22).

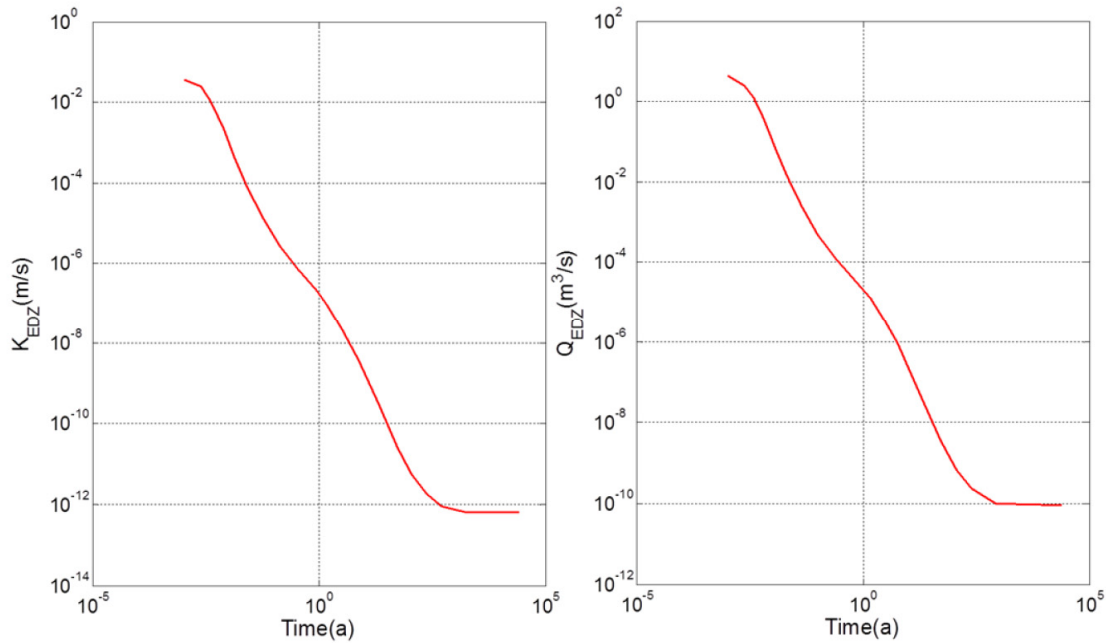


Figure 22: Temporal evolution of simulated equivalent hydraulic conductivity of the EDZ and of the axial flow rate across the abstracted EDZ (from Alcolea et al. 2014).

Matrix conductivity changes were derived from a simplified version of the Kozeny-Carman law (Horseman et al. 1996). Based on the mapped distribution of fractures and matrix in a radially symmetric finite element mesh, equivalent continuum porosity, hydraulic conductivity, and flow rate have been derived for a radially symmetric EDZ model (Figure 23).

Conclusions of Alcolea et al (2014)

The main conclusions drawn by Alcolea et al. (2014) regarding the long-term EDZ evolution of a HLW repository are listed below:

- Specific axial fluxes of the EDZ (standardized axial flow to area) drop by approximately 10 orders of magnitude from early to late times, regardless of in situ stresses and other parameters modelled in the sensitivity cases, although there is a difference of one order of magnitude from all sensitivity cases.
- Fracture porosity drops from 0.12 to approximately 10^{-6} from early to late times and it is generally not sensitive to local conditions or strength parameters used.
- At late times the EDZ is restricted to a radial zone with a thickness of less than two tunnel diameters. Significant enhancement of hydraulic conductivity is observed only in a zone with a thickness of less than half a tunnel diameter. The enhancement is less than one order of magnitude with respect to the intact matrix and corresponds to an increase in porosity of less than 20%.
- For the simplified radially symmetric EDZ the changes in the effective properties with increasing distance away from the excavation boundary are shown in Figure 23.

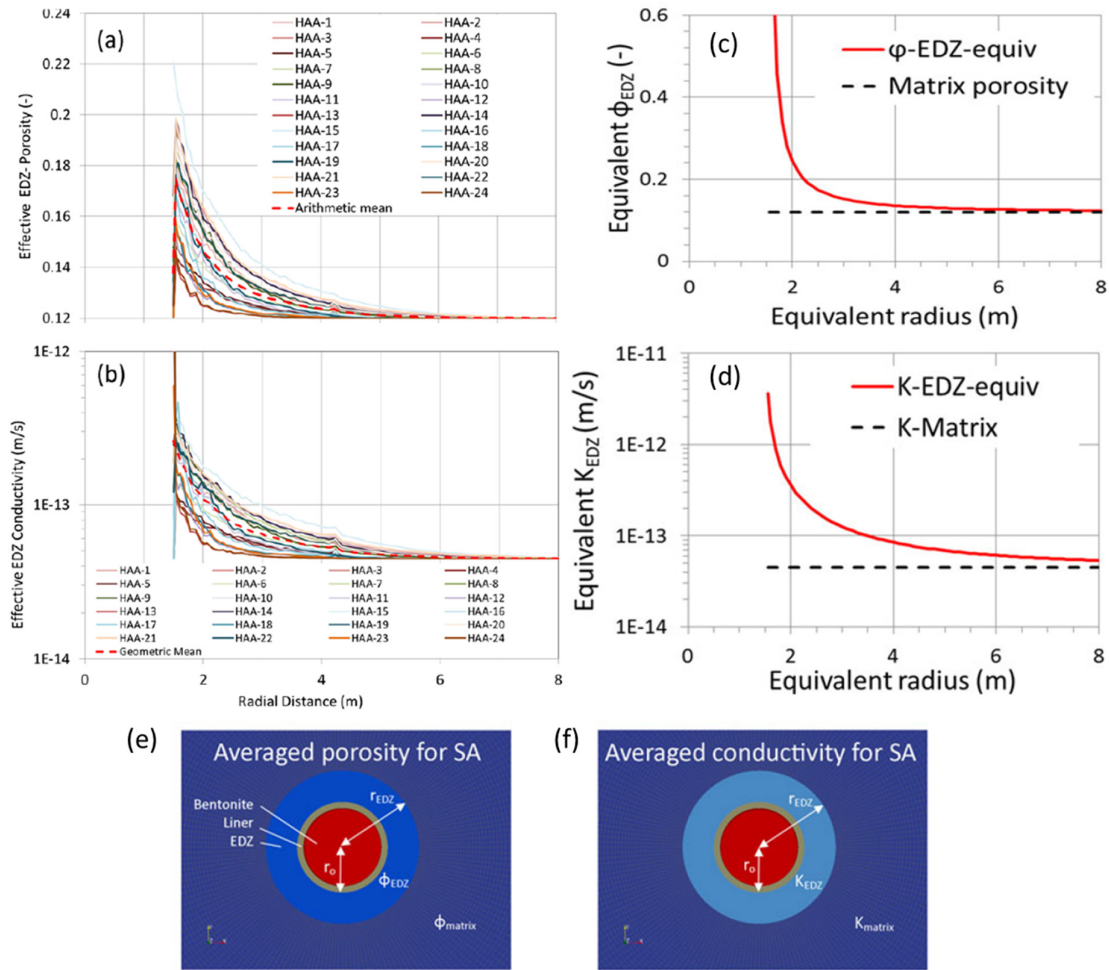


Figure 23: Profiles of effective porosity (a) and effective hydraulic conductivity (b) for all HLW simulations of the “late times” EDZ with increasing distance from the excavation boundary. The safety case analysis “average” (c) equivalent porosity and (d) conductivity values with distance from the excavation surface taken from the HLW simulations which show values equal to the matrix for a radius of 8 m and illustrations of the averaged (e) porosity and (f) conductivity for safety assessment (from Alcolea et al 2014).

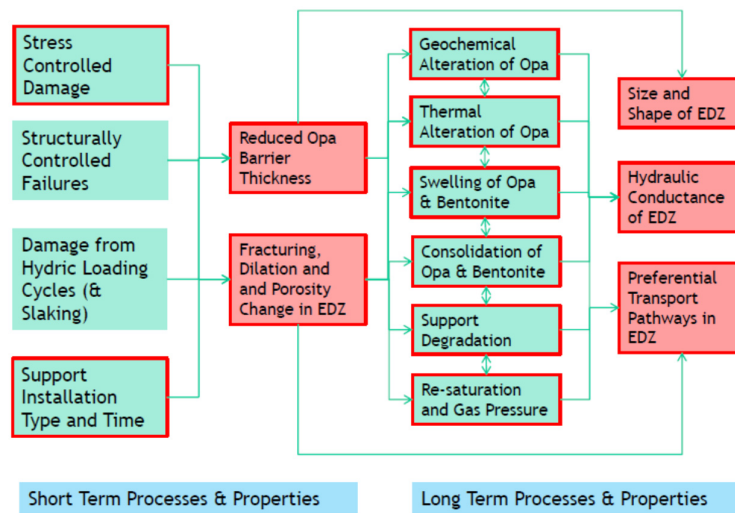


Figure 24: Key processes controlling EDZ short- and long-term properties.

4.2 ETH Assessment of long-term EDZ properties

4.2.1 Overview of long-term evolution of HLW repository near field

Figure 24 gives an overview of the main processes changing near field properties in the pre- and post-sealing repository stages. While all of these processes are discussed in various NAGRA reports, this review only focusses on long-term hydro-mechanical aspects and ignores couplings with thermal or chemical processes (including gas pressures). The hydro-mechanical processes can generally be categorized into three main areas, which may act independently or dependently, depending on the situation. The three main types of hydro-mechanical processes are deformations (swelling or consolidation), stress changes (relaxation), and strength degradation. Their conceptual influence on the EDZ with time is illustrated in Figure 25.

Swelling can be caused by chemical alteration of the rock mass caused by oxidation (sulfides to sulfates), hydration (anhydrite to gypsum, clay mineral water absorption), new crystal growth or by dilution of pore water fluid without chemical alteration to the rock mass (osmosis, diffusion, pore pressure increases). It has been shown that swelling can be suppressed with the application of confinement (Hawladar et al. 2003). The amount of confinement required to suppress swelling is rock type dependent. Swelling is considered as a key processes contributing to self-sealing of the EDZ.

Consolidation causes deformations and hydraulic property changes around an underground opening. A distinction should be made between deformation resulting from the opening of the excavation in the short term (influence of tunnel face and stress re-distribution) and those that occur long after repository sealing, e.g. primary and secondary consolidation composed of viscous deformations (creep) and poro-elastic effects.

Long-term strength degradation is a reduction of the mechanical properties of the rock mass from peak to residual with time within the plastic yield zone. This is distinguished from plastic yielding due to stress re-distribution from the initial excavation process and affects the damaged rock mass within the plastic yield zone whose mechanical properties are not yet at residual level. This is an important process occurring in brittle rocks and can be caused by a number of environmental (e.g. humidity fluctuations) and geochemical processes happening within the EDZ with time. Figure 25 shows how some of these mechanisms influence the yield envelopes with time and the changes that could occur to the EDZ.

Figure 25 and most investigations carried out in the past by NAGRA are related to an EDZ, which is composed of variably fractured material, but not containing any overbreak or material missing from the outside the designed perimeter of the excavation. As shown in various reports and discussed in section 3, structurally and stress controlled failures can lead to buckling, slab or wedge failures creating large overbreak. In extreme situations these damage zones can reach dimensions of up to 3 excavation diameters (Kupferschmied et al. 2015). Such large overbreak is of very high significance for long-term safety, because they can seriously impact bentonite buffer support pressure and self-sealing of EDZ fractures, if not backfilled properly.

4.2.2 Lab and in-situ experiments

The new lab tests on the consolidation and swelling behavior of the Opalinus Clay samples from the Schlattingen borehole are of high quality and provide a reliable contribution to the understanding of self-sealing mechanisms (Ferrari et al. 2012). However, the laboratory testing results currently available do not directly relate to long-term processes happening within the EDZ since this was not the goal of the consolidation and swelling tests. The mechanisms have been included in the numerical simulations conceptually, although not using direct values from the laboratory results. The in-situ experiments carried out in the Mont Terri URL empirically support the concept of fracture and EDZ self-sealing over several orders of magnitude. The individual processes contributing to self-sealing are difficult to comprehensively understand and assess from the existing in-situ experiments.

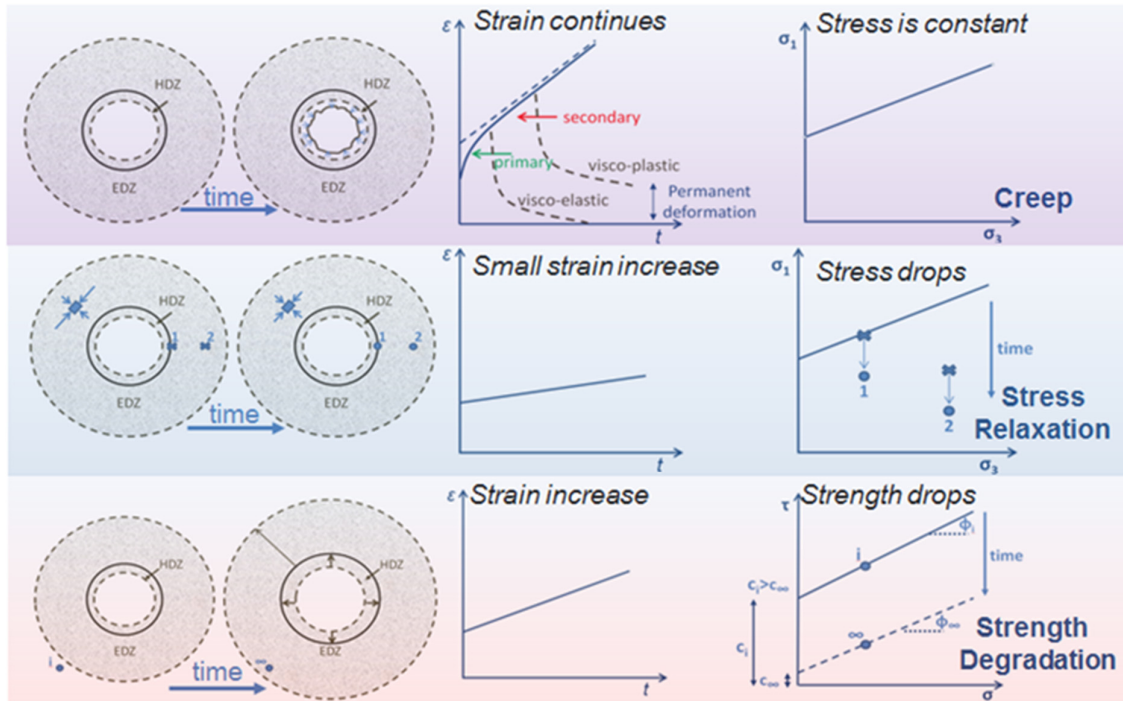


Figure 25: Three fundamental long-term mechanical effects (creep, stress relaxation, strength degradation) on the EDZ expressed in terms of strain-time and principal stress space (after Paraskevopoulou et al. 2015).

The data from the HG-A experiment offer very valuable insight into the reversibility of self-sealing as a function of fracture fluid pressure, support pressure and effective stress (Figure 20). The reviewers suggest to put more emphasis on experimental evidences at excavation scale and to critically test numerical models with data from these experiments.

4.2.3 Numerical Simulations

The models discussed in section 4.2 refer to the long-term property changes of the EDZ around a HLW repository resulting from swelling, consolidation and support degradation (Geomechanica 2013, Alcolea et al. 2014). These processes have not been modelled in an explicit physical formulation but as changes in boundary conditions or material properties. All these simulations refer to an idealized damaged EDZ without large overbreak.

Regarding the impacts on long-term safety and the requirements of stage 2 reporting, as formulated by the regulator in ENSI 33/075, several scenarios that could be considered relevant have not been presented in the documents submitted by NAGRA for stage 2:

- All numerical simulations by Geomechanica (2013) and by Alcolea et al. (2014) do not consider tunnels oriented perpendicular to the maximum horizontal stress (SH max) which would give rise to the largest EDZ. Although the majority of the excavations will be oriented parallel to SHmax there are uncertainties in the stress field orientation and there will be local variations, which should be considered.
- The numerical approach only considers an 'intact' EDZ without large overbreak, such as observed in excavations at the Mont Terri URL and in boreholes (see Figure 18). Such overbreak might be localized in occurrence, but the impact on the long-term EDZ needs to be evaluated, particularly for the intermediate sealing sections (discussed in previous section 3).

A more detailed review of the derivation of the long-term EDZ properties (without overbreak) from numerical simulations for the analysis of long-term safety is discussed in the following subsections for each numerical code and the geomechanical behavioral influences on the EDZ.

4.2.3.1 Assessment of Geomechanica (2013) Simulations

The Y-Geo code is a combined finite/discrete element method (FEMDEM) which allows the creation of fractures along mesh element boundaries. The code shows potential to become a leading software package in geomechanics, however, currently rigorous testing and comparison with analytical and empirical solutions have not been shown or referenced in Geomechanica (2013) to support the validity of the numerical results.

In the report the model is described in detail and the input calibration process is explained. However, the calibration process for the micro-mechanical input parameters is not directly compared with laboratory stress-strain measurements, although peak values have been shown to be reproducible. The calibration to measured excavation deformations at the Mont Terri URL in the FE tunnel is shortly mentioned in section 10 of the report by Geomechanica (2013). In order to correctly capture the deformations the lab calibrated micro-mechanical parameters had to be increased by a factor of 2.75 to get comparable numerical excavation deformations. Calibration to in-situ fracture density, spacing, aperture or other fracture properties has not been documented or reported, although it has been commented by Geomechanica (2013) and Alcolea et al. (2014) that the modelling approach over estimates the fracture density. Since the Y-Geo modelling is being used for hydraulic model inputs for safety assessment cases, calibration to real fracture networks within the Opalinus Clay is a fundamental step. Stating that the fracture network density is overestimated by a factor of 5 to 10 times is not a satisfactory quantification of the impact on the evaluation process. The Y-Geo simulations capture various aspects of the time-dependent behavior around underground excavations. Two time frames are considered, namely the short-term construction and the long-term “re-saturation” phases.

In the short-term two aspects which influence the EDZ development (and starting point for the long-term EDZ evolution) are the influence of the tunnel face on damage creation and delayed rock support installation. Capturing the 3D “face support” in a 2D code using a core softening (utilized in Y-Geo) or by a gradual pressure reduction approach is common practice. Incorporating the rock support will not change the dimension of the EDZ significantly, however, it will influence fracture apertures. The fracture aperture is highly important as it has been utilized in the subsequent simulations, which in turn have been used in the safety assessment. Short-term rock mass behaviors that would influence fracture apertures, such as swelling of the rock mass, consolidation, or poro-elastic effects, cannot be simulated with Y-Geo.

In the long-term re-saturation phase swelling of the bentonite and reduction of the stiffness of the excavation liner have been simulated using Y-Geo. These are important mechanisms which re-consolidate the EDZ and are simulating the mechanical effect that would be caused by saturation of the bentonite backfill material after closure. Although no reference to where the swelling pressure (P_s) range comes from is given, it does fall within the requirements set by NAGRA ($0.2 \text{ MPa} < P_s < S_h$ from Leupin et al. 2014). The application of an internal pressure to simulate the bentonite swelling is a reasonable approach, however in reality at the same time the rock mass swells, which will influence the fracture apertures. During this re-saturation phase swelling and effective stress changes within the rock mass have not been considered in the Y-Geo modelling. The swelling and pore water pressure influences will act during the same time period and will have a coupled effect on the fracture aperture and matrix porosity. This aspect has been discussed by Alcolea et al. (2014) and will be addressed separately.

The method used to simulate installation of the liner in the numerical simulation could also influence the fracture apertures due to the timing of installation and the confinement it provides. The timing of support installation was determined as either when the model total displacements stopped changing with

model time or when the model convergence reached 4%. In Geomechanica (2013) the support installation has not been related (or discussed relative) to a distance from the tunnel face, following such methods suggested by Vlachopoulos and Diederichs (2009). Also, the rock – liner interface has not been discussed in detail and leads to questions on how well the method used to employ the liner installation influences the EDZ properties and how realistic the interface evolution represents the in-situ behavior. Full sealing by application of a closing pressure is not realistic. In reality re-consolidation of the EDZ and degradation of the liner may close some voids at the rock-shotcrete interface, however, it is doubtful whether full closure would be achieved. This is one of the reasons NAGRA's repository design has direct contact of the bentonite with the rock surface in intermediate sealing sections.

Overall the Y-Geo modelling represents a substantial step forward in geomechanical modelling, however, there are questions regarding the reliability of the results, since they appear to give substantially different fracture patterns and densities in comparison to those observed at the Mont Terri URL. More rigorous documentation is needed to compare the code with analytical solutions, empirical observations and measurements, as well as to discuss the limitations of and assumptions used in the software regarding its influence on the EDZ extent, properties and porosity determination.

4.2.3.2 Assessment of Simulations by Alcolea et al. (2014)

The approach utilized by Alcolea et al. (2014) was to take the EDZ fracture network from the Y-Geo simulations, convert it into an equivalent porous media, mapping the discrete fracture networks to a cell base porosity and conductivity, and to create a radially symmetric continuum model with average porosity and conductivity. The starting point of this process are the fracture mechanics simulations, as discussed above.

The approach presented is well documented, however, some assumptions and critical elements (which code was used or if analytical equations only were used) are not explicitly stated. A quantification of the uncertainty of these major limitations regarding the predicted reduction of the EDZ conductivity with time has not been fully addressed. The most critical assumptions and limitations that were outlined and reported include:

- The modified Bandis et al. (1983) equation influence on the re-saturation process is unknown and it is recommended by Alcolea et al. (2014) to conduct laboratory experiments to address this limitation.
- The fundamental parameter in this equation that controls the closure process is the exponent α . This value was determined by calculating the residual aperture required for the fracture transmissivity to be similar to the matrix transmissivity of intact Opalinus Clay after resaturation.
- The uncertainty in the EDZ geometry is unknown and it is suggested by Alcolea et al. (2014) to address this uncertainty by means of Monte Carlo analysis.

The modified Bandis et al. (1983) equation has been stated by Alcolea et al. (2014) to be dimensionally incorrect and that the 'goodness' of the suggested model to represent self-sealing by swelling has not been fully evaluated. The fundamental parameter in this equation that controls the time component of the closure process is the exponent α . This value was determined by calculating the residual aperture required for the fracture transmissivity to be similar to the matrix transmissivity of intact Opalinus Clay after resaturation. This aperture is then used in the modified Bandis et al. (1983) equation to determine the alpha parameter for the most conductive cell in the model (i.e. that with the largest initial aperture). This in effect forces the model to a desired solution consistent with observed or measured in-situ values and does not allow the model to evolve in a manner that can be used as a predictive tool. By forcing the solution to the desired hydraulic conductivity, also the time dependence of fracture closure becomes pre-defined. In fact, the model time to reduced hydraulic conductivity is much greater than that measured in experiments at the Mont Terri URL, which is also acknowledged by the authors. The use of the modified Bandis et al. (1983) equation needs to be critically evaluated to determine if it accurately

reflects the in-situ behavior, including evaluation of the input parameters and the method in which it is applied.

The uncertainty of the EDZ geometry and fracture properties from the Y-Geo modelling is a fundamental concern (discussed in the previous section). The Monte Carlo analysis suggested by Alcolea et al. (2014) to address this uncertainty will not fully capture the uncertainty, since each Y-Geo EDZ fracture network is not a unique representation of the EDZ dimensions and properties for that specific stress and strength scenario. Other stress, stiffness and strength scenarios could yield the same EDZ dimensions and properties. Therefore relating the convergence from the Y-Geo modelling with the hydraulic properties using the method of Alcolea et al. (2014) will yield inconsistent results due to the non-unique Y-Geo EDZ representation.

It is recommended that future numerical simulations should be first carried out to capture the laboratory and in-situ observations to ensure that the realistic mechanisms can be simulated, before many iterations are computed and used as a prediction tool.

5 Conclusions

Feasibility studies for civil tunnels are based on the assumption that the entire spectrum of excavation support and tunnel excavation methods are available. Thus, an optimized excavation and support concept that accounts for the anticipated ground behavior or geological hazards can be designed. This is, however, different for the assessment of the technical feasibility of a nuclear waste repository. Limitations exist with respect to the support elements, which are related to the long-term safety of the repository, i.e. reduction of cement-based material, such as shotcrete, due to chemical transformation of bentonite and host rock, a limited amount of steel due to long-term corrosion and associated gas production, and organics (chemical reactions). The limitations of support measures according to NAGRA (2014b) include a maximum shotcrete thickness of 30 cm and a not-quantified maximum amount of steel and organics (e.g., GFK bolts). Due to these limitations in support measures unwanted events, such as large excavation damage zones or overbreak associated with unravelling, shearing or buckling, which can be controlled in civil tunneling with proper support measures and excavation concepts, can become a major issue for long-term safety of a nuclear waste repository. It is therefore reasonable to limit the depth of the repository and define a maximum depth for which successful construction, proper sealing and post-closure safety can be demonstrated in a robust way.

For the geological conditions in Northern Switzerland, the maximum depth below ground surface influences to a large extent the perimeters of the potential repositories. Since the discussion of the maximum depth below ground surface is directly related to limitations in support measures, the analysis needs to include structural analysis of support options with increasing depth and an evaluation of the depth at which the available support elements can no longer mitigate unwanted ground response in a reliable and robust way.

In the following sections the specific key questions asked by ENSI are addressed and answered.

5.1 Are the rock mechanical fundamentals and scoping calculations for Opalinus Clay provided by NAGRA reproducible, complete and correct?

The constitutive framework and the behavioral aspects described by NAGRA, in particular the effective stress dependent strength and stiffness of the tested rock, are in agreement with many other studies on clay shales (e.g. Aristorenas 1992) and are well described and documented in the literature. NAGRA introduced simplification to the constitutive framework to overcome limitations in numerical and analytical methods used for the engineering feasibility study (i.e. omitting the Roscoe yield surface). This simplified model is reasonable for engineering feasibility studies, providing that the consequences of omitting the Roscoe yield surface are considered in the choice of elastic properties. A single set of effective strength properties and a single E-Modulus was considered by NAGRA for a relatively wide

range of effective stress conditions / depth (i.e. between 400 and 900 m). Thus, an increase in effective rock or rock mass strength properties and E-Modulus, as suggested by NAGRA's constitutive framework, is not considered for the relevant depth range. This may have relevant consequences for the engineering feasibility assessment.

The analysis and interpretation of rock mechanical tests provided by NAGRA to derive geomechanical properties for numerical and analytical calculations (i.e. effective strength, elastic properties and undrained shear strength) is not reproducible and partially inconsistent. Both effective strength properties and the undrained strength were established from triaxial data which are inadequate and/or largely do not fulfill the requirements of a successful state-of-the-art consolidated undrained or consolidated drained test. The detailed analysis of Amann and Vogelhuber (2015) shows that only two triaxial test results can be used for defining effective strength properties, and 8 triaxial test results for the undrained shear strength. Both, the undrained shear strength and effective strength properties for intact Opalinus Clay suggested by NAGRA tend to overestimate the actual strength.

The weighting of data points of different test series, which were assigned different qualities, and a regression analysis through the weighted data are not considered appropriate. A large amount of inadequate test results overbalance the final result of a regression analysis through the weighted data points and lead to wrong conclusions.

5.2 Are both the numerical calculations and evidences for defining the maximum depth below ground surface in NAB 14-81 in terms of the expected rock mass behavior reproducible?

Given the limitation for support elements (i.e. maximum 30 cm of shotcrete, steel arches only in the sealing sections, etc.) and experience gained from underground research laboratories and other tunnels, a restriction of the maximum depth for a HLW repository is, in general, reasonable. The maximal depth of 700 m suggested by NAGRA for high-level waste emplacement drifts is, however, quantitatively not reproducible. This is primarily related to the considered strength properties which tend to overestimate the actual strength of the rock, the choice of the elastic properties (undrained E-Modulus rather than drained E-Modulus for effective stress calculation; not considered consequences of omitting the Roscoe yield surface in defining the elastic properties; a single set of effective strength properties and E-Modulus for the relevant depth range between 400 and 900 m), the design criteria (i.e., tunnel strain based criteria) defined by NAGRA, and limitations of the utilized methods for the given rock mass characteristics and behavioral aspects. In addition, tunnel support was not systematically considered (except for the GRC analysis) to estimate the depth below the ground surface where the load bearing capacity is exceeded and to confirm results obtained from the GRC analysis. Results obtained from the GRC analysis show that the load bearing capacity of the proposed support for intermediate sealing sections is exceeded between 400 and 500m, considering the so called "Widerstandsprinzip", and between 600 and 700m considering the so called "Ausweichprinzip". Thus, not all construction and safety related requirements can be satisfied. The GRC analysis is, however, largely uncertain due to the various assumptions made by NAGRA to overcome limitation of the method. Overall the analyses provided by NAGRA show that the plastic zone and deformation increase with depth and therefore also the likelihood for relevant problems, such as overbreak. An appropriate depth classification and the maximum depth below ground surface remain, however, unreliable and need to be demonstrated using a more robust approach.

5.3 Is the optimized delineation of the disposal perimeter in NTB 14-01 in terms of maximum depth below ground surface and its assessment reproducible?

As outlined above, the quantification of the maximum depth below ground surface provided by NAGRA is uncertain and not reproducible. The depth classification and maximum depth suggested by NAGRA has a major impact on the optimization of the repository perimeter at the HLW site Nördlich Lägern

and to a lesser degree at the site Zürich Nordost. In these siting regions the optimized perimeters outlined by NAGRA in NTB 14-01 are not reproducible.

5.4 Are potential effects of the longer term EDZ development after repository closure covered and assessed by NAGRA? Are these effects reproducible and plausible?

The results from lab experiments and in-situ experiments support the hypothesis of self-sealing in a moderately damaged EDZ in Opalinus Clay. Experiments lasting only a few years and including a passive support pressure already suggest a reduction of EDZ transmissivity by several orders of magnitude, down to 10^{-8} or 10^{-9} m²/s, which is required for long-term safety. Active support pressure further reduces EDZ transmissivity and hydraulic conductance. The additional modelling results provided by NAGRA are not based on physically sound assumptions and cannot be considered independent evidence for long-term self-sealing. They are also not reproducible given that some assumptions and limitations are not discussed in enough detail. While the impact of a moderately damaged EDZ on long-term safety has been studied carefully and in sufficient detail, the effects of large overbreak on long-term safety have not been quantified. Overbreak scenarios (different potential failure mechanisms) and corresponding technical counter measures should be discussed in a more systematic and rigorous way.

6 References

- Amann, F., Löw, S. (2009) Vorschlag geologischer Standortgebiete für das SMA- und das HAA-Lager: Beurteilung und Anwendung der bautechnischen Auswahlkriterien. Expertenbericht im Rahmen der Beurteilung des Vorschlags geologische Standortgebiete für das SMA- und das HAA-Lager, Etappe 1, Sachplan geologische Tiefenlager
- Amann, F., Vogelhuber, M. (2015) Assessment of Geomechanical Properties of Intact Opalinus Clay. ENSI Expert Report 33/461, Brugg.
- Anagnostou, G. (2009) The effect of advance-drainage on the short-term behaviour of squeezing rocks in tunneling. In: Proceedings International Symposium on Computational Geomechanics (ComGeoI). Juan- les-Pins, Cote d'Azur, France.
- Aristorenas, G.V. (1992) Time-dependent behaviour of tunnels excavated in shale. PhD thesis, Massachusetts Institute of Technology.
- Bandis, S.C., Lumsden, A.C., Barton, N.R. (1983) Fundamentals of rock joint deformation. Int. J. Rock Mech. Min. Sci. and Geomech. Abstr, 20(6), 249 - 268.
- Bobet, A., Aristorenas G., Einstein H. (1998) Feasibility analysis for a radioactive waste repository tunnel. Tunnelling and Underground Space Technology, 13, 4, 409-426
- Chern, J.C., Yu, C.W., Kao, H.C. (1998) Tunneling in squeezing ground. In: Proceedings 4th Int. Conference on Case Histories in Geotech. Eng., St. Louis, Missouri, USA.
- Czaikowski, O., Wolters, R., Düsterloh, U., Lux, K.H. (2005) Gebirgsmechanische Beurteilung von Tonsteinformationen im Hinblick auf die Endlagerung radioaktiver Abfälle – Abschlussbericht. Clausthal-Zellerfeld, Deutschland.
- Diederichs, M.S., Kaiser, P.K., Eberhardt, E. (2004) Damage initiation and propagation in hard rock during tunneling and the influence of near-face stress rotation. Int. J. Rock Mech. Min. Sci., 41, 785-812.
- Duncan, J.M., Goodman, R.E. (1968) Finite element analysis of slopes in jointed rock. Contract report 8-68-3. US Army of Engineers Waterways Experimental Station, Vicksburg.

Geomechanica (2012) The excavation of a circular tunnel in a bedded argillaceous rock (Opalinus Clay): short-term rock mass response and numerical analysis using FEM/DEM. Mont Terr Technical Note 2012-06

Hawladar, B.C., Lee, Y.N., Lo, K.Y. (2003) Three-dimensional stress effects on time-dependent swelling behavior of shaly rocks. *Can. Geotech. J.*, 40, 501-511.

Hoek, E., Marinos, P. (2000) Predicting tunnel squeezing problems in weak heterogeneous rock masses. *Tunnels and Tunneling International*, Dec., 2000.

Horseman, S.T., Higgs, J.J.W., Alexander, J., Harrington, J.F. (1996) Water, gas, and solute movement through argillaceous media. NEA working group on measurement and physical understanding of groundwater flow through argillaceous media. Report CC-96/1.

Kovári, K. (1985) Probleme der Gebirgsverformungen bei der Anwendung von Vollvortriebsmaschinen im Fels. Sonderdruck aus SIA-Dokumentation 91, Tunnel- und Stollenbau im Fels mit Vollvortriebsmaschinen. Sammelband der Referate der FGU-Studentagung (SIA-Fachgruppe Untertagebau).

Kovári, K. (1998) Tunnelbau in druckhaftem Gebirge/Tunneling in squeezing rock. *Tunnel*, 5.

Kovári, K., Staus, J. (1996) Basic considerations on tunneling in squeezing ground. *Rock Mech. Rock Eng.*, 29(4), 203-210.

Kupferschmied, N., Wild, M.W., Amann, F., Nussbaum, C.H., Jaeggi, D., Badertscher, N. (2015) Time-dependent fracture formation around a borehole in clay shale. *Inter. J. Rock Mech. Min. Sci.*, 77, 105 – 114.

Labious, V., Vietor, T. (2014) Laboratory and in-situ simulation tests of the excavation damaged zone around galleries in Opalinus Clay. *Rock Mech. Rock Eng.*, 47(1), 57-70

Lisjak, A., Garitte, B., Grasselli, G., Muller, H.R., Vietor, T. (2015) The excavation of a circular tunnel in a bedded argillaceous rock (Opalinus Clay): Short-term rock mass response and FDEM numerical analysis. *Tunnelling and Underground Space Tech.*, 45, 227-248

Marschall, P., Lanyon, B. Gaus, I., and Rüedi J. (2013) Gas transport processes at Mont Terri Test Site (EDZ and host rock) - Field results and conceptual understanding of self-sealing processes. FORGE Report D4.16, 61pp.

Neerdael, B., DeBruyn, D., Mair, R.J., Taylor, R.N. (1999) Geotechnical behaviour of Boom Clay. Commission of the European Communities, Nuclear Science and Technology, Pilot tests on radioactive waste disposal in underground facilities, EUR 13985EN1999, 223–238.

Paraskevopoulou, C., Diederichs, M., Amann, F., Loew, S., Perras, M.A. (2015) Long-term static load laboratory testing behavior of different rock types. In: *Proceeding of the Canadian Geotechnical Society's Annual Conference - GeoQuebec*, Quebec City, Canada.

Steiner, W. (2014) Erfahrungen beim Tunnelbau im Opalinuston des Tafel- und Faltenjuras. In: *Symposium Rock Mechanics and Rock Engineering of Geological Repositories in Opalinus Clay and Similar Claystones*, ETH Zurich.

Valley, B.C. (2007) The relation between natural fracturing and stress heterogeneities in deep-seated crystalline rocks at Soltz-sous-Forets (France). PhD thesis, ETH Zurich, No. 17385.

Vlachopoulos, N., Diederichs, M.S. (2009) Improved longitudinal displacement profiles for convergence confinement analysis of deep tunnels. *Rock Mech Rock Eng*, 42, 131-146

ENSI 33/460

ENSI, CH-5200 Brugg, Industriestrasse 19, Telefon +41 (0) 56 460 84 00, info@ensi.ch, www.ensi.ch